

1.5 UV Radiation Effects on Photosynthesis

Stomatal and non-stomatal responses to various environmental stimuli can limit photosynthetic carbon assimilation (Farquhar and Sharkey, 1982; Flexas *et al.*, 2008). Stomatal limitations are caused by reduced stomatal conductance, which limits CO₂ uptake (Farquhar and Sharkey, 1982), which can result from stomatal closure or changes in stomatal development. If prolonged, limited carbon assimilation eventually restricts growth (Farquhar and Sharkey, 1982). However, stomata may also close in response to a reduction in photosynthesis due to reduced need for CO₂ uptake (Allen *et al.*, 1998). Non-stomatal limitations can also occur in the boundary layer and mesophyll. The boundary layer can affect photosynthesis by reducing the concentration of CO₂ at the leaf surface, reducing CO₂ uptake, if wind speed is insufficient to mix the air surrounding the leaf. This occurs at the level of individual leaf surfaces, but also the crop canopy as a whole (Jones, 1985). Increased epicuticular wax and pubescence can also enhance the boundary layer resistance (Lambers *et al.*, 2008). Mesophyll limitations can occur in the transport of CO₂ from substomatal cavities, after diffusion through the stomata, to carboxylation sites in the chloroplast, along which there are many resistances such as cell walls (Flexas *et al.*, 2008). Thus many potential limitations to photosynthesis exist.

Studies relating to UV radiation and photosynthetic performance have found both stomatal and non-stomatal limitations in many species (e.g. Allen *et al.*, 1998; Lidon *et al.*, 2012). Others have found no effect on photosynthetic parameters at all, perhaps due to the applied irradiance or dose, or because UV radiation was applied from seed allowing defensive mechanisms such as sunscreen from increased flavonoid content to initiate earlier (Noguès *et al.*, 1998; Allen *et al.*, 1999). Some studies have suggested

stomatal limitations occur when UV radiation induces partial closure (Noguès *et al.*, 1999). Others have found that limitation of photosynthesis results from a loss of Rubisco content and activity, and the activity of other Calvin cycle enzymes (Allen *et al.*, 1997). Acute application of UV-B radiation for 30 or 60 minutes each day significantly reduced assimilation rate, with 30 minute daily treatments inhibiting photosynthetic electron transport and 60 minute treatments compromising Rubisco activity (Reyes *et al.*, 2018), but PAR was only $100 \mu\text{mol m}^{-2} \text{s}^{-1}$ which may have exaggerated the results (Aphalo *et al.*, 2012). Many studies have shown that photosystem II (PSII) in the thylakoid membrane is particularly sensitive to UV-B although other studies have found a reduction in photosynthesis without significant effect on PSII in some species (Allen *et al.*, 1998; Noguès and Baker, 1995; Tyystjarvi, 2008 Dobrikova *et al.*, 2013). In the Calvin cycle ribulose 1,5-biphosphate carboxylase/oxidase (Rubsisco) content and activity may also be reduced (Jordan *et al.*, 1992; Allen *et al.*, 1997). Reduced capacity for synthesis of adenosine triphosphate (APT) in the thylakoid membrane can affect regeneration of ribulose 1,5-biphosphate (RuBP), as can the loss of other enzymes in the Calvin cycle, limiting CO_2 assimilation (Allen *et al.*, 1998; Flexas and Medrano, 2002). Leaf morphology can also reduce assimilation rate, a reduction in leaf area under UV-B decreases whole leaf photosynthesis indirectly (Kakani *et al.*, 2003b). In the majority of studies UV radiation limits photosynthesis but when it does there is no consensus on whether this is stomatal limited, or the exact location of any non-stomatal limitation.

It has been suggested that a low ratio of PAR to UV-B also exaggerates photosynthetic responses to UV-B radiation (Cen & Bornman, 1990; Aphalo *et al.*, 2012) which appears to be the case when assimilation rate was reduced by >80% in rice after PAR was reduced from 400 to $100 \mu\text{mol m}^{-2} \text{s}^{-1}$ in conjunction with the

UV-B treatment (Lidon and Ramalho, 2011). Above ambient UV radiation levels, mainly related to ozone depletion studies, often induce the most consistent response (Allen *et al.*, 1997; Noguès *et al.*, 1998, 1999), but not always (Allen *et al.*, 1999). However, solar UV exclusion studies, with a consistent PAR to UV ratio, or above ambient UV doses, have also shown that UV-B reduces assimilation rate (Kataria *et al.*, 2013). There are clearly many different factors affecting the photosynthesis response to UV radiation, including experimental methods, and different mechanisms of response, stomatal and non-stomatal. Generally there is a reduction in assimilation rate and possibly several mechanisms act together, varying between species and cultivars, according to the experimental conditions.

1.6 UV Radiation Effects on Water Use Efficiency

Instantaneous water use efficiency (WUE_i), the ratio of carbon assimilation rate through photosynthesis to the rate of water loss by transpiration, is an important factor for agriculture in arid environments. If photosynthesis is reduced by UV radiation, whether stomatal or non-stomatal related, then total water use must decrease proportionally more to enhance water use efficiency, but if photosynthesis were unaffected then a reduction in water use would increase water use efficiency.

There is little consistency in the relatively limited literature on the effect of UV radiation on WUE_i . A glasshouse study of wheat, rice and soybean with supplemental UV-B found no changes in either assimilation or transpiration rate and hence WUE_i (Teramura *et al.*, 1990). A review of elevated UV-B effects on WUE_i found decreases in most terrestrial vegetation (Runeckles & Krupa, 1994). A field study of spring wheat with supplemental UV-B lighting found that it reduced water use but instantaneous water use efficiency was also significantly reduced (Zhao *et al.*, 2009).

Gaberscik *et al.* (2002) also found a decrease in WUE_i in an outdoor pot trial of buckwheat (*Fagopyrum esculentum*), particularly during early development, but attributed this to a large increase in transpiration rate even though assimilation rate also reduced significantly. A glasshouse experiment of enhanced UV-B found increased WUE_i in 3 of 4 isolines of soybean (Gitz *et al.*, 2005). The different cultivars varied in their response, two significantly reduced transpiration rate while photosynthesis was statistically unchanged, another significantly reduced transpiration rate more than the significant reduction in photosynthesis, the fourth showed no significant changes (Gitz *et al.*, 2005). An ambient UV exclusion study found variable response of soybean, with increases and decreases in two cultivars each, with reduced conductance caused by changes in stomatal density rather than closure (Gitz III *et al.*, 2013). This demonstrates the variability of responses to UV radiation in terms of assimilation rate, transpiration rate and resulting WUE_i , dependent on species, cultivar and experimental conditions.

1.7 Biological Spectral Weighting Functions

Biological spectral weighting functions (BSWFs) were originally designed to calculate effective UV radiation doses relating to ozone depletion studies, because spectral composition of UV radiation varies with ozone column depth and solar elevation (Aphalo *et al.*, 2012). With the change in focus of UV radiation studies, from ozone depletion to plant regulatory responses to ambient levels of UV, the BSWFs can be applied to UV radiation from lamps so that lamp treatments can be compared with solar UV radiation treatments, because the emission spectrum from artificial radiation sources cannot replicate solar radiation. BSWFs are therefore vital to compare scientific studies because UV radiation sources, whether artificial or solar, emit radiation of variable quantities at different wavelengths. If BSWFs are not given,

comparing different UV radiation studies is difficult. Once the action spectrum of a specific biological response is determined it can be applied as a BSWF (Aphalo *et al.*, 2012). The irradiance at each wavelength is weighted based on a BSWF (e.g. growth inhibition), resulting in a UV biologically effective irradiance, or dose when duration of exposure is integrated (Aphalo *et al.*, 2012). A number of different BSWFs exist for plants e.g. a plant growth inhibition action spectrum (PGIAS: Flint and Caldwell, 2003), a flavonoid accumulation action spectrum (FLAV: Ibdah *et al.*, 2002), and even for stomatal opening in broad bean (Eisinger *et al.*, 2000). Where different BSWFs are employed the weighted irradiance or dose cannot be compared, even where they are expressed in the same units, as they are measured on different scales (Aphalo *et al.*, 2012). BSWFs allow specific UV irradiances to be calculated so that an appropriate level of UV radiation (whether applicable to a specific geographical location or to ozone depletion studies) is applied to plants (Flint and Caldwell, 2003) and its relationship to crop production under solar radiation around the globe known. Incorrect use of BSWFs, or use of the wrong BSWF, can cause erroneous interpretation of results (Caldwell & Flint, 2006).

The action spectrum most widely used as a BSWF for terrestrial plants is the generalised plant action spectrum (GPAS: Caldwell, 1971; Caldwell *et al.*, 1986). It combines nine non-growth related UV-B plant responses and predicts no action by UV-A. More recently, a growth-related action spectrum was derived that included action in the UV-A range because there was clear evidence that growth was affected (Flint and Caldwell, 1996). This resulted in the plant growth inhibition action spectrum (PGIAS), which predicts similar plant responses in the UV-B range to the GPAS but with additional sensitivity to UV-A (Flint and Caldwell, 2003). Clearly, as their names suggest, neither of these action spectra was designed with UV-induced

stomatal closure in mind. Using both of the above action spectra allows direct comparison with past studies under artificial or solar radiation.

A major consequence of which BSWF is applied to an unweighted UV spectral irradiance is the relevance of the resulting weighted UV irradiance, or dose, to the natural solar radiation range globally. Depending on the BSWF used the maximum natural solar UV irradiance weighted by the PGIAS ($\sim 1.2 \text{ W m}^{-2}$) is numerically much greater than weighted by GPAS ($\sim 0.375 \text{ W m}^{-2}$). Therefore a PGIAS weighted irradiance of 1.0 W m^{-2} would be deemed relevant to current UV radiation levels but under GPAS it would be considered over double the current global maximum (Fig. 1.4). This has great pertinence for interpretation of the results in terms of their applicability to global agricultural production.

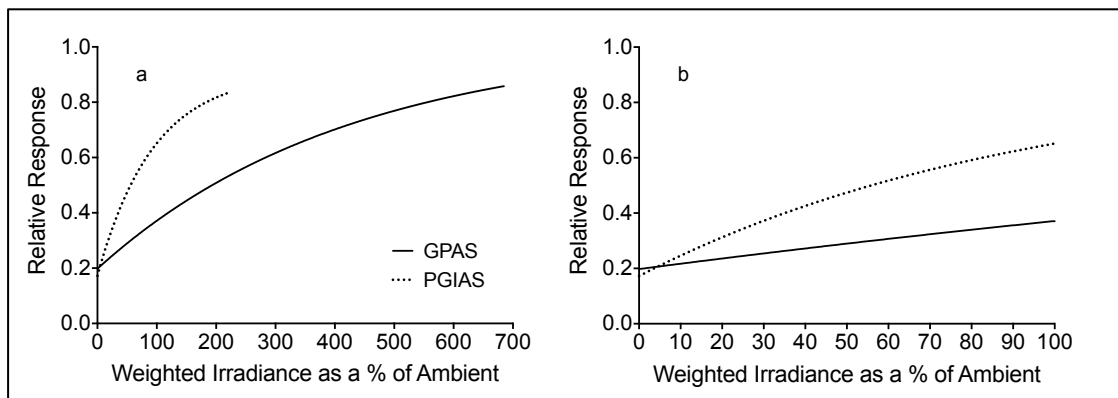


Figure 1.4: A comparison of the same relative plant response to UV radiation weighted by the generalised plant action spectrum (GPAS) and plant growth inhibition action spectrum (PGIAS) to demonstrate the difference in biological effectiveness predicted by the two different action spectra from an identical UV source. (a) The full range of UV irradiances applied throughout this thesis, and (b) magnification of the relative response up to 100% of the modelled current global maximum UV irradiance (Atmospheric Chemistry Observations & Modeling 2019).

1.8 Project Aims

Commercial growers utilising UV-transparent (UV-T) plastic cladding for polytunnels have reported higher leaf temperatures in crops grown under the UV-T plastics than under “conventional” plastics that are opaque to all or part of solar UV radiation. The

plethora of UV radiation plant and crop research demonstrates many plant responses to UV radiation, some of which would be expected to affect leaf temperature. The literature indicates that UV radiation generally causes reduced stomatal conductance, often caused by partial stomatal closure, which would be expected to cause a concurrent reduction in transpiration rate. It was therefore hypothesised that a UV-induced transpiration rate reduction would lead to this increase in leaf temperature observed commercially. This may have beneficial repercussions for crop water use efficiency depending on the UV radiation effect on photosynthesis. Tomato was chosen as the model crop for three reasons: (i) the initial leaf temperature data was collected from a commercial tomato farm (Table 1.2) making it a good model crop for investigation of the hypothesis, (ii) tomato is the world's largest vegetable crop (N8 Research Partnership, 2019), and (iii) the effects of UV radiation on stomata do not appear to have been investigated previously in tomato.

The project aims are:

1. Corroborate the reports from commercial growers that UV radiation increases leaf temperature. This will be conducted in controlled environment experiments to ensure any increase is a result of UV radiation and not other factors co-varying in the field.
2. Test the hypothesis that the mechanism of any increase in leaf temperature is reduced transpiration rate caused by UV-induced partial stomatal closure by developing a high throughput controlled environment experimental system.
3. Investigate the effect of hypothesised stomatal closure, in conjunction with the response of photosynthesis, on instantaneous water use efficiency in the same high throughput experimental system.

4. Upscale the experiments spatially, temporally and environmentally: from high throughput short duration UV applications in growth cabinets to longer duration (multi-day) experiments in field conditions that more accurately reflect commercial growing environments to determine whether the responses observed in tightly controlled environments exist in polytunnels in a field environment.

2 General Materials and Methods

2.1 Plant Material at the Lancaster Environment Centre

Tomato (*Solanum lycopersicum* cv. 'Money Maker') plants were propagated in the absence of UV-B radiation in a south facing glasshouse at the Lancaster Environment Centre (Lancaster University, Lancaster, UK; 54.04°N, 2.80°W) that transmits longwave UV-A but no UV-B radiation. Temperature was partially controlled by passive ventilation, thermal blinds and heating. Passive ventilation and shading blinds were deployed gradually as ambient total radiation exceeded 600 W m^{-2} , and fully deployed when total radiation reached 1000 W m^{-2} . Thermal blinds were deployed when ambient total radiation reduced below 200 W m^{-2} or ambient temperature below 2°C . The minimum glasshouse temperature set point for heating was 15°C and the maximum 24°C . Supplementary light emitting diode (LED) lamps (Senmatic FL300 Grow, Denmark) were set to switch on when ambient total radiation reduced below 450 W m^{-2} and switch off above 500 W m^{-2} , or if glasshouse temperature exceeded 30°C , with a 16-h photoperiod. Seeds sown in modular tray inserts (15-cell, 7.5x7.5 cm cells) containing a peat-based substrate (Levington Advance M3, ICL Everris Ltd,

Ipswich) were at the 3-leaf stage (~3 weeks old depending on the season) when they were transplanted individually into 2 L pots (150 mm diameter) containing the same substrate.

2.2 Quantifying UV Irradiances

UV radiation in the climate cabinets (Chapter 3), controlled environment (CE; Chapter 4) room and polytunnels at Lancaster University (Chapter 5) was quantified with a scanning spectroradiometer with double monochromator (model SR9910-V7, Macam Photometrics, Livingston, UK) with cosine head attachment that provided the spectral transmission (260-800 nm) of UV radiation and PAR sources (artificial or solar).

Solar radiation transmission in Antalya (Turkey; Chapters 6 and 7) was quantified on a clear sunny day immediately prior to the experimental period with broadband radiation sensors (silicon cell pyranometer: SKS 1110; PAR quantum sensor: SKP 215; UV-A sensor: SKU 421; UV-B sensor: SKU 430; Skye Instruments Ltd., Llandrindod Wells, UK) that provided the broadband (total radiation 310-2800 nm; PAR: 400-700 nm; UV-A: 315-400 nm; UV-B: 280-315 nm) solar radiation within each polytunnel. From this the mean maximum irradiances were calculated. Daily UV radiation doses were calculated from UV irradiances measured half-hourly from 06:00-20:00.

2.3 Quantifying Plastic Radiation Transmission

The spectral transmission of plastics used to clad the polytunnels in Lancaster (UK) and Antalya (Turkey) was measured in the laboratory at Lancaster with a 75 W xenon arc lamp (LOT Oriel, Leatherhead, UK), a 10 cm integrating sphere and a scanning spectroradiometer with double monochromator (model SR9910-V7) that provided the

spectral transmission (260-800 nm) of radiation through each plastic. A section of plastic from each polytunnel and a control (without plastic) were used for calculation of the percentage transmission at each wavelength.

2.4 Quantifying Radiation Loading

Radiation loading, measured as total radiation, was measured with the scanning spectroradiometer with double monochromator (model SR9910-V7; 260-800 nm) with cosine head attachment (see Section 1.3). Measurements were made under the LI-6400XT cuvette ‘clear window’ attachment for the climate cabinet experiments (Chapter 3), under the LED attachment of the LI-6400XT for experiments in the controlled environment room (Chapter 4) and Antalya (Chapter 6), and in the polytunnels at Lancaster (Chapter 5). These measurements were duplicated for each experiment, except in the Lancaster polytunnels, with the Skye broadband total radiation sensor (310-2800 nm; see Section 2.2).

2.5 Biological Spectral Weighting Functions

The UV radiation data can be presented in different formats. UV treatments are expressed as (i) unweighted UV irradiances; (ii) irradiances weighted using the plant growth inhibition action spectrum (PGIAS; Flint and Caldwell, 2003); and the (iii) irradiances weighted using the generalised plant action spectrum (GPAS; normalised to 300 nm; Caldwell, 1971; Caldwell *et al.*, 1986) unless otherwise stated. PGIAS has been quoted primarily but because GPAS has been used in the majority of UV radiation studies utilising a biological spectral weighting function (BSWF), referencing it allows direct comparison with previous studies.

2.6 Leaf Temperature

Air temperature fluctuations profoundly influence leaf temperature, especially if stomata are not transpiring fully due to partial closure, reducing the plant's ability to regulate leaf temperature. To account for this, where possible the difference between leaf and air temperature ($T_{leaf} - T_{air}$) is used instead of T_{leaf} .

3 Leaf Temperature and Gas Exchange Responses to a Range of Ultraviolet Irradiances

3.1 Introduction

Stomatal control of leaf temperature has already been well elucidated, particularly in relation to energy balance modelling (Lambers *et al.*, 2008; Section 1.3). The effect of UV radiation on stomatal aperture has also been extensively investigated (e.g. Kakani *et al.*, 1999; Tab. 1.2). Yet leaf temperature responses to UV radiation have rarely been studied (Novotná *et al.*, 2016; Tab. 1.2) and the ramifications for crop water use efficiency (Runeckles & Krupa, 1994; Section 1.6) have received little attention. Very little work has investigated short-term (over minutes) responses (Reyes *et al.*, 2018; Tab. 1.2) that avoid long-term (over weeks) effects on plant and stomatal development. Similarly, leaf physiological responses to a range of UV irradiances do not appear to have been assessed.

The aim of this chapter is to assess the fundamental science of the leaf physiological responses to a range of ultraviolet (UV) irradiances, as it relates to the effect of UV radiation on leaf temperature. It is based on the hypothesis that leaf temperature would increase due to partial stomatal closure, with possible effects on instantaneous water use efficiency. A high throughput method was developed to apply varied UV irradiances ranging from a sunny midwinter day in Lancaster (UK) to double the global maximum for agriculture (based on PGIAS UV radiation weighting). This method required short (90 minutes) acute UV irradiances to be applied to assess the response of multiple plants in a time efficient manner in closely controlled experimental conditions.

Specific to this chapter is the use of unfiltered UV radiation from an artificial UV source. When UV radiation treatments are applied from UV lamps, it is common practice to filter the lamp output with cellulose acetate or cellulose diacetate to omit wavelengths <293 nm. This is done to match the wavelength spectrum of solar radiation in the field as closely as possible. An exception to this is a study of quinoa in which UV lamps were unfiltered and the UV application was acute, similar to the method employed in this chapter (Reyes *et al*, 2018; Tab. 1.2). However, given the proposed use of supplemental UV radiation in horticulture, understanding the effects of UV treatments beyond those occurring in the field becomes relevant. UV applications in horticultural cultivation could be static, or mobile on a rail system, to apply short UV radiation exposure to plants either throughout the growth cycle or at specific developmental stages, such as to limit stem elongation (Innes *et al*, 2018) or increase colouring of fruits (Paul *et al.*, 2005). In this chapter, both filtered (293-400 nm) and unfiltered (280-400 nm) UV treatments were applied separately to compare the effectiveness of the additional short-wave UV-B radiation (280-293 nm), included

in the unfiltered treatments, on stomatal closure and the resulting physiological consequences.

It was hypothesised that UV-B radiation causes partial stomatal closure that limits transpiration rate, thereby increasing leaf temperature (relative to air temperature). The hypothesis was tested by investigating the stomatal and leaf temperature responses of individual tomato leaves to UV radiation of different wavelength spectrums (e.g. UV-A and UV-B, filtered or unfiltered), appropriately weighted by biological spectral weighting functions, over 90 minutes. In addition, any effect on leaf photosynthesis and instantaneous water use efficiency (WUE_i) was analysed.

3.2 Material and Methods

3.2.1 Plant Material

Tomato plants were cultivated at the Lancaster Environment Centre following the procedure outlined previously (Section 2.1). Approximately 4 weeks after seed sowing, the most uniform plants were selected and transferred to a climate cabinet to acclimate for 1 week prior to the experiments. At the end of acclimation, when plants were ~5 weeks old, the most uniform plants were selected and transferred to a second climate cabinet, with a leaflet from the youngest fully developed leaf pair on the 5th internode used for the experiments.

3.2.2 Climate Cabinet Conditions and Radiation Sources

The experiments were conducted in a climate cabinet (Microclima 1750, Snijder Scientific, Tilburg, Holland). This provided relatively stable temperature and humidity control, and constant background photosynthetically active radiation (PAR) for each experiment. As noted above, a second climate cabinet was used to acclimate plants

transferred from the glasshouse. Each cabinet provided the same conditions: $\sim 300 \mu\text{mol m}^{-2} \text{s}^{-1}$ PAR for a 16-h photoperiod (provided by a combination of Sylvania: T5 FHO/54W/840/1149mm, T5 FHO/24W/840/549mm and Brite Grow T8/58W/1200mm fluorescent tubes). UV radiation ($<400 \text{ nm}$) from the fluorescent tubes was blocked with a wavelength selective filter (Lightworks Sun Master plastic film, Arid Agritec Ltd., Lancaster, UK; Fig. 3.1) to ensure plants were not exposed to UV radiation prior to experimentation, or background UV radiation during experiments. The climate cabinet temperature was $25 \pm 1.5^\circ\text{C}$, relative humidity was $60 \pm 10\%$ and CO_2 was 400 ppm. Both climate cabinets had identical environmental conditions to avoid any “transfer shock” when plants were moved between cabinets.

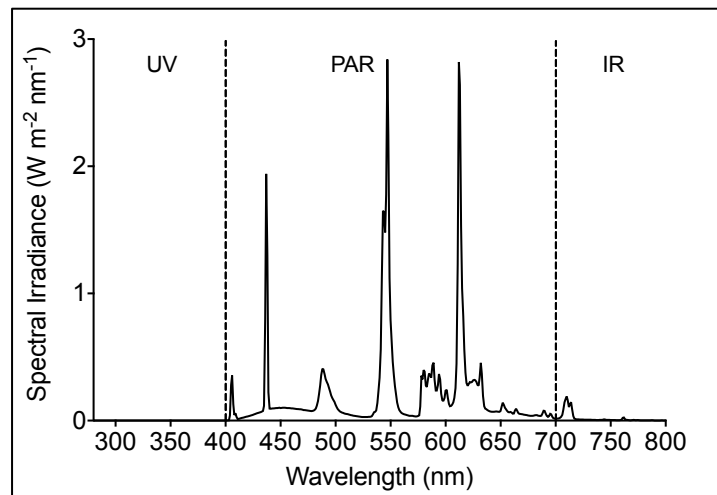


Figure 3.1: Spectral irradiance (280-800 nm) of the photosynthetically active radiation (PAR) from the climate cabinet (Sylvania T5s and T8s, see above), with ultraviolet (UV) radiation ($<400 \text{ nm}$) filtered out with UV-opaque plastic film (Lightworks Sun Master plastic film, Arid Agritec Ltd., Lancaster, UK). The range of photosynthetically active radiation (PAR) and infrared radiation (IR) are also highlighted.

The UV radiation and PAR sources were separate, providing a range of wavelengths (UV-A and UV-B: 293-400 nm) and irradiances ($0.008\text{-}2.64 \text{ W m}^{-2}$ PGIAS weighted). Firstly, compact fluorescent lamps (CFLs) provided UV-A (Helix 25W Black Light Blue UV, Prolite, Ritelite (Systems) Ltd, Stamford, UK) or UV-B (ZooMed ReptiSun 10.0 UV-B Desert, ZooMed Laboratories Inc., San Luis Obispo, USA) radiation (Fig. 3.2a,c). Secondly, to ensure that the specific UV source did not affect experimental

results and to provide a higher range of irradiances, fluorescent tubes (FTs) were used to provide UV-A (Q-Lab UVA-340) or UV-B (Q-Lab UVB-313 EL, both Q-Panel Lab Products, Cleveland, USA) radiation in separate experiments (Fig. 3.2b,d). The UV-B FT was filtered with cellulose acetate to eliminate wavelengths $<293\text{nm}$ for the ‘filtered’ UV radiation treatments, which is standard experimental practice to mimic solar radiation, but not so for the ‘unfiltered’ treatments (Fig. 3.2d).

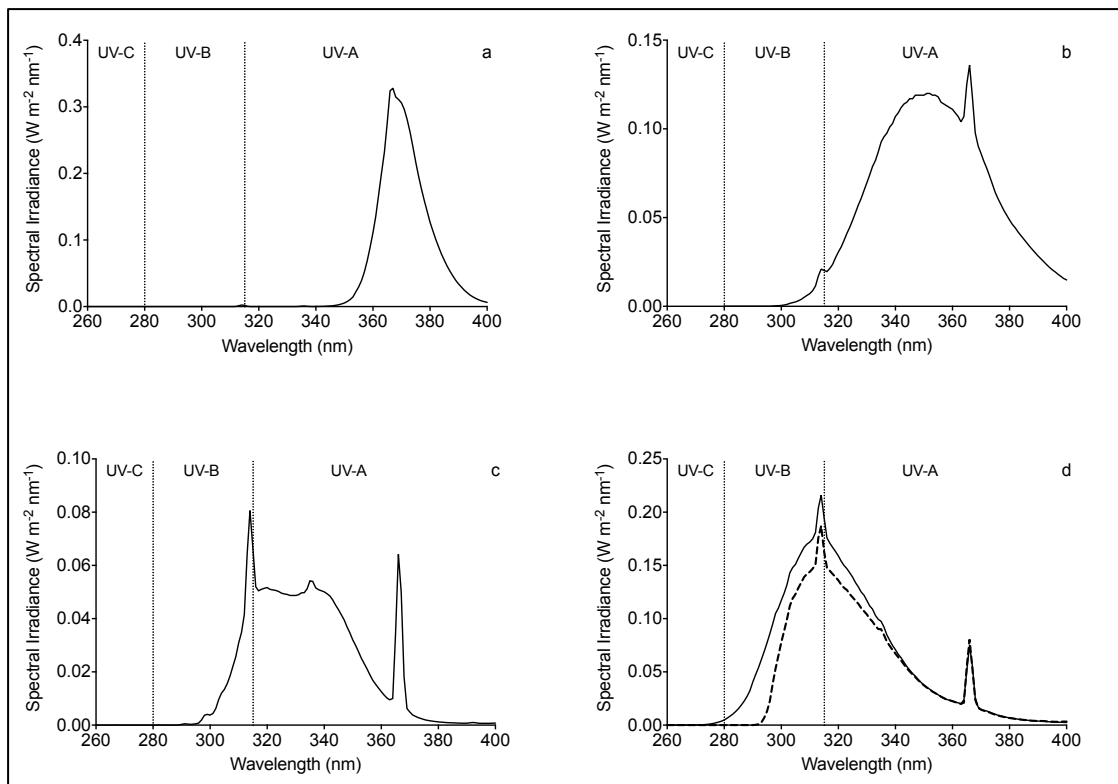


Figure 3.2: Spectral irradiance (260-400 nm) of the ultraviolet (UV) sources used. (a) UV-A compact fluorescent lamp (CFL), (b) UV-A 340 fluorescent tube (FT), (c) UV-B CFL, (d) UV-B 313 FT unfiltered (solid line) and filtered with cellulose acetate (dashed line). UV-A, UV-B and UV-C are identified by the vertical dotted lines.

To investigate the effect of the excluded wavelengths (280-293nm), the UV treatments were divided into ‘filtered’ and ‘unfiltered’ treatments. However, it should be noted that UV treatments labelled as ‘filtered’, such as those from the CFL sources or the UV-A FT, were not actually filtered because the sources do not include wavelengths 280-293nm. Thus the UV treatments identified as ‘filtered’ do not include wavelengths $<293\text{ nm}$, but may not have been specifically filtered with cellulose

diacetate. UV radiation was quantified with a spectroradiometer (Section 2.2) that provided the spectral irradiance (260-800 nm) of each source (Fig. 3.2). UV treatments are expressed as unweighted, and weighted by the PGIAS and GPAS biological spectral weighting functions (Section 2.5; Tab. 3.1). UV-A irradiances (unweighted) were matched with the unweighted UV-B irradiances (applicable to the selected weighted irradiances) to ensure an equal total radiation loading independent of the UV wavelengths applied. UV irradiance was varied by either changing the distance between the experimental leaf and the UV radiation source, ensuring that leaves remained equidistant from the PAR source by raising or lowering the UV lamp on a clamp, or through cabinet control of the UV intensity.

Table 3.1: The UV irradiances and doses (280-400 nm) applied. These are unweighted, and weighted by the generalised plant action spectrum (GPAS: Caldwell, 1971; Caldwell *et al.*, 1986) and the plant growth inhibition action spectrum (PGIAS: Flint and Caldwell, 2003). The UV treatments are divided into those that do not include wavelengths <293 nm ('filtered' UV) and those that were unfiltered (unfiltered UV).

UV Treatment	Unweighted Irradiance 280-400 nm (W m^{-2})	GPAS Weighted UV Irradiance (W m^{-2})	GPAS Weighted UV Dose (kJ m^{-2})	PGIAS Weighted UV Irradiance (W m^{-2})	PGIAS Weighted UV Dose (kJ m^{-2})
Control	0.00	0.000	0.000	0.000	0.000
'Filtered' UV: Wavelengths 293-400 nm					
UVBCFL0.102	0.44	0.100	0.540	0.102	0.551
UVBCFL0.259	2.19	0.255	1.377	0.259	1.399
UVACFL0.102e	0.42	0.000	0.000	0.008	0.043
UVACFL0.259e	2.07	0.000	0.000	0.037	0.200
UVBFT0.097	0.74	0.100	0.540	0.097	0.524
UVBFT0.208	1.76	0.196	1.058	0.208	1.123
UVBFT0.251	1.91	0.260	1.404	0.251	1.355
UVAFT0.251e	5.23	0.029	0.157	0.111	0.599
UVBFT0.297	2.41	0.280	1.512	0.297	1.604
Unfiltered UV: Wavelengths 280-400 nm					
UVBFT0.155	0.50	0.145	0.783	0.155	0.837
UVBFT0.300	0.97	0.280	1.512	0.300	1.620
UVBFT0.707	2.55	0.648	3.499	0.707	3.818
UVBFT1.120	3.40	1.080	5.832	1.120	6.048
UVBFT1.798	5.58	1.680	9.072	1.798	9.709
UVBFT2.640	7.92	2.550	13.770	2.640	14.256

3.2.3 Leaf Gas Exchange and Temperature Measurements

Leaf gas exchange and temperature measurements were made using a LI-COR 6400XT (LI-COR Inc., Lincoln, NE, USA). The LI-COR 6400XT 'clear window'

(‘Teflon’) cuvette attachment transmitted PAR and UV radiation to the experimental leaf enclosed inside. The cuvette block temperature was 25°C, relative humidity ranged 45-55%, CO₂ was 400 ppm and flow rate was 500 μmol s⁻¹. Once a leaf was enclosed inside the cuvette, leaf gas exchange was allowed to stabilise for 15 minutes before applying UV for 90 minutes. The LI-COR 6400XT also provided an additional level of environmental control, which dampened the cyclic fluctuations in controlled environment temperature that are inherent to climate cabinet temperature control. It could also be controlled remotely minimising the risk of UV-B exposure to the operator.

3.2.4 Leaf Temperature (ΔT) Derivation and Example Treatments

Variation in leaf temperature was assessed as $T_{leaf} - T_{air}$ (Section 2.6). The change in this difference was then measured over the treatment period. The effect of UV radiation on this difference between leaf and air temperature over this time period is referred to here as ΔT , and was calculated as follows:

$$\Delta T = (T_{leaf} - T_{air})_{START} - (T_{leaf} - T_{air})_{FINAL} \quad (3.1)$$

where $(T_{leaf} - T_{air})_{START}$ is the difference between leaf and air temperature before UV radiation was applied and $(T_{leaf} - T_{air})_{FINAL}$ is the difference afterwards. Example time courses of the three types of treatments (control, excised leaves, UV radiation; Fig. 3.3) demonstrate the typical leaf temperature response and how ΔT was derived from T_{leaf} and T_{air} . For each experiment, after the leaf was enclosed in the LI-COR 6400XT cuvette, data logging was started and the leaf gas exchange allowed to stabilise for the initial 15 minutes. Then this treatment was maintained for control plants (Fig. 3.3a), or the leaf excised with scissors inducing full stomatal closure to determine the maximum possible leaf warming in that specific environment (Fig. 3.3b), or UV

radiation was applied (Fig. 3.3c). In the first two examples, T_{air} remained stable throughout but when UV was applied, T_{air} fluctuated slightly ($\pm 0.2^\circ\text{C}$). Control leaves exhibited relatively stable T_{leaf} resulting in a stable ΔT . Excised leaves exhibited a slightly delayed increase in T_{leaf} and ΔT compared to the response to UV radiation. This demonstrates that the technique detects the brief and rapid responses in transpiration rate associated with leaf excision. The delayed response of excised leaves was followed by a sharp increase in T_{leaf} and ΔT just minutes later, which gradually plateaued. UV treated leaves exhibited a more immediate but consistent rate of increase in T_{leaf} and ΔT . The air temperature fluctuations in the UV radiation example illustrates why ΔT must be determined to avoid any effect of air temperature on leaf temperature (Fig. 3.3c). This demonstrates the time course of T_{leaf} , T_{air} and ΔT for each type of treatment.

3.2.5 Analysing the Separate Effects of the UV Source and Stomatal Response on Leaf Warming

The effect of the UV lamp heat output on leaf temperature was determined by analysing the relationship between the change in transpiration rate (ΔE) and ΔT . The data were divided into two groups. ‘No UV’ data consisted of treatments that excluded UV radiation (control leaves that were not irradiated with UV radiation and leaves that were excised rather than irradiated with UV radiation) and ‘UV’ data comprised of the various UV treatments. The vertical displacement of the regression lines indicated radiative heating from the UV source, quantified by the Y-intercept.

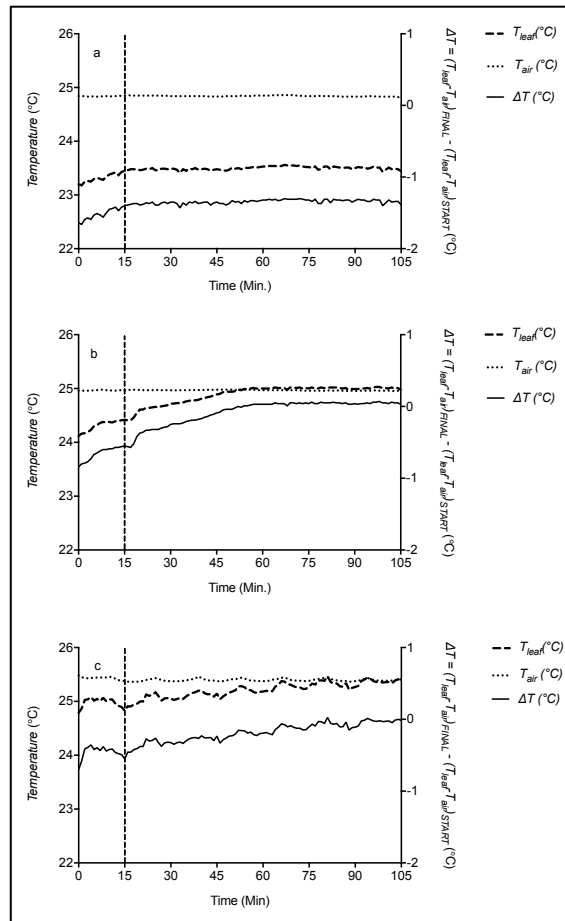


Figure 3.3: Example time courses of T_{leaf} , T_{air} and the resulting $\Delta T = (T_{leaf} - T_{air})_{FINAL} - (T_{leaf} - T_{air})_{START}$ ($^{\circ}\text{C}$) for (a) control, (b) leaf excision and (c) UV radiation treatments. At zero minutes the leaf was enclosed in the LI-COR 6400XT cuvette and data logging without further treatment. The conditions inside the cuvette were allowed to stabilise for 15 minutes. After 15 minutes the treatment was maintained, the leaf was excised or UV radiation was applied (vertical dashed line), and continued for 90 minutes.

3.2.6 Statistical Analysis

Regression analysis was performed using GraphPad Prism version 7.0d for Mac OS X (GraphPad Software, La Jolla California USA, www.graphpad.com) to determine the nature of the relationship between PGIAS / GPAS weighted UV irradiance and each dependent parameter. For the combined filtered and unfiltered UV treatment data set, and the separated data sets, a test determined whether a linear or non-linear model (one-phase association / decay) best fitted the data ($P < 0.05$), with linear as the null hypothesis. In most cases a one-phase association / decay model best fitted the data but for others a linear regression or none at all was most appropriate. If the same

model best fitted the filtered and unfiltered UV treatments when analysed separately, a second test was performed to determine whether these two data sets fitted a single line / curve (null hypothesis) or significantly different lines / curves. The regression coefficients were used to determine how much of the variation in each dependent parameter can be explained by the PGIAS weighted UV irradiance.

Regression analysis aimed to understand the relative effects of transpiration rate and assimilation rate on water use efficiency increases using GraphPad Prism (Section 3.3.6). Further regression analysis determined the effect of the UV lamp heat output on leaf temperature by analysing the relationship between the change in transpiration rate (ΔE) and ΔT using GraphPad Prism (Section 3.3.8).

3.3 Results

Since experiments were conducted between 2017 and 2019, each encompassing several weeks with many batches of plants, variation in the pre-treatment values of the physiological variables appeared to affect the resulting post-treatment values. Analysing the percentage change from pre- to post-treatment normalised the data. The results are presented as the percentage change over the course of UV radiation application for each parameter, except leaf temperature where the absolute change ($^{\circ}\text{C}$) was more appropriate due to the small magnitude of change. Analysing the change from pre- to post-UV treatment also represents the effect of transferring crops from under standard plastic (low UV environment) to UV-transparent plastic (high UV environment) as often occurs in commercial production when plants can be propagated under standard plastic and transplanted into a UV-inclusive polytunnel, or outside in the field, for continuation to maturity. All UV irradiances quoted are

PGIAS weighted unless otherwise stated (see Table 3.1 for equivalent GPAS or unweighted values).

3.3.1 Leaf Temperature

UV radiation increased leaf temperature, relative to air temperature (ΔT), in response to a range of UV irradiances (Fig. 3.4). Regression analysis of the whole data set (filtered and unfiltered UV treatments) indicated that a single positive one-phase association model was a significantly better fit than linear ($P=0.018$) with PGIAS weighted UV irradiance explaining 48% of the leaf temperature increase (R^2 : 0.48; Fig. 3.4). The Y-intercept indicates that even in the absence of UV radiation leaf temperature increased $0.17\pm 0.03^\circ\text{C}$, indicating non-stomatal related warming. However, ΔT in control leaves barely changed in the absence of UV radiation ($-0.04\pm 0.07^\circ\text{C}$), which demonstrates that this warming was related to the UV source (for further analysis see Section 3.3.8). The plateau of the one-phase association curve shows that the maximum increase possible in the controlled environment was predicted to be $0.90\pm 0.13^\circ\text{C}$ (Fig. 3.4).

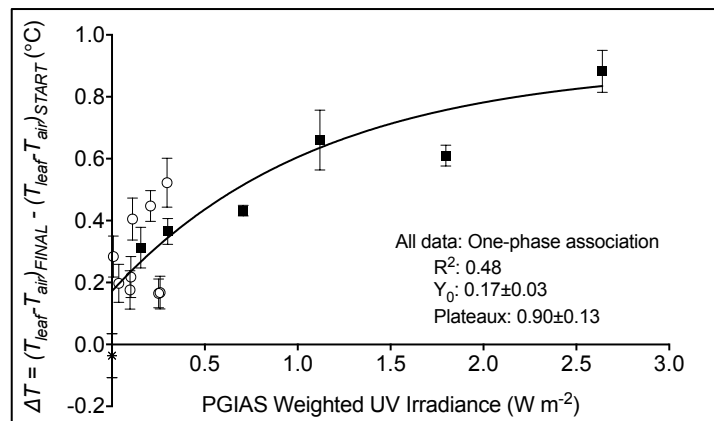


Figure 3.4: The UV irradiance response of leaf temperature ($\Delta T = (T_{leaf} T_{air})_{FINAL} - (T_{leaf} T_{air})_{START}$) to the combined data set (filtered and unfiltered UV treatments) fitted with a one-phase association regression model (solid line). All UV irradiances are weighted by the plant growth inhibition action spectrum (PGIAS; Flint & Caldwell, 2003). The symbols represent control (asterisk), filtered (open) and unfiltered (closed) UV treatments. Climate cabinet and cuvette temperature were 25°C during measurements. Error bars represent ± 1 SE ($n=4$ or 8 depending on the treatment) but if not visible they were smaller than the symbol.

There was no significant difference between the one-phase association models for each data set ($P=0.091$) meaning the single curve of the combined data sets is most appropriate. However, I did explore the relationships for filtered and unfiltered UV radiation. When these data were separated into filtered (293-400 nm) and unfiltered (<293-400 nm) UV treatments, a positive one-phase association was again the more appropriate model for each (filtered: $P=0.011$; unfiltered: $P=0.002$). However, these relationships explained more of the variation for the unfiltered UV treatments (R^2 : 0.72) than the filtered treatments (R^2 : 0.18). Unfiltered UV treatments increased leaf temperature more than the filtered treatments because it was possible to apply greater irradiances when the lamps were unfiltered, with all treatments fitting a single one-phase association model.

3.3.2 Transpiration Rate

Regression analysis of the whole data set (filtered and unfiltered UV treatments) indicated that a significant one-phase decay model was more appropriate than a linear model ($P=0.019$). UV irradiance explained 41% of the decrease in transpiration rate (R^2 : 0.41; Fig. 3.5a). The Y-intercept demonstrates that even in the absence of UV radiation, transpiration rate decreased by $8.1\pm 1.6\%$ in response to enclosing the leaf inside the LI-6400XT cuvette. This was supported by the transpiration response of control leaves ($6.1\pm 3.8\%$ decline) when enclosed in the cuvette without UV radiation. The plateau of the one-phase decay curve predicts that the maximum possible reduction in transpiration rate due to this UV radiation was $37.5\pm 5.9\%$ (Fig. 3.5a).

When only the unfiltered UV (280-400 nm) treatment data was analysed, a one-phase decay regression was a significantly better fit than linear ($P=0.015$; R^2 : 0.55; Fig. 3.5b). There was no significant relationship between transpiration rate and the limited

range of UV irradiances provided by the filtered UV treatments (293-400 nm) (Fig. 3.5b). However, considering the linear phase of the UV irradiance response only, i.e. when the unfiltered treatments $>0.3 \text{ W m}^{-2}$ (PGIAS) were excluded from analysis, there was no significant difference between the individual linear regressions (Slope: $P=0.297$; Y-intercept: $P=0.372$). This suggests that if the filtered irradiances could have been increased to the same extent as the unfiltered treatments, that the one-phase decay response would have been replicated (Fig. 3.5b).

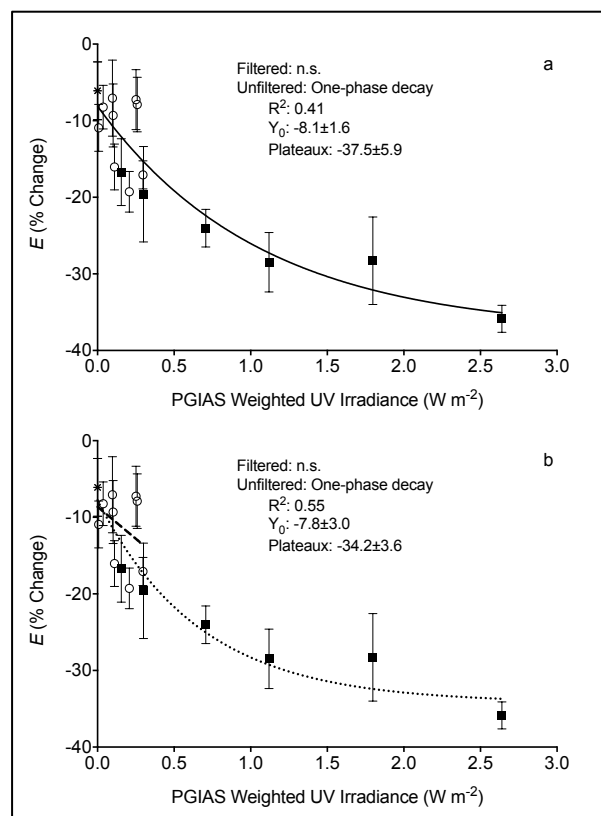


Figure 3.5: The UV irradiance response of transpiration rate (E) to (a) the combined data set (filtered and unfiltered UV treatments) fitted with a one-phase decay regression model (solid line) and (b) the separated data sets (filtered and unfiltered UV treatments) where the unfiltered data are fitted with a significant one-phase decay regression model (dotted line) and the filtered data fitted with a linear regression (not significant: dashed line). All UV irradiances are weighted by the plant growth inhibition action spectrum (PGIAS; Flint & Caldwell, 2003). The symbols represent control (asterisk), filtered (open) and unfiltered (closed) UV treatments. Climate cabinet and cuvette temperature were 25°C during measurements. Error bars represent ± 1 SE ($n=4$ or 8 depending on the treatment) but if not visible they were smaller than the symbol.

3.3.3 Stomatal Conductance

Regression analysis of the whole data set (filtered and unfiltered UV treatments) for stomatal conductance indicated that a negative linear relationship was marginally more appropriate than a one-phase decay model ($P=0.057$). The linear regression was highly significant ($P<0.001$) with PGIAS weighted UV radiation explaining 34% of the decrease in stomatal conductance (R^2 : 0.34; Fig. 3.6a). Enclosing the leaf inside the cuvette decreased stomatal conductance even in the absence of UV radiation, as the Y-intercept was -19.71% and control leaves reduced $-13.6\pm 5.3\%$. Together with the transpiration rate response, this demonstrates that leaf enclosure inside the cuvette induced some stomatal closure prior to UV application.

When only the unfiltered UV (280-400 nm) treatment data was analysed, a one-phase decay regression model was more appropriate than linear ($P=0.025$; Fig. 3.6b). The one-phase decay regression explained 51% of the decrease in stomatal conductance (R^2 : 0.51; Fig. 3.6b). The plateau of the one-phase decay indicates that the maximum possible reduction was $49.5\pm 4.5\%$ (Fig. 3.6b). There was no significant relationship between filtered PGIAS weighted UV radiation (293-400 nm) and reduced stomatal conductance (Fig. 3.6b). However, when the unfiltered treatments $>0.3 \text{ W m}^{-2}$ were excluded from analysis there was no significant difference between the individual linear regressions (Slope: $P=0.247$; Y-intercept: $P=0.459$). This again suggests that if the filtered irradiances could have been increased to the same extent as the unfiltered treatments, the one-phase decay response would have been replicated (Fig. 3.6b).

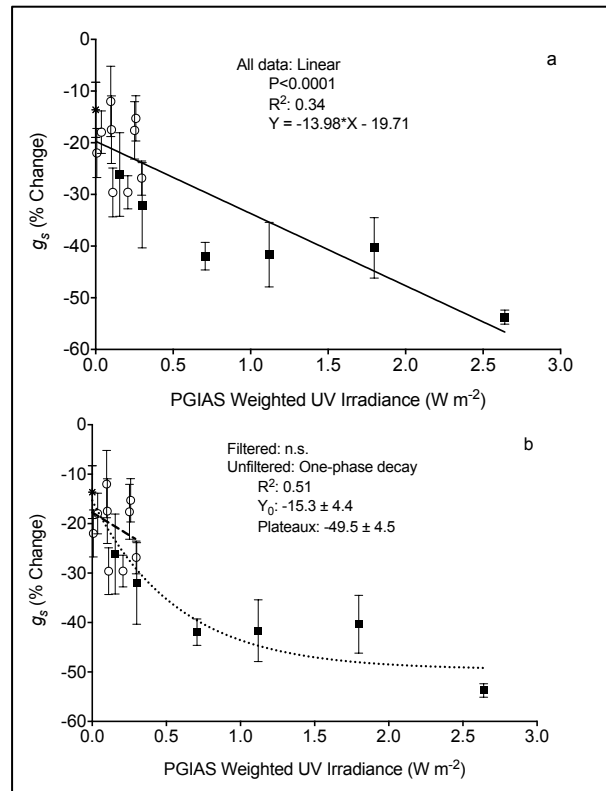


Figure 3.6: The UV irradiance response of stomatal conductance (g_s) to (a) the combined data set (filtered and unfiltered UV treatments) fitted with a one-phase decay regression model (solid line) and (b) the separated data sets (filtered and unfiltered UV treatments) where the unfiltered data are fitted with a significant one-phase decay regression model (dotted line) but the filtered data did not significantly fit any regression model (dashed line). All UV irradiances are weighted by the plant growth inhibition action spectrum (PGIAS; Flint & Caldwell, 2003). The symbols represent control (asterisk), filtered (open) and unfiltered (closed) UV treatments. Climate cabinet and cuvette temperature were 25°C during measurements. Error bars represent ± 1 SE ($n=4$ or 8 depending on the treatment) but if not visible they were smaller than the symbol.

3.3.4 Photosynthesis

Regression analysis of the whole data set (filtered and unfiltered UV treatments) indicated that only a negative linear model fitted the data ($P < 0.001$; R^2 : 0.59; Fig. 3.7a). Although assimilation rate generally increased (<11%) in response to each applied irradiance, the overall relationship with PGIAS weighted UV irradiance was negative. The greater the UV irradiance the lower the assimilation rate increased. The Y-intercept (7.9%) indicates that assimilation rate increased when UV radiation was not applied and control leaves also increased ($6.3 \pm 1.6\%$) in the absence of UV radiation, perhaps in response to enclosure within the cuvette or possibly reflecting natural variation between leaves. When only the unfiltered UV treatment data (280-

400 nm) was analysed, a negative linear regression model again best explained most of the change in assimilation rate ($P=0.003$; $R^2: 0.86$; Fig. 3.7b). No regression model significantly fitted the filtered UV treatment response (Fig. 3.7b). Assimilation rate decreased linearly as unfiltered UV radiation increased.

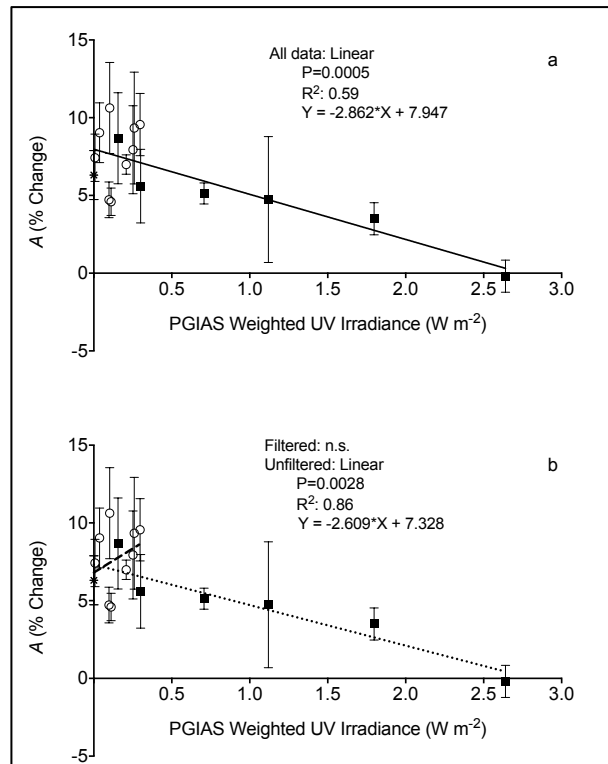


Figure 3.7: The UV irradiance response of assimilation rate (A) to (a) the combined data set (filtered and unfiltered UV treatments) fitted with a significant negative linear regression model (solid line) and (b) the separated data sets (filtered and unfiltered UV treatments) where the unfiltered data are fitted with a significant negative linear regression model (dotted line) but the filtered data did not significantly fit any regression model (dashed line). All UV irradiances are weighted by the plant growth inhibition action spectrum (PGIAS; Flint & Caldwell, 2003). The symbols represent control (asterisk), filtered (open) and unfiltered (closed) UV treatments. Climate cabinet and cuvette temperature were 25°C during measurements. Error bars represent ± 1 SE ($n=4$ or 8 depending on the treatment) but if not visible they were smaller than the symbol.

Increased assimilation rate, observed for all but the greatest UV irradiance, may be attributed to the UV source. The UV lamps not only emitted UV radiation but also radiation at longer wavelengths (>400 nm; Fig. 3.8), including photosynthetically action radiation (PAR), which cannot be filtered from the source. This increased PAR by $\sim 10\%$ when the UV lamp was switched on, causing a similar increase ($\sim 10\%$) in assimilation rate. However, it is interesting to note that increasing the unfiltered UV

irradiance gradually reduced the gains in assimilation with the maximum irradiance (2.64 W m^{-2}) resulting in no overall change. Thus with increasing irradiance UV-induced inhibition of photosynthesis counteracted assimilation gains from the increase in PAR. This can explain why there was a general increase in assimilation rate in response to UV radiation.

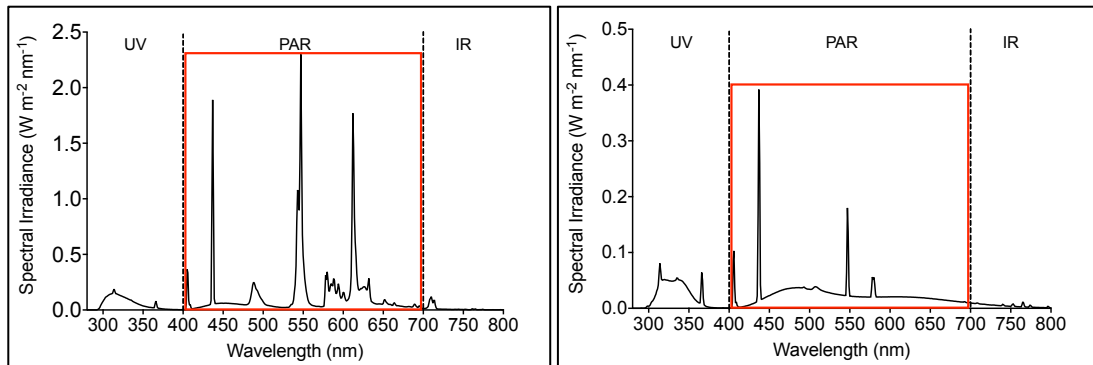


Figure 3.8: Spectral irradiance (280-800 nm) of (a) the UVB313 fluorescent tube (FT) ultraviolet (UV) radiation source and (b) the UV-B compact fluorescent lamp (CFL). The wavelengths are separated between UV radiation (UV), photosynthetically active radiation (PAR) and infrared radiation (IR) by dashed vertical lines demonstrating that not only does the UV source emit UV radiation but also PAR (red outline). This additional PAR would affect assimilation rate when the UV source was switched on.

3.3.5 Intracellular Carbon Dioxide (CO_2) Concentration

Regression analysis of the whole data set (filtered and unfiltered UV treatments) indicated that a negative linear model was most appropriate ($P < 0.001$) explaining 82% of the change in intracellular CO_2 ($R^2: 0.82$; Fig. 3.9a). However, the magnitude of the decreases was small ($< 15\%$).

When only the unfiltered UV treatment data (280-400 nm) was analysed, a negative linear regression again best explained most of the reduction in intracellular CO_2 ($P = 0.003$; $R^2: 0.85$; Fig. 3.9b). No significant regression model fitted the UV irradiance response to the filtered UV treatments (Fig. 3.9b). When the unfiltered treatments $> 0.3 \text{ W m}^{-2}$ were excluded from analysis there was no significant difference between the individual linear regressions (Slope: $P = 0.170$; Y-intercept: $P = 0.172$) which could indicate that if the filtered irradiances were increased to the

same range as the unfiltered treatments that the same negative linear response would occur. Increased irradiances of unfiltered UV radiation decreased intracellular CO₂ concentrations.

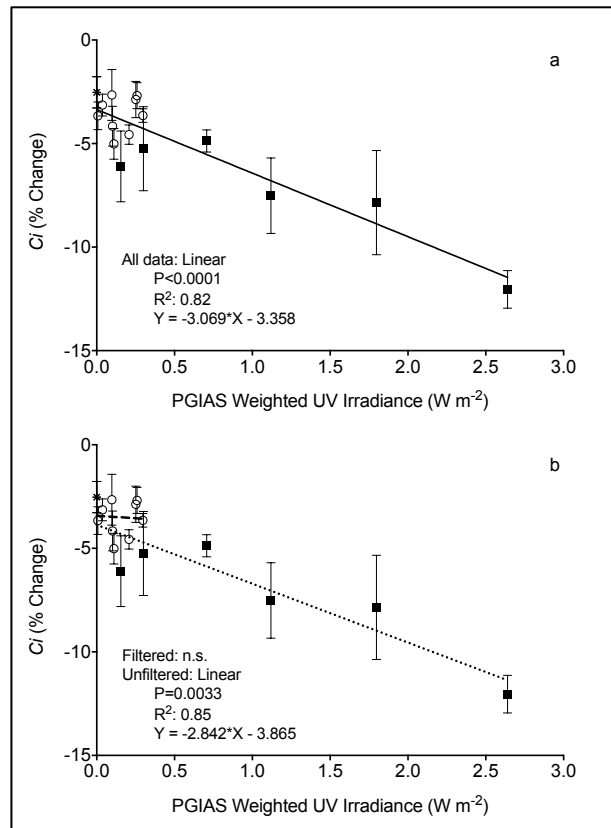


Figure 3.9: The UV irradiance response of intracellular CO₂ (*C_i*) to (a) the combined data set (filtered and unfiltered UV treatments) fitted with a significant negative linear regression model (solid line) and (b) the separated data sets (filtered and unfiltered UV treatments) where the unfiltered data are fitted with a significant negative linear regression model (dotted line) but the filtered data did not significantly fit any regression model (dashed line). All UV irradiances are weighted by the plant growth inhibition action spectrum (PGIAS; Flint & Caldwell, 2003). The symbols represent control (asterisk), filtered (open) and unfiltered (closed) UV treatments. Climate cabinet and cuvette temperature were 25°C during measurements. Error bars represent ± 1 SE (n=4 or 8 depending on the treatment) but if not visible they were smaller than the symbol.

3.3.6 Instantaneous Water Use Efficiency (*WUE_i*)

Analysis of the irradiance response of *WUE_i* to the whole data set (filtered and unfiltered UV treatments) indicated that a positive one-phase association model was the best fit ($P < 0.001$) explaining 39% of the increase ($R^2: 0.39$; Fig. 3.10a). The Y-intercept demonstrates that even in the absence of UV radiation, *WUE_i* increased $17.5 \pm 2.6\%$, similar to control leaves ($14.6 \pm 4.8\%$). Again, this was caused

predominantly by transpiration rate decreasing in response to enclosing the leaf inside the cuvette (for all treatments) and to some extent by assimilation rate increasing in response to the additional PAR emitted by the UV radiation source (except for control leaves as the UV lamp was not switched on). The plateau of the one-phase association curve indicates that the maximum increase possible due to UV radiation under these experimental conditions was $57.7 \pm 6.9\%$ (Fig. 3.10a).

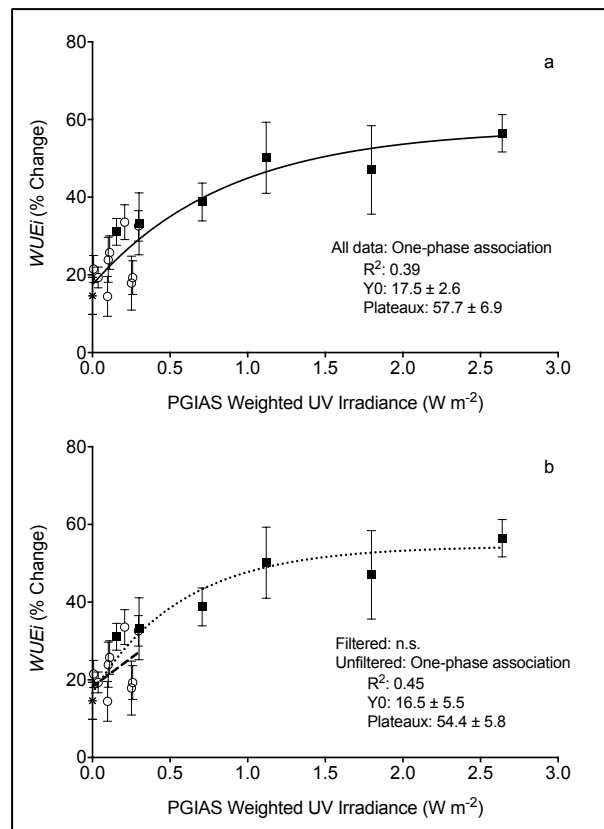


Figure 3.10: The UV irradiance response of instantaneous water use efficiency (WUE_i) to (a) the combined data set (filtered and unfiltered UV treatments) fitted with a significant one-phase association model (solid line) and (b) the separated data sets (filtered and unfiltered UV treatments) where the unfiltered data are fitted with a significant one-phase association model (dotted line) but the filtered data did not significantly fit any regression model (dashed line). All UV irradiances are weighted by the plant growth inhibition action spectrum (PGIAS; Flint & Caldwell, 2003). The symbols represent control (asterisk), filtered (open) and unfiltered (closed) UV treatments. Climate cabinet and cuvette temperature were 25°C during measurements. Error bars represent ± 1 SE ($n=4$ or 8 depending on the treatment) but if not visible they were smaller than the symbol.

When only the unfiltered UV treatment data (280-400 nm) was analysed again a positive one-phase association model was most appropriate, explaining more of the

increase than when the UV treatments were combined; R^2 : 0.45; Fig. 3.10b). No significant regression model fitted the UV irradiance response to the filtered UV treatments (Fig. 3.10b). However, when the unfiltered treatments $>0.3 \text{ W m}^{-2}$ were excluded from analysis there was no significant difference between the individual linear regressions (Slope: $P=0.375$; Y-intercept: $P=0.421$). This suggests that if the filtered irradiances could have been increased to the same extent as the unfiltered treatments, that the one-phase association response would have been replicated (Fig. 3.10b).

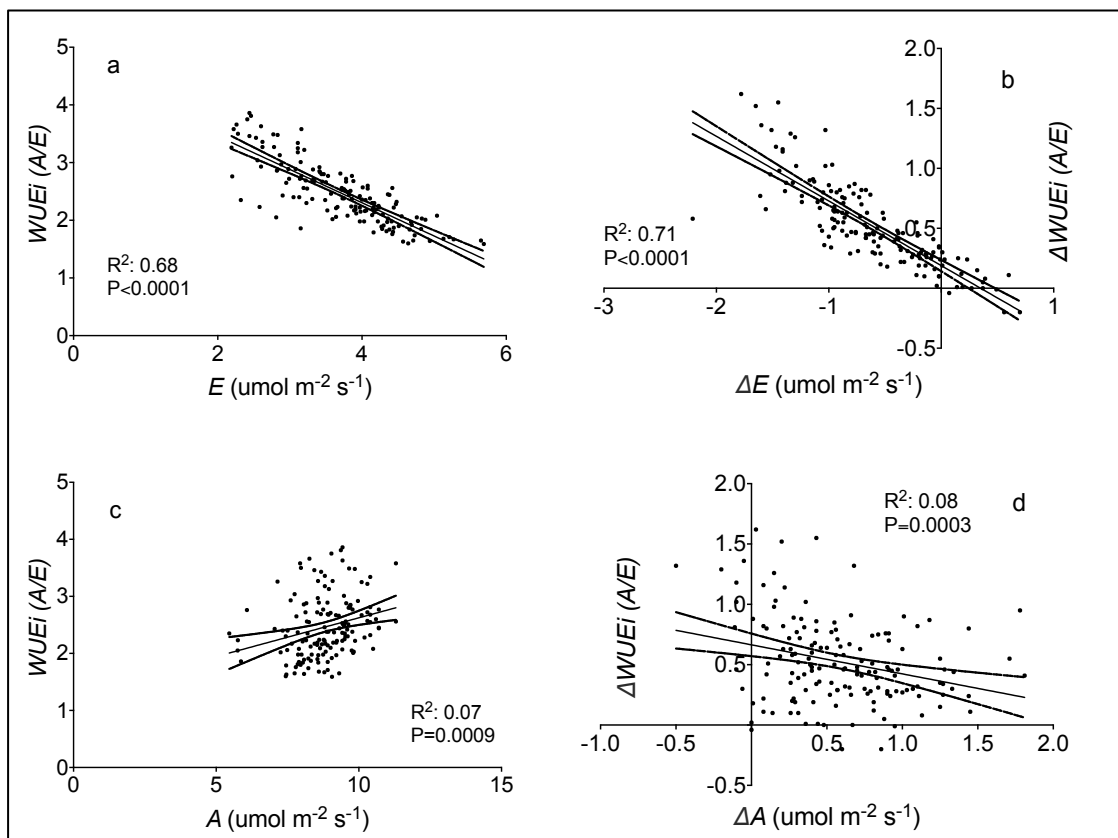


Figure 3.11: Relationships between $WUE_i (A/E)$ and post-treatment (a, c) and changes in (b, d) transpiration rate (a, b) and assimilation rate (c, d) with R^2 and P values for the linear regressions reported. The dashed line represent the 95% confidence interval of the linear regression.

Unfiltered UV irradiances enhanced WUE_i because they decreased transpiration rate more (up to 37%) than they increased assimilation rate ($<11\%$). WUE_i was better correlated with post-treatment transpiration rate (E ; R^2 : 0.68; $P < 0.001$; Fig. 3.11a),

and the change in transpiration rate (ΔE ; R^2 : 0.71; $P < 0.001$; Fig. 3.11b) than either post-treatment assimilation rate (A ; R^2 : 0.07; $P < 0.001$; Fig. 3.11c) or the change in assimilation rate (ΔA ; R^2 : 0.08; $P < 0.001$; Fig. 3.11d). This clearly demonstrates that decreased transpiration rather than increased assimilation had more effect in enhancing WUE_i across the range of UV irradiances applied.

3.3.7 Quantifying the Maximum Leaf Warming Possible

Leaves were also excised to determine the maximum leaf warming that could occur in response to complete stomatal closure in those specific controlled environmental conditions (Section 3.2.4). Leaf excision initiates stomatal closure within minutes, after a brief and transient opening, causing complete closure (based on stomatal conductance alone) within 90 minutes (Ceulemans *et al.*, 1989). The greater the initial transpiration rate of a leaf immediately prior to excision, the larger the reduction through complete stomatal closure, and therefore the subsequent increase in ΔT . A range of pre-excision transpiration rates provided a range of ΔT increases that may be caused by partial stomatal closure in response to the UV treatments. These ‘No UV’ data (‘control’ & ‘excised leaf’ data) show that the maximum degree of leaf warming (ΔT) that could occur due to complete stomatal closure in the specific radiative loading environment of the climate cabinet, in the absence of a UV lamp, was 1.14°C (Fig. 3.12).

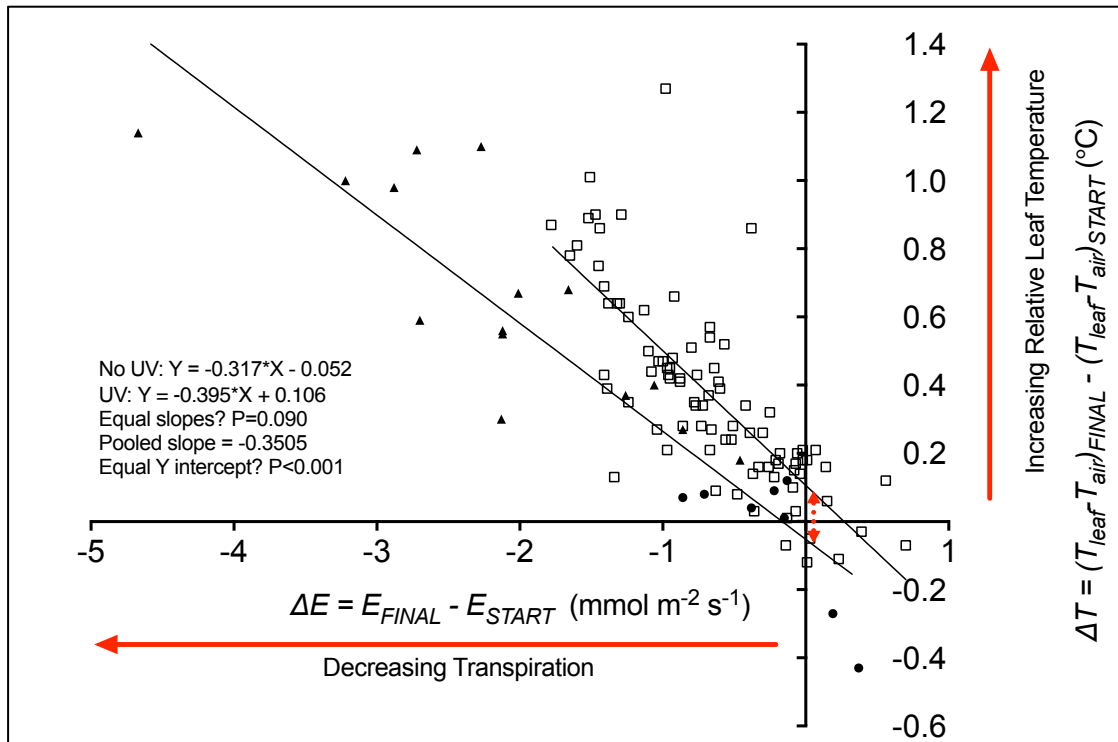


Figure 3.12: The change in relative leaf temperature ($\Delta T = (T_{leaf}T_{air})_{FINAL} - (T_{leaf}T_{air})_{START}$), plotted against the change in transpiration rate ($\Delta E = E_{FINAL} - E_{START}$) in response to various treatments in the CE cabinet experiments. Each symbol represents a separate individual leaf ($n=111$). The ‘No UV’ data are derived from unirradiated treatments, the controls of all experiments (closed circles) and from the excised leaf experiments (closed triangles). The excised leaf data demonstrates the maximum ΔT increase possible in the controlled experimental environment. These ‘No UV’ data were plotted separately to the ‘With UV’ data (open squares) from all experiments. Linear regressions were fitted separately to the ‘No UV’ and ‘With UV’ data. The two fitted regressions were highly significant (both $P<0.001$). The slopes of the fitted lines for the two datasets were not significantly different ($P=0.09$) but the Y intercepts were highly significantly different ($P<0.001$). This difference in Y intercept is the vertical offset between the linear regression lines when there is no difference in transpiration rate (indicated by the dashed double-headed arrow), taken as a measure of direct radiative heating from the UV lamps used to apply UV radiation.

3.3.8 Dissecting the Individual Effects of the UV Source and Partial Stomatal Closure on Leaf Warming

It is important to note that leaves were also exposed to infrared radiation from the artificial UV radiation source in all treatments except the control and leaf excision (the ‘No UV’ data) experiments (Fig. 3.13), potentially causing radiative heating of the leaf regardless of stomatal behaviour. Radiative heating has been partially included in the analysis of leaf temperature relative to air temperature (ΔT) by taking account of air temperature. Radiative heating from the UV source could increase air temperature indirectly, as the near infrared radiation from the lamp is absorbed and re-emitted as

far infrared radiation from the surfaces inside the climate cabinet, which is then absorbed by trace gases in the air such as water vapour thus increasing air temperature (Liang, 2013). Additionally, this indirect heating of air temperature would be small in comparison to the direct radiative heating of the leaf because a leaf is similar to a black body that absorbs near infrared radiation directly from the lamp.

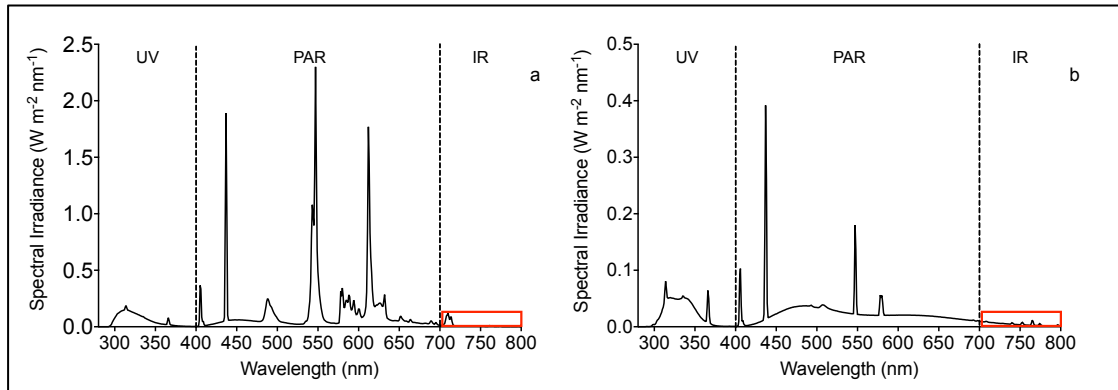


Figure 3.13: Spectral irradiance (280-800 nm) of (a) the UVB313 fluorescent tube (FT) and (b) the UV-B compact fluorescent lamp (CFL) ultraviolet (UV) radiation sources. The wavelengths are separated between UV radiation (UV), photosynthetically active radiation (PAR) and infrared radiation (IR) by dashed vertical lines demonstrating that not only does the UV source emit UV radiation but also infrared radiation (red outline) that can cause radiative heating of leaves when the UV source was switched on.

Clearly, radiative heating from the UV source occurred in all UV treatments so this effect should be separated from effects caused by partial stomatal closure. The effect of direct radiative heating from the UV source was determined through linear regression analysis of the ‘With UV’ and ‘No UV’ treatment data. Analysis of the difference between the ‘No UV’ data and ‘With UV’ treatment data demonstrated direct radiative heating from the UV lamp via vertical displacement of the plotted linear regression lines (indicated by the double-headed arrow: Fig. 3.12), because the ‘No UV’ data received no additional heat input of infrared radiation from a lamp whereas all the UV treatments did. The significant ($P < 0.001$, Fig. 3.12) displacement of the Y-intercepts was $0.16 \pm 0.09^\circ\text{C}$ demonstrating that when transpiration rate did not change, ΔT increased regardless of any stomatal response, caused by direct

radiative heating from the UV source. Linear regression analysis indicates that the slopes of the ‘No UV’ and ‘With UV’ treatment data did not significantly differ ($P=0.181$; pooled slope: -0.3435 ; Fig. 3.12).

Increases in ΔT beyond the vertical displacement of the slopes can be attributed to partial stomatal closure and decreased transpiration rate. The mean increase in ΔT for all UV treatments ranged 0.17 ± 0.05 to $0.88\pm0.07^\circ\text{C}$. This indicates that ΔT increases, resulting from UV-induced partial stomatal closure decreasing transpiration rate, corrected for the effect of radiative heating, can be calculated as follows:

$$\Delta T_{corrected} = \Delta T_{uncorrected} - \text{Radiative heating} \quad (3.2)$$

$$\Delta T_{corrected} = 0.17\pm0.05 \text{ to } 0.88\pm0.07^\circ\text{C} - 0.16\pm0.09^\circ\text{C}$$

$$\Delta T_{corrected} = 0.01\pm0.14 \text{ to } 0.72\pm0.16^\circ\text{C}$$

This results in corrected leaf warming, relative to air temperature (ΔT), of up to $0.72\pm0.16^\circ\text{C}$. These calculations dissect the individual effects of direct radiative heating from the UV source and partial stomatal closure on the ΔT increases. These increases were in response to a UV radiation range of 0.097 W m^{-2} (PGIAS) equal to a sunny midwinter day in Lancaster, UK, to 2.64 W m^{-2} (PGIAS) that is similar to the global maximum (based on PGIAS weighting), though both were applied over 90 minutes rather than a full day.

3.4 Discussion

It is inferred that the UV irradiance responses to the filtered UV treatments would have been equal to the unfiltered treatments because when comparing the difference between them, up to the maximum range of the filtered treatments (0.297 W m^{-2}

PGIAS), there was no statistical difference ($P>0.05$). Therefore, interpretation of the filtered UV irradiance responses will be considered the same as the response to the greater range of unfiltered UV treatments. Commercial supplemental UV lighting is unlikely to be filtered with cellulose acetate or another material. Thus including shorter wavelengths (280-293 nm) in the unfiltered UV treatments likely represents commercial supplemental UV lighting.

3.4.1 UV Radiation Increases Leaf Temperature

Irrespective of whether the UV treatments were filtered or unfiltered, PGIAS weighted UV radiation increased leaf temperature (ΔT) (Fig. 3.4). The maximum degree of individual leaf warming relative to air temperature (ΔT) possible in that specific radiative loading environment in the absence of UV radiation was 1.14°C (Fig. 3.12). The greatest ΔT increase attributable to UV-induced partial stomatal closure was 0.72°C . This is after direct radiative heating from the UV source is deducted ($0.16\pm 0.09^{\circ}\text{C}$: Section 3.3.8), which is also demonstrated by the Y-intercept of the leaf temperature response curve ($0.17\pm 0.03^{\circ}\text{C}$: Fig. 3.4) that is substantially greater than the response of control leaves ($-0.04\pm 0.07^{\circ}\text{C}$: Fig. 3.4). This demonstrates that UV radiation increased leaf temperature.

The leaf temperature increase of 0.72°C may appear small but was a significant proportion (63%) of the maximum possible in those climate cabinet conditions with limited radiation loading. However, it is considerably smaller than the leaf temperature increase upon UV exposure found in mountain grassland ($\sim 2^{\circ}\text{C}$: Novotná *et al.*, 2016) and the original reports from commercial growers in southern Turkey ($\sim 2^{\circ}\text{C}$: Williams *et al.*, 2020), where in both cases solar radiation (compared to artificial lamps) would provide greater radiation loading and therefore heat input to

leaves. In polytunnels around the Mediterranean, the ΔT increase would likely be considerably higher than observed in the climate cabinet for the same percentage decrease in transpiration rate due to the greater radiation loading, as observed by Williams *et al.*, (2020). The ΔT increase observed may be even greater where radiation loading is more intense.

3.4.2 Leaf Temperature Increased by UV-Induced Partial Stomatal Closure

The consistency of the UV irradiance responses of leaf temperature (increased; Fig. 3.4), transpiration rate (decreased; Fig. 3.5) and stomatal conductance (decreased; Fig. 3.6) indicate that stomatal closure was the main cause of increased leaf temperature. Partial stomatal closure can be inferred as the cause of reduced transpiration rate due to rapid (within 90 minutes) responses to UV application and the use of fully expanded leaves meaning stomatal development (decreases in density or index) could not have occurred.

UV-induced stomatal closure has been observed previously without investigating leaf temperature. Similarly, unfiltered acute UV radiation treatments of 30 and 60 minutes, applied for 9 consecutive days, significantly reduced stomatal conductance to 20% of control in quinoa, with both low and high background PAR (Reyes *et al.*, 2018). This greater stomatal response probably results from repeated daily treatments compared to a single day in this study. Stomatal conductance was halved in pea leaves over 14 hours (Noguès *et al.*, 1999) whereas a similar reduction was observed in this study (Fig. 3.6) by applying 4x the GPAS weighted UV irradiance over 90 minutes. This demonstrates the balance between UV irradiance and duration of application on UV-induced stomatal closure. However, stomatal conductance reduced only marginally less by a considerably lower irradiance in this study (Fig. 3.6), indicated by the one-

phase decay regression, demonstrating that lower irradiances have a proportionally greater effect on stomatal conductance in tomato than higher irradiances. A difference in the timescale of response to UV radiation is also apparent. When the UV irradiances were similar, two hours exposure scarcely affected stomatal conductance compared to control leaves in pea, with a stated lag time of 4.3 hours (Noguès *et al.*, 1999) but in this study UV radiation decreased stomatal conductance by almost half over 90 minutes (Fig. 3.6). This demonstrates a much faster response to UV radiation in tomato than pea.

It was highlighted already (Section 3.3.4) that the UV source contained PAR that it was not possible to filter. This resulted in the plants being irradiated not only with UV radiation but also additional PAR beyond that provided by the lighting of the climate cabinet. This would have counteracted UV-induced stomatal closure because two of the main components of PAR, red and blue light, both act as stimuli to open stomata (Shimazaki *et al.*, 2007). Additionally, an increase in PAR enhances photosynthesis that results in stomatal opening to facilitate greater conductance (Ballarè, 2014). Switching the UV source on provided both UV radiation that acted to partially close the stomata, and increased PAR that acted to open them. Thus the additional PAR reduced the apparent effects of UV radiation on stomatal closure.

3.4.3 UV Radiation Increases Instantaneous Water Use Efficiency (WUE_i)

WUE_i was enhanced because UV radiation substantially reduced transpiration rate but had relatively little effect on assimilation rate (Figs. 3.5, 3.7, 3.10). Regression analysis showed that transpiration rate explained 68-71% of the variation in WUE_i whereas assimilation rate accounted for only 7-8% (Fig. 3.11). Decreased transpiration rate restricts total water use but this does not benefit crop production if

stomatal closure limits CO₂ uptake and consequently photosynthesis. Enhancing instantaneous water use efficiency (*WUEi*) by increasing the ratio of assimilation rate to transpiration rate would be beneficial in arid environments where water is limited, such as those around the Mediterranean where protected cropping is ubiquitous.

Table 3.2: Summary of instantaneous water use efficiency (*WUEi*) responses to UV radiation in various crops. UV doses are weighted by the generalised plant action spectrum (GPAS: Caldwell, 1971; Caldwell *et al.*, 1986) or plant growth inhibition action spectrum (PGIAS, Flint & Caldwell, 2003).

<i>WUEi</i> Response	Crop Species	UV Dose (kJ m ⁻²)	UV Filter	Growth Environment	Reference
Decrease (<i>A</i> reduced proportionally more than <i>E</i>)	Spring wheat	13.1 (GPAS)	Cellulose acetate (blocking <280 nm)	Field	Zhao <i>et al.</i> , 2009
Decrease (<i>E</i> increased and <i>A</i> decreased)	Buckwheat	Unspecified (17% ozone depletion)	Cellulose diacetate (blocking <280 nm)	Outdoor pot trial	Gaberscik <i>et al.</i> , 2002
Cv. 1. Increase (<i>E</i> reduced) Cv. 2. Increase (<i>E</i> reduced) Cv. 3. Increase (<i>E</i> reduced more than <i>A</i>) Cv. 4. No change	Soybean (4x cultivars)	13.0 (GPAS)	Cellulose diacetate (blocking <290 nm)	Glasshouse	Gitz III <i>et al.</i> , 2005
Increase (<i>E</i> reduced substantially, <i>A</i> increased marginally)	Tomato	Up to 14.3 (PGIAS) / 13.8 (GPAS)	Cellulose acetate (blocking <293 nm)	Climate cabinet	This study (Fig. 11)

Previous work found variable responses of *WUEi* to UV radiation across different species (Tab. 3.2). However, none have been conducted in a controlled environment, on a timescale similar to this study or in tomato. Supplemental UV-B decreased *WUEi* in field-grown spring wheat even though total water use decreased, because photosynthesis reduced proportionally more (Zhao *et al.*, 2009: Tab. 3.2). An outdoor pot trial of buckwheat from July to October with supplemental UV-B filtered with cellulose diacetate also decreased *WUEi*, caused by increased transpiration rate and reduced photosynthesis (Gaberscik *et al.*, 2002: Tab. 3.2). Supplemental UV-B filtered with cellulose diacetate increased *WUEi* by up to 25% in 3 out of 4 soybean cultivars grown in a glasshouse for 5 weeks from seed (Gitz *et al.*, 2005: Tab. 3.2) compared to 57% in this study (Fig. 3.10). These reports identify varying *WUEi*

responses, but none occurred in a controlled environment, tomato or over a similarly short duration to this study.

It is important to highlight that the UV source in all cases also included additional PAR as well as the UV and infrared radiation discussed previously (Fig. 3.8). Switching on the UV radiation source increased PAR up to ~10% (increasing with greater UV irradiance), which can explain the increased assimilation rate (up to 9%) observed. However, WUE_i was predominantly increased by the transpiration reduction (68-71%; Fig. 3.11a,b) rather than increased assimilation rate (7-8%; Fig. 3.11c,d), so the increased assimilation rate caused by the additional PAR from the UV source was a relatively small component of increased WUE_i .

Additional PAR from the UV source may not be ideal when attempting to assess the effect of UV radiation on WUE_i , but likely reflects commercial cultivation of crops under supplemental UV lighting. With supplementary UV radiation the plant would also receive additional emitted PAR depending on the type of UV radiation source i.e. broadband or narrowband, and specific manufacturer. Therefore the occurrence of PAR in the UV source and subsequent increase in assimilation rate may mimic commercial practice.

3.4.4 The Effect of Shortwave UV-B Radiation on Photosynthesis

Shortwave UV-B radiation (280-293 nm) inhibited the increase in photosynthesis that should occur due to the enhanced output of PAR from the UV radiation source. As UV irradiance, and therefore PAR, intensified the increase in assimilation rate diminished (Fig. 3.7b), the opposite of the best fitting regression model for the filtered UV treatments (positive linear: $P=0.354$; Fig. 3.7b). This demonstrates that the increasing unfiltered UV (280-400 nm) irradiances inhibited the increase in

photosynthesis caused by the additional PAR emitted by the UV lamp, whereas increasing the filtered treatments (293-400 nm) appeared to have the opposite effect (Fig. 3.7b). Although the maximum and actual efficiency of photosystem-II was not assessed here, similar UV applications found photosynthetic electron transport was inhibited 1 day after 30 or 60 minute applications of daily unfiltered 1.69 W m^{-2} UV-B (Reyes *et al.*, 2018), which could explain the inhibition of assimilation rate increases in the current work (Fig. 3.7b). Shortwave UV-B radiation (280-293 nm) inhibits assimilation rate, which should be investigated further by applying unfiltered UV radiation to horticultural crops in protected cultivation.

3.4.5 Interpreting the UV Irradiance Responses

Interpretation of a linear regression model is different to a non-linear one-phase model at the upper and lower ends of the UV irradiance scale. A linear relationship would indicate that the higher UV irradiances applied in this work would cause greater stomatal closure than observed, to the point that it would probably be detrimental to CO_2 uptake and photosynthesis, but in the one-phase relationship it would not. The nature of the non-linear one-phase stomatal (conductance and transpiration rate), leaf temperature and WUE_i responses (Figs. 3.4-3.6, 3.10) indicate that lower UV irradiances have proportionally greater effect on crop physiology than higher irradiances. This means closure would not be proportional to UV irradiance thus the effect on stomata gradually plateaux to the point that any increase in irradiance has no further effect. The difference in the mean leaf temperature increases at the highest irradiances ($1.12\text{-}2.64 \text{ W m}^{-2}$ PGIAS) was relatively small, due to the plateaux of this relationship.

The biological spectral weighting function (BSWF) used to weight UV irradiances affects the interpretation of these results in terms of their global relevance. When weighted by the PGIAS, the irradiance at which responses plateau (1.12 W m^{-2}) is close to the global maximum, while the maximum irradiance in this study (2.64 W m^{-2} PGIAS) is approximately double the global maximum (Fig. 1.4). When weighted by the GPAS the irradiance at which responses plateau (1.08 W m^{-2}) is almost 3x the global maximum and 2.55 W m^{-2} is $\sim 7x$ greater (Fig. 1.4), clearly demonstrating the difference in the BSWFs because of the inclusion of UV-A in the PGIAS and how this affects interpretation of the UV irradiances applied.

The one-phase association UV irradiance responses demonstrate that short acute UV irradiance applications (UV doses when the timescale of application is considered with irradiance) could be very effective at increasing leaf temperature and WUE_i in horticulture. The mechanism causing stomatal closure is initiated at very low irradiances. This is particularly important in terms of applying UV radiation to crops in protected cultivation such as glasshouses and plant factories where excessive UV radiation can adversely affect photosynthesis (Allen *et al.*, 1997, 1998), particularly if lamps are unfiltered (observed in this study; Reyes *et al.*, 2018). UV lights may be broadband fluorescent lamps, that have been available for some time, or rapidly developing narrowband light emitting diodes (LEDs) that may provide a more targeted approach to light manipulation dependent of specific plant process (Wargent, 2016; Huche-Thelier *et al.*, 2016). Supplemental UV lighting can operate on a rail system designed to ensure only periodic application, moderating doses to be low enough to avoid adverse effects but sufficient to control plant size (Innes *et al.*, 2018; Jenkins *et al.*, 2009), enhance factors such as fruit pigmentation and flavour (Paul *et al.*, 2005) and nutritional quality (Neugart and Schreiner, 2018), reduce pesticide

residue (Weber *et al.*, 2009a,b) or inhibit pests (Caldwell *et al.*, 2007) and disease (Demkura and Ballarè, 2012). Indeed, sustained increases of moderate UV radiation can affect plant growth more than short acute applications of higher doses (Suchar and Robberecht, 2015). These data indicate that short acute UV irradiance / dose application would be sufficient to partially close stomata thus increasing leaf temperature and WUE_i , both desirable physiological responses in protected cultivation when attempting to increase resource use efficiency in terms of water use and reducing the time required for a cropping cycle while minimising energy costs.

3.5 Conclusions

UV radiation increased leaf temperature (ΔT) up to 0.7°C after air temperature fluctuations and direct radiative heating from the UV source were taken into account. This was caused by reduced transpiration rate. UV-induced partial stomatal closure was inferred since short (90 minutes) treatments were applied to fully expanded leaves. The combination of reduced transpiration rate and relatively unaffected photosynthesis increased WUE_i . The unavoidable inclusion of PAR within the UV source was shown to have had a far smaller effect on WUE_i than reduced transpiration rate that resulted from the UV-induced stomatal closure. Unfiltered UV radiation inhibited any increase in assimilation rate, which may affect crop development over a longer timescale. The non-linear UV irradiance responses indicates that acute applications of low to moderate UV radiation may benefit protected crop production by partially closing the stomata, thereby increasing leaf temperature, plant development and WUE_i , which would be highly beneficial in commercial crop cultivation utilising supplemental UV lighting. Further work will assess this response over a longer timescale (multiple days) in a controlled environment setting (Chapter 4) in addition to work in polytunnels planned in Lancaster (UK; Chapter 5) and Antalya

(Turkey; Chapter 6) which will elucidate the effect of solar UV radiation on assimilation rate and WUE_i over a longer timescale.

4 Leaf Temperature and Gas Exchange Responses to Ultraviolet Radiation in a Controlled Environment

4.1 Introduction

The UV irradiance responses (Chapter 3) demonstrate that 90 minute exposure increases leaf temperature and instantaneous water use efficiency non-linearly. The non-linearity of the UV irradiance responses mean that lower irradiances have a proportionally greater effect than higher irradiances. It was concluded that partial stomatal closure was the cause. Despite the lack of work addressing UV radiation effects on leaf temperature, UV-induced stomatal closure has been reported many times (e.g. Kakani *et al.*, 2003b; Tab. 1.2). Only one previous study has reported that exposure to solar UV radiation leads to an increase in leaf temperature, albeit not statistically significant, and inferred partial stomatal closure as the mechanism (Novotná *et al.*, 2016; Tab. 1.2). The reports of reduced stomatal conductance in response to UV radiation have resulted in the effect of UV radiation on WUE_i also

being investigated previously, but to a lesser extent, with variable responses across different species in different experimental conditions reported (e.g. Teramura *et al.*, 1990, Gitz III *et al.*, 2005).

This chapter acts as a bridge between experiments conducted in the tightly controlled environment conditions of the climate cabinet (Chapter 3) and those conducted in uncontrolled polytunnel structures (Chapters 5-6). This is achieved by linking the fundamental science of the leaf physiological responses to a range of acute UV radiation treatments in a climate cabinet (Chapter 3) to the multi-day experiments conducted under wavelength attenuated solar radiation in the UK (Chapter 5), and in particular Turkey (Chapter 6), an important location for protected cultivation crop production. The ‘bridge’ is provided by a controlled environment setting, that avoided the natural variability of field conditions, but allowed treatments to be extended to the 6-day experimental duration used in the polytunnel experiments in the field. The controlled environment used in this chapter was considerably larger than the climate cabinet employed for the leaf physiological UV irradiance responses, providing the space required to experiment with multiple plants simultaneously, negating the need for a high throughput system of individual plants that would otherwise be impossible for investigation of the longer term responses. The facility provided the ability to apply UV-A and UV-B simultaneously as a combined treatment.

In the programmes of experiments described in this chapter it was hypothesised that UV radiation causes partial stomatal closure that reduces stomatal conductance and transpiration rate resulting in increased leaf temperature (relative to air temperature). The hypothesis was tested by investigating the stomatal and leaf temperature responses of individual tomato leaves in plants subjected to a combined UV-B and

UV-A radiation treatment, weighted by BSWFs to mimic solar radiation, over 6 days. It was also hypothesised, based on previous work (Chapter 3), that leaf photosynthesis would not be affected by UV radiation thus increasing instantaneous water use efficiency through the reduction in transpiration rate.

4.2 Material and Methods

4.2.1 Plant Material

Three separate experiments of 6 days duration were conducted. In each case tomato (*Solanum lycopersicum* cv. 'Money Maker') plants were propagated in the absence of UV-B radiation in a glasshouse at the Lancaster Environment Centre (Section 2.1). At the 4-leaf stage (after ~4 weeks of growth from seed), the twenty most uniform plants were selected and transferred to the controlled environment (CE) room. After 2 days acclimation to the CE room conditions in the absence of UV radiation, 12 uniform plants were selected for treatment. These were divided in two (6 plants for each UV treatment regime for each repeat experiment), based on their physiological properties (leaf temperature, transpiration rate, stomatal conductance, assimilation rate and instantaneous water use efficiency) to eliminate any differences prior to UV radiation application and ensure any subsequent differences were the result of UV radiation and not pre-treatment physiology. A leaflet from the most recent fully developed leaf pair on the 3rd internode was used for the experiments. Plant positions on the bench were rotated daily to eliminate any effect of small variations in radiation caused by position, each plant spending 24 hours in each of 6 positions, undertaken within both UV treatment regimes.

4.2.2 UV Treatments

The experiments were conducted in a specially designed controlled environment (CE) room at the Lancaster Environment Centre (LEC), Lancaster, UK. The CE room maintained temperature at $25\pm 2^{\circ}\text{C}/16\pm 2^{\circ}\text{C}$ (day/night) with air conditioning (Airedale Mistral DX, Airedale International, Leeds, UK) controlled by Hortisystems central computer (Hortisystems UK Ltd, Pulborough, UK). Plants were positioned on a bench with artificial lighting 0.65 m above. Photosynthetically active radiation (PAR) of $450\ \mu\text{mol m}^{-2}\ \text{s}^{-1}$ was provided by light emitting diodes (LEDs: B100 and B150, Valoya, Helsinki, Finland) for a 16-h photoperiod. The LEDs produce no UV-A which contrasts with other PAR sources widely used in the past, including fluorescent tubes and metal halide discharge lamps. Thus all UV radiation (UV-A and UV-B) was provided by specific UV sources.

There were two UV radiation treatments: UV+ and UV-. For the UV+ treatment UV radiation of $17.8/13.0\ \text{kJ m}^{-2}\ \text{d}^{-1}$ (PGIAS/GPAS weighted) was applied for a 14-h photoperiod with separate fluorescent tubes (UV-A: Q-Lab UVA-340; UV-B: Q-Lab UVB-313 EL, Q-Panel Lab Products, Cleveland, USA; Fig. 4.1). The bench was divided in two, separated by UV-opaque plastic film (UV-O; Lightworks Sun Master: Arid Agritec, Lancaster, UK) that transmits 2.2% UV radiation. Equal lighting (PAR, UV-A and UV-B) was positioned above each half of the bench. Positioned between the artificial lighting and plants were wavelength selective filters to manipulate the UV regime on each bench half. The UV-opaque plastic was used to create the UV-exclusive environment (UV-). UV-transparent plastic (UV-T; Lightworks Sun Smart, Arid Agritec, Lancaster, UK) was used in the UV-inclusive (UV+) side to mimic the effect of the UV-O plastic on the UV-exclusive side, with the addition of cellulose acetate to block wavelengths $<293\ \text{nm}$, to mimic sunlight as closely as possible.

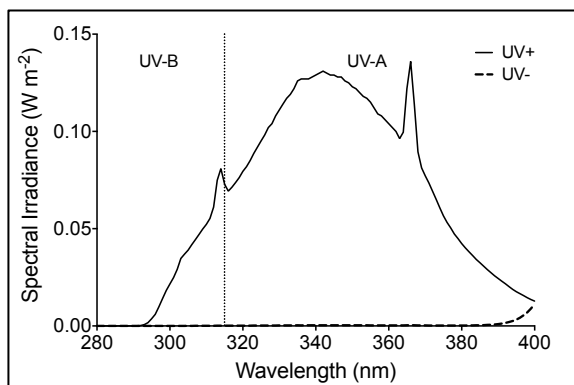


Figure 4.1: Ultraviolet spectral irradiance (280-400 nm) of the UV-inclusive (UV+: solid line) and UV-exclusive (UV-: dashed line) treatments provided by the Q-Lab UVA340 and UVB313 EL fluorescent tubes. The wavelength ranges of UV-A and UV-B are separated by the vertical dotted line.

UV radiation was quantified with a Spectroradiometer (model SR9910-V7) that provided the spectral transmission (260-700 nm) of each source (Section 2.2; Fig. 4.1). UV treatments are expressed unweighted, and weighted by the PGIAS and GPAS biological spectral weighting functions (Section 2.5; Tab. 4.1)

Table 4.1: Daily irradiances and doses applicable to the UV-inclusive (UV+) and UV-exclusive (UV-) treatment regimes. UV is weighted by generalised plant action spectrum (GPAS; Caldwell, 1971; Caldwell *et al.*, 1986) and the plant growth inhibition action spectrum (PGIAS; Flint and Caldwell, 2003).

UV Regime	Unweighted Irradiance 280-400 nm (W m ⁻²)	GPAS Irradiance 280-400 nm (W m ⁻²)	PGIAS Irradiance 280-400 nm (W m ⁻²)	Unweighted Dose 280-400 nm (kJ m ⁻²)	GPAS Weighted UV Dose (kJ m ⁻² d ⁻¹)	PGIAS Weighted UV Dose (kJ m ⁻² d ⁻¹)
UV+	6.87	0.258	0.354	346.2	13.0	17.8
UV-	0.068	0.001	0.002	3.4	0.0	0.1

4.2.3 Leaf Gas Exchange and Temperature Measurements

Leaf gas exchange and temperature measurements were made using a LI-6400XT (LI-COR Inc., Lincoln, NE, USA). The LI-6400XT light emitting diode (LED) cuvette attachment provided the specified PAR (1600 μmol m⁻² s⁻¹), without any UV radiation, to the experimental leaf enclosed inside. Using the LED attachment avoided any effect of spatial variations in temperature, or differences in radiation loading, inside the CE room on leaf temperature measurements that could occur if not using a

cuvette for air temperature control, or LED for radiation, respectively. Once a leaf was enclosed inside the cuvette, the internal environment (cuvette block temperature: 26°C, relative humidity: 45-55%, CO₂: 400 ppm, flow rate: 500 μmol s⁻¹) was allowed to stabilise (1-2 minutes) before data was recorded. These settings were selected because they closely matched the conditions inside the CE room. All leaf gas exchange measurements were centred around the middle of the photoperiod to minimise diurnal stomatal effects on the results.

4.2.4 Data analysis

The results are presented as the absolute post-UV treatment values for each parameter, except leaf temperature where the absolute change in $T_{leaf}-T_{air}$ was used to take account of any variations in air temperature that could swamp the small leaf temperature changes expected based on the climate cabinet experiments (Chapter 3). For each repeat experiment the day zero data was obtained prior to UV exposure. UV radiation was switched on immediately afterwards, meaning day one data was obtained 24 hours after the treatments had begun, and so on. Three separate experiments were conducted, the combined results of all three are presented as the results (Section 4.3) and the three individual experiments are presented as an appendix (Appendix 1).

4.2.5 Statistical Analysis

The three repeat experiments of 6-day duration were tested for normal distribution and equal variances in SPSS version 18 (SPSS Inc., Chicago, USA). These data were statistically analysed for differences between the UV treatments (UV+ / UV-) using a repeated measures ANOVA in SPSS, with UV treatment and experiment as the main factors, and day as the repeated measure. The experiments were analysed as a

combined data set initially but where there was an interaction between experiment and UV treatment e.g. for assimilation rate, the experiments were also analysed individually. To determine daily differences between UV radiation treatments, unpaired t-tests were performed for each day (corrected for multiple comparisons) using the Sidak-Bonferroni method, in GraphPad Prism version 7.0d for Mac OS X (GraphPad Software, La Jolla California USA, www.graphpad.com). An unpaired two-tailed t-test was performed to analyse whether the increases in leaf temperature observed in the climate cabinet (Chapter 3) and this study (Section 4.4.1) in response to comparable UV irradiances were significantly different, in GraphPad Prism.

4.3 Results

Analysis of the combined data (Experiments 1, 2 and 3) shows that although each leaf physiological parameter varied significantly between experiments ($P < 0.001$ for each parameter; Tab. 4.2) the treatment response was consistent across all three experiments for all parameters (treatment x experiment: $P > 0.05$; Tab. 4.2) except assimilation rate (treatment x experiment: $P = 0.025$; Tab. 4.2). Thus, the data were pooled across all three experiments for analysis except for assimilation rate, for which each experiment is analysed separately. The results of the three individual experiments are included as an appendix (Appendix 1).

When data were pooled across all three experiments UV radiation significantly ($P < 0.001$; Tab. 4.2) increased leaf temperature ($T_{leaf} - T_{air}$) compared to control leaves (UV-), by up to 0.23°C (Day 1; Fig. 4.2a). Leaf temperature ($T_{leaf} - T_{air}$) varied between days ($P = 0.003$; Tab. 4.2) but treatment differences were not affected by this (treatment x day: $P = 0.140$; Tab. 4.2). This daily variation in leaf temperature ($T_{leaf} - T_{air}$) was not consistent across each experiment (experiment x day: $P < 0.001$; Tab. 4.2),

it varied $<0.8^{\circ}\text{C}$ within each 6 day experiment, likely due to small differences in transpiration rate. There was also no interaction between day, experiment and treatment ($P=0.428$; Tab. 4.2). This demonstrates that UV radiation significantly enhanced leaf temperature ($T_{leaf} - T_{air}$) regardless of the effect that individual experiments and days had on the magnitude of response.

Table 4.2: Summary of P values for each factor and factor interaction from the repeated measures ANOVA analysis for each leaf physiological parameter measured.

ANOVA Factors	$T_{leaf} - T_{air}$	E	g_s	A	WUE_i	C_i
Experiment	$<0.001^{***}$	$<0.001^{***}$	$<0.001^{***}$	$<0.001^{***}$	$<0.001^{***}$	$<0.001^{***}$
Treatment	0.007**	0.002**	0.008**	$<0.001^{***}$	0.541	0.812
Day	0.003**	$<0.001^{***}$	$<0.001^{***}$	$<0.001^{***}$	$<0.001^{***}$	$<0.001^{***}$
Treatment x Experiment	0.489	0.684	0.804	0.025*	0.773	0.488
Treatment x Day	0.140	$<0.001^{***}$	$<0.001^{***}$	$<0.001^{***}$	0.032*	0.003**
Experiment x Day	$<0.001^{***}$	$<0.001^{***}$	$<0.001^{***}$	$<0.001^{***}$	$<0.001^{***}$	<0.001
Day x Experiment x Treatment	0.428	0.083	0.159	0.066	0.264	0.164

The leaf temperature difference observed above was associated with significantly ($P=0.008$; Tab. 4.2) reduced stomatal conductance and transpiration rate ($P=0.002$; Tab. 4.2) in the presence of UV radiation. Stomatal conductance and transpiration rate were up to $118 \text{ mmol m}^{-2} \text{ s}^{-1}$ and $0.85 \text{ mmol m}^{-2} \text{ s}^{-1}$ lower respectively (Day 1; Fig. 4.2b,c). Both parameters varied significantly between days ($P<0.001$ for each; Tab. 4.2) and this interacted with the treatment effect (treatment x day: $P<0.001$ for each; Tab. 4.2), with small fluctuations in the magnitude of response from day to day (Fig. 4.2bc). This was most evident after 1 day of UV radiation exposure (Fig. 4.2), thereafter the fluctuations were small (g_s : Days 2-6 = $<15\%$ change; E : Days 2-6 = $<6\%$ change). These daily fluctuations were inconsistent between experiments (experiment x day: $P<0.001$ for each; Tab. 4.2). There was also no interaction between day, experiment and treatment ($P>0.05$ for each; Tab. 4.2). UV radiation reduced

stomatal conductance and transpiration rate even though their values fluctuated daily, interacting with the magnitude of treatment response.

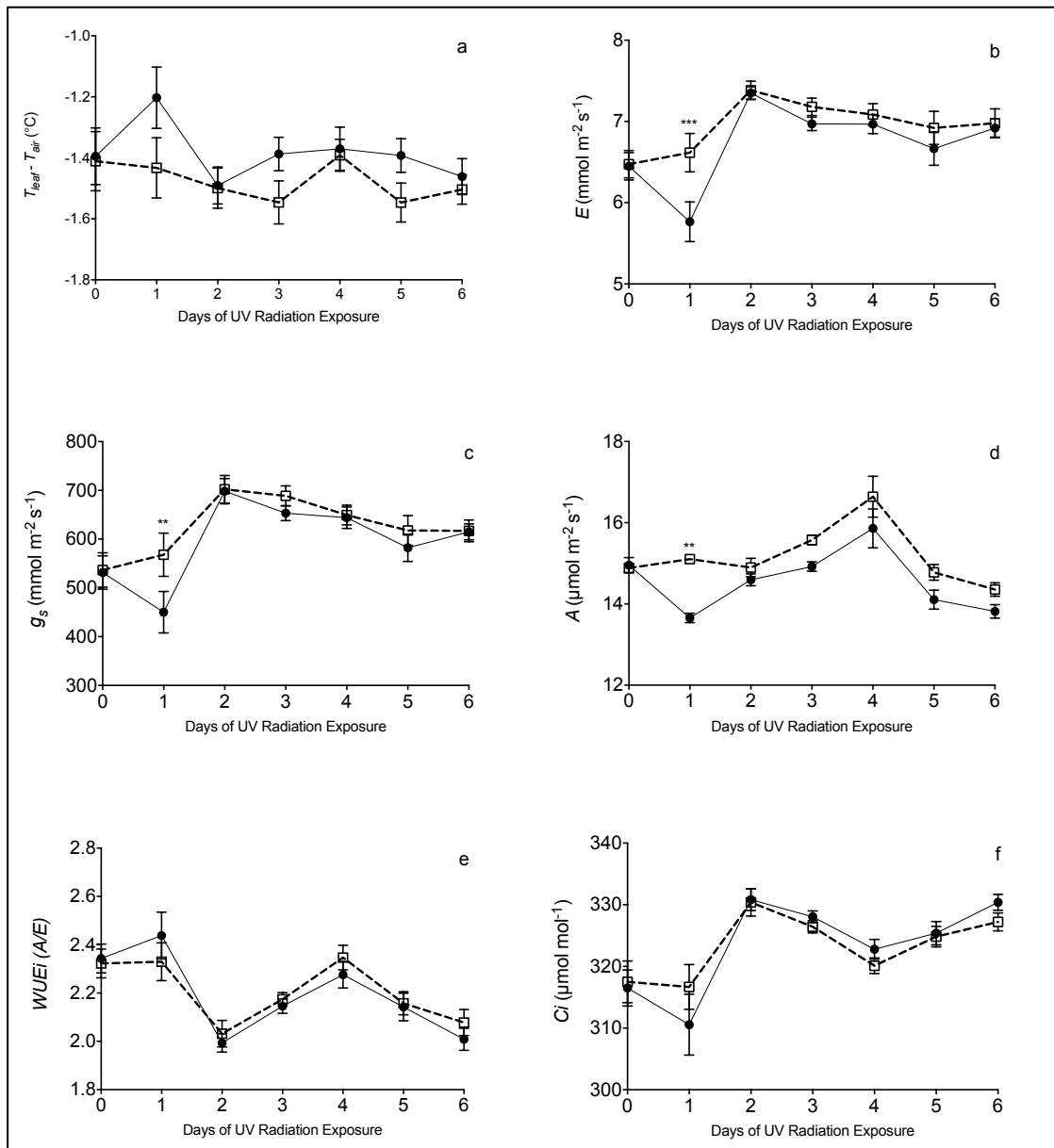


Figure 4.2: The response to UV+ (closed circles and solid line) and UV- (open squares and dashed line) of (a) leaf temperature ($T_{leaf} - T_{air}$), (b) transpiration rate (E), (c) stomatal conductance (g_s), (d) assimilation rate (A), (e) instantaneous water use efficiency (WUE_i), and (f) intracellular CO_2 (C_i) when all three experiments were combined and analysed together. The asterisks represent individual days where there was a significant difference between treatments (**: $P < 0.01$; ***: $P < 0.001$) corrected for multiple t-tests. CE room and cuvette temperature were 26°C during measurements. Each symbol is the mean of 18 leaves ($n=18$). Error bars represent ± 1 SE but if not visible they were smaller than the symbol. See Table 4.2 for full statistical analysis.

Pooled analysis of assimilation rate showed significant ($P < 0.001$; Tab. 4.2) differences between experiments, causing the effect of UV treatment to also vary

between experiments (treatment x experiment: $P=0.025$; Tab. 4.2). This appears to be caused by the magnitude of treatment response, which was greater in Experiment 1 than 2, both of which were greater than Experiment 3 (Fig. 4.3). Analysing the experiments individually revealed a significant effect of UV treatment ($P<0.027$ for each experiment; Tab. 4.2), assimilation rate was up to $1.22\text{-}1.58\ \mu\text{mol m}^{-2}\text{s}^{-1}$ lower in response to UV+ across the three experiments (Day 1; Fig. 4.3). Assimilation rate significantly varied between days ($P<0.001$ in each experiment; Tab. 4.2), which affected the treatment response (treatment x day: $P<0.05$ for each experiment; Tab. 4.2), meaning the response to UV radiation was more apparent on some days than others. This is evident as small fluctuations from day to day, with the treatment effect appearing greater on some days than others (Fig. 4.3). The variation between days was not consistent across each experiment (experiment x day: $P<0.001$; Tab. 4.2). There was also no interaction between day, experiment and treatment ($P=0.066$; Tab. 4.2). Thus UV radiation significantly reduced assimilation rate, but the magnitude of the response varied daily and with experiment.

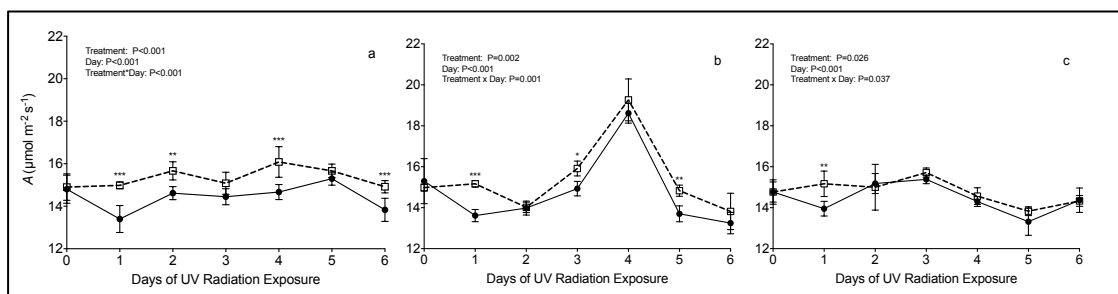


Figure 4.3: The assimilation rate response to UV+ (closed circles and solid line) and UV- (open squares and dashed line) radiation treatments for (a) experiment 1, (b) experiment 2, and (c) experiment 3. The asterisks represent individual days where there was a significant difference between treatments (**: $P<0.01$; ***: $P<0.001$) corrected for multiple t-tests. CE room and cuvette temperature were 26°C during measurements. Each symbol is the mean of 6 leaves ($n=6$). Error bars represent ± 1 SE but if not visible they were smaller than the symbol.

The concurrent reductions in transpiration rate and assimilation rate resulted in no significant effect of UV radiation treatment on WUE_i ($P=0.541$; Tab. 4.2; Fig. 4.3).

Although not significant, the greatest treatment difference occurred on day 1 (0.11 $\mu\text{mol CO}_2 / \text{mol}^{-1} \text{H}_2\text{O}$; Fig. 4.3). WUE_i varied between days ($P < 0.001$; Tab. 4.2), which affected the differences observed between treatments (treatment x day: $P = 0.032$; Tab. 4.2), with very small fluctuations from day to day. However, these daily fluctuations were inconsistent across the three experiments (experiment x day: $P < 0.001$; Tab. 4.2). There was also no interaction between day, experiment and treatment ($P = 0.066$; Tab. 4.2). Thus UV radiation did not affect WUE_i because transpiration and assimilation rate reduced proportionally.

Similar results were observed for intracellular CO_2 (C_i), pooled across the three experiments, with no significant effect of UV treatment ($P = 0.812$; Tab. 4.2; Fig. 4.2) although the greatest difference between treatments was observed on day 1 (Fig. 4.2). Again, there was variation between days in C_i ($P = 0.003$; Tab. 4.2) and this clearly affected the difference between treatments (treatment x day: $P < 0.001$; Tab. 4.2) where the weak response reversed over the course of the week. However, this was not consistent across the three experiments (experiment x day: $P < 0.001$; Tab. 4.2). There was no interaction between day, experiment and treatment ($P = 0.164$; Tab. 4.2). There was no consistent UV radiation effect on C_i .

Linear regression analysis of leaf temperature ($T_{\text{leaf}} - T_{\text{air}}$) for each treatment was undertaken to determine whether leaf warming unrelated to reduced transpiration rate occurred while measuring leaf temperature (Fig. 4.4). Radiative heating differences between treatments was not hypothesised to have occurred because the method used meant that there should be no differences in total radiation for each treatment at the time of leaf temperature measurements. For both treatments the leaf was enclosed within the gas exchange analyser cuvette, set up with identical environmental

conditions and PAR. The analysis shows that there was no significant difference between the slopes of the treatments ($P=0.923$; Fig. 4.4) or significant vertical displacement of the Y intercepts ($P=0.777$; Fig. 4.4) demonstrating that no significant radiative heating occurred.

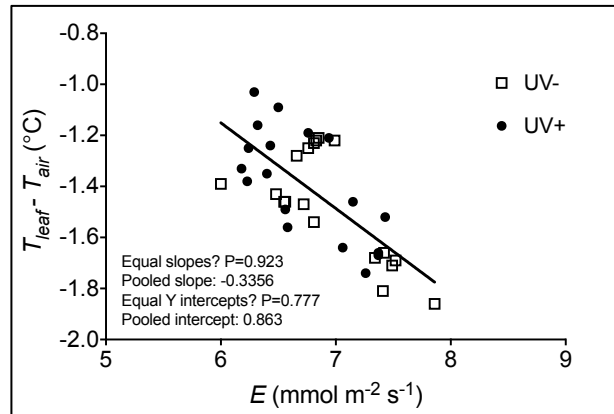


Figure 4.4: Linear regression analysis (summarised) of radiative heating for the three experiments combined. This demonstrates that the slopes and Y intercepts of each treatment were not significantly different meaning there was no significant radiative heating in the UV+ treatment compared to the UV- treatment during measurement. The pooled linear regression is highlighted (solid line). CE room and cuvette temperature were 26°C during measurements. Each symbol is the mean of 18 leaves ($n=18$).

4.4 Discussion

4.4.1 UV Radiation Increases Leaf Temperature by Reducing Transpiration Rate

UV radiation significantly increased leaf temperature ($T_{leaf} - T_{air}$) over 6 days by decreasing transpiration rate, even though there were significant differences in this response between the three experiments (Section 4.6). The increase ($0.23 \pm 0.10^{\circ}\text{C}$) was less than at a comparable UV irradiance in the climate cabinet (0.297 W m^{-2} : $0.52 \pm 0.08^{\circ}\text{C}$; Chapter 3). It was also much lower than reported in a field study of mountain grass in the Czech Republic ($\sim 2^{\circ}\text{C}$: Novotná *et al.*, 2016; Chapter 1) and the original reports from commercial growers in southern Turkey (1.9°C : Williams *et al.*, 2020). As discussed below, these leaf temperature responses could be explained by a difference in the UV radiation (irradiance and dose) the plants were exposed to which

affects the magnitude of stomatal closure and transpiration rate reduction, and/or the total radiation loading in the different environment / locations.

The differences in leaf temperature increases observed in the controlled environments (Chapters 3 and 4), under solar conditions in the Czech Republic ($\sim 2^{\circ}\text{C}$: Novotná *et al.*, 2016; Chapter 1) and in southern Turkey (1.9°C : Williams *et al.*, 2020) partly reflect the UV irradiance / dose applied. The irradiances applied in the comparable climate cabinet (Chapter 3) and CE room work (Section 4.4.1) were $\sim 0.3 \text{ W m}^{-2}$ (whether weighted by PGIAS or GPAS). In the field in the Czech Republic (July) and in Turkey (June) the UV irradiances would be considerably higher, possibly triple according to modelling of UV irradiance (Atmospheric Chemistry Observations & Modeling 2019), even after plastic UV radiation transmission is taken into account. Based on work conducted already (Chapter 3) a tripling of the UV irradiance would enhance partial stomatal closure and therefore leaf temperature increase. However comparison between the field and laboratory results is dependent on which biological spectral weighting function (BSWF) is used to weight the UV irradiance. The irradiances of $\sim 0.3 \text{ W m}^{-2}$ equates to $\sim 25\%$ of ambient maximum (PGIAS) or $\sim 80\%$ (GPAS), so the BSWF determines whether irradiances of $\sim 0.3 \text{ W m}^{-2}$ are deemed low or high, and whether they are comparable with ambient maximums in the field (if GPAS weighted) or not (if PGIAS weighted). Therefore comparison of the artificial UV irradiances applied (Chapters 3 and 4) with those under solar radiation conditions are dependent on which BSWF is most accurate.

Radiation loading is determined by the net balance of downwelling and upwelling UV, PAR and infrared radiation (Section 1.3), affected by the different locations and environments. Under solar conditions in the field the net radiation loading would be

greater than was present within the LI-6400XT cuvette under the LED attachment, which can explain the large difference in those leaf temperature responses. The leaf temperature differences observed between the climate cabinet (Section 3.4.1) and the CE room (Section 4.4.1) can be explained by differences in radiation loading. Direct radiative heating in the climate cabinet was quantified as $0.16 \pm 0.09^\circ\text{C}$ (Section 3.4.7). This was caused by the UV radiation source, which was only switched on 15 minutes after continuous data logging began (to allow leaf gas exchange to stabilise inside the cuvette prior to UV application). Control leaves were not subjected to UV radiation and therefore radiative heating from the UV source (Section 3.3.3). In this chapter, direct radiative heating did not occur because leaf temperature data was derived with equal radiation conditions inside the LI-6400XT cuvette during measurements. Deducting the direct radiative heating effect from the leaf temperature increase in the climate cabinet for the most comparable UV irradiance treatment (0.297 W m^{-2}) gives the leaf warming relating to partial stomatal closure alone as:

$$\Delta T_{corrected} = \Delta T_{uncorrected} - \text{Radiative heating} \quad (4.1)$$

$$\Delta T_{corrected} = 0.52 \pm 0.08^\circ\text{C} - 0.16 \pm 0.09^\circ\text{C}$$

$$\Delta T_{corrected} = 0.36 \pm 0.17^\circ\text{C}.$$

This results in a negligible difference between the climate cabinet ($0.36 \pm 0.17^\circ\text{C}$: Section 3.4.1) and the CE room ($0.23 \pm 0.10^\circ\text{C}$: Fig. 4.2), confirmed by an unpaired t-test ($P=0.495$). This demonstrates that comparable UV irradiances in different types of experiment induced a similar leaf temperature increase.

In response to the most comparable UV irradiance ($\sim 0.3 \text{ W m}^{-2}$), transpiration decreased by $0.92 \pm 0.11 \text{ mmol m}^{-2} \text{ s}^{-1}$ (17%) in the climate cabinet and in the CE room

it reduced by $0.85 \pm 0.25 \text{ mmol m}^{-2} \text{ s}^{-1}$ (13%; Fig. 4.2). These comparable reductions are reflected in the similar leaf temperature responses identified above, after radiative heating that occurred in the climate cabinet experiments was deducted. Comparing these transpiration rate or stomatal conductance responses with the field experiment in the Czech Republic (Novotná *et al.*, 2016) is not possible because these parameters were not measured directly; a reduction in the latter was inferred (Novotná *et al.*, 2016). Similarly, the reports from growers in southern Turkey only referenced leaf temperature (Williams *et al.*, 2020).

4.4.2 UV Radiation Causes Partial Stomatal Closure

UV radiation significantly decreased stomatal conductance, thereby decreasing transpiration rate. Since experiments were conducted on fully expanded tomato leaves, and on a time scale that meant changes in cell, epicuticular wax and stomatal development (density and index) could not have occurred, partial stomatal closure is inferred as the cause. This is consistent with the general consensus of UV-induced stomatal conductance reduction (Kakani *et al.*, 2003b; Tab. 1.2), demonstrating UV radiation can cause partial stomatal closure.

Treatment differences in stomatal and leaf temperature responses fluctuated from day to day. ANOVA of the combined experiments showed that that a significant daily fluctuation in stomatal conductance and transpiration rate significantly interacted with the effect of the UV treatments (Tab. 4.2), causing the difference between the treatments to fluctuate from day to day (Fig. 4.2). Fluctuations have occurred previously in mature pea leaves that were either previously unexposed or cultivated from seed in the presence of UV radiation (Noguès *et al.*, 1998, 1999). In previously exposed pea leaves subjected to a similar UV irradiance to this study (Tab. 4.1), but

with a concurrent UV- treatment, the difference between treatments was clear on some days but not on others, even reversing at times, between days 21-30 of UV treatment (Noguès *et al.*, 1999). In that study, and this one, these fluctuations were sometimes daily but at other times occurred over multiple days, with little consistency in the periodicity (Fig. 4.2). In a similar experiment on previously exposed pea plants large variations in stomatal conductance over multiple days also occurred in response to the same UV radiation treatment (Noguès *et al.*, 1998). This demonstrates a fluctuating stomatal response of pea and tomato plants to UV radiation but the cause of this is unknown.

4.4.3 Greatest Response to UV Radiation Observed After 24 Hours

The greatest difference between treatments for all measured parameters occurred on day 1, after 24 hours UV exposure (Fig. 4.2). This is particularly clear for leaf temperature, stomatal conductance, transpiration rate and assimilation rate. It is probably a result of using plants that were previously unexposed to UV radiation, having greater sensitivity due to lack of acclimation, being suddenly subjected to a relatively high dose that would be similar to the maximum globally. It is apparent that the response lessened in the following days, probably due to acclimation of the plants to the UV environment (Fig. 4.2). A similar experiment that applied double the UV radiation to previously unexposed pea leaves produced a particularly large stomatal conductance reduction (>50%) after 24 hours, compared to 15% in this study (Fig. 4.2) with a subsequent lessening of the reduction over the following 4 days (Noguès *et al.*, 1999). There is very little other work on the UV response of leaves over the course of hours and days. The UV response of previously unexposed pea and tomato plants appears to be greatest after 24 hours exposure.

4.4.4 No Effect of UV Radiation on Instantaneous Water Use Efficiency

Transpiration rate and assimilation rate reduced proportionally resulting in no significant difference in WUE_i between treatments. It was hypothesised, based on the results obtained from the climate cabinet irradiance response work (Chapter 3), that WUE_i would increase because UV radiation would decrease transpiration rate without changing assimilation rate. However, assimilation rate was significantly reduced by UV radiation resulting in WUE_i not changing significantly. Only two previous studies reported no effect on WUE_i (Shumaker *et al.*, 1997; Gitz III *et al.*, 2005). Within polytunnel-like structures covered in either cellulose diacetate (UV+) and polyester (UV-) films during June to August, UV radiation decreased the transpiration rate, stomatal conductance and assimilation rate of immature and mature leaves of poplar cuttings (Shumaker *et al.*, 1997). In the other study, supplemental UV-B radiation did not affect either transpiration rate or assimilation rate in one of four cultivars of soybean grown in a glasshouse for 28 days (Gitz III *et al.*, 2005). In three other soybean cultivars, WUE_i increased, mainly caused by reduced transpiration rate rather than changes in assimilation rate (Gitz III *et al.*, 2005). UV radiation also decreased WUE_i , in spring wheat where assimilation rate reduced proportionally more than transpiration rate (Zhao *et al.*, 2009) and in buckwheat where transpiration rate increased while assimilation rate decreased (Gaberscik *et al.*, 2002). This suggests great variation between crop species and even within different cultivars of the same species, however none was conducted in controlled environment conditions. However, the experiments conducted in different controlled environments over different timescales in this thesis so far have shown similar variability in WUE_i responses.

4.5 Conclusions

A combined UV radiation treatment incorporating UV-A and UV-B increased leaf temperature ($T_{leaf} - T_{air}$) by decreasing stomatal conductance and transpiration rate, which corroborates the responses observed in the climate cabinet experiments (Chapter 3). There was no apparent change in WUE_i because photosynthesis and transpiration rate reduced proportionally, in contrast to the increases that occurred in the climate cabinet experiments (Chapter 3). This was caused by a decrease in assimilation rate that was not observed in the climate cabinet, possibly due to the difference in UV exposure duration. In these tomato plants that had not been exposed to UV radiation previously, stomatal sensitivity to UV was greatest within the first 24 h with partial recovery thereafter. This demonstrates that UV radiation induces partial stomatal closure that increases leaf temperature but does not affect WUE_i . It is therefore expected that leaf temperature and WUE_i will respond similarly in field experiments of the same duration to be conducted in polytunnels in Lancaster (UK) and Antalya (Turkey) under solar radiation conditions.

5 Leaf Temperature and Stomatal Conductance Responses to Ultraviolet Radiation in Polytunnels at Lancaster (UK)

5.1 Introduction

The ultraviolet (UV) irradiance response work (Chapter 3) aimed to understand the fundamental science behind a range of acute (90 minutes) UV irradiance treatments on leaf physiology. This was followed by longer term experiments (6 days) where plants were treated with or without UV radiation (UV+/UV-: Chapter 4), still in a controlled environment setting. This was designed to bridge the high throughput experiment system in a tightly controlled growth chamber to the multi-day experiments planned in polytunnel structures in the UK (this chapter) and in Turkey (Chapter 6). The current chapter progresses the work from artificial to natural conditions by investigating the

effect of solar UV radiation in small polytunnel structures on stomata and leaf temperature.

The work in the current chapter was conducted at the Lancaster Environment Centre (UK) to gain an understanding of how the fundamental science gleaned in a controlled environment (Chapters 3 and 4) would relate to responses of the same tomato cultivar in a setting more closely resembling the ‘real world’ of commercial protected horticultural crop production. This work was enabled by a period of unusually consistent good weather for the north of England during which outside air temperature reached 28°C immediately following the summer solstice, when UV irradiance and dose are greatest. The weather is pertinent because a year earlier a UV exclusion experiment was conducted at the Hazelrigg field station of Lancaster University (only a few miles from the current experiment location). That work is not presented because of numerous problems that occurred, from flooding to animal predation of plants, but above all low UV irradiances in an unusually cloudy and wet summer even for the north of England.

This project was instigated by reports from commercial growers that crops cultivated under UV-transparent (UV-T) polytunnels had a 1.9°C higher leaf temperature than those grown under UV blocking (UV-O) polytunnels (Williams *et al.*, 2020; Tab. 1.1). The work in this chapter will utilise similar plastic polytunnel claddings, from the same developer (Arid Agritech Ltd.), which either transmit or block the majority of solar UV radiation. These plastics act in a similar way to the plastics used in conventional experimental UV radiation exclusion studies, blocking solar radiation below specific wavelengths (e.g. UV-O that blocks <400 nm), but are actually the same plastics as those used commercially on polytunnels. Examples of plastics used in

conventional exclusion studies, and in the experimental campaign at Hazelrigg highlighted earlier, are Teflon and cellulose diacetate (UV-transparent), and different wavelength selective polyester films (e.g. blocking <320nm or <400 nm). This chapter therefore directly links experimental practice and commercial use to investigate the reports from commercial growers.

UV exclusion studies are common when investigating the effects of ambient UV radiation on plants. The only report of leaf temperature responses to UV radiation was conducted in this way, though it was designed to investigate drought and UV radiation effects on biomass rather than leaf temperature (Novotná *et al.*, 2016; Tab. 1.2). The study identified a $\sim 2^{\circ}\text{C}$ decrease in canopy temperature when UV radiation was excluded using rainout shelters formed by plastic lamellas of different acrylic materials that either transmitted 90% of UV, or blocked UV-B and part of UV-A, radiation (Novotná *et al.*, 2016; Tab. 1.2). UV exclusion studies using wavelength selective filters increased stomatal conductance and photosynthesis in a tropical climate field trial, often without identifying the cause (Indore, India: Dehariya *et al.*, 2012; Kataria *et al.*, 2013; Kataria *et al.*, 2014; Tab. 1.2) and in one case increased stomatal aperture (Kataria and Guruprasad, 2015; Tab. 1.2). Another UV exclusion study in the US found UV radiation reduced stomatal conductance by decreasing stomatal density (Gitz III *et al.*, 2013; Tab. 1.2). However, each of these studies was conducted over a longer duration than the present study meaning UV-induced changes in stomatal distribution could occur, not only stomatal closure. Although none of this research considered leaf temperature, they demonstrate that UV radiation generally decreases stomatal conductance, which would be expected to result in enhanced leaf temperature.

Following on from the work already conducted (Chapters 3 and 4) it was hypothesised that UV radiation would cause partial stomatal closure, measured as reduced stomatal conductance, thereby increasing leaf temperature. This was tested in a campaign of experiments where the stomatal conductance and leaf temperature responses of tomato plants to solar UV radiation was investigated in small polytunnel structures clad with different plastics (UV-T = UV+ and UV-O = UV-) by subjecting glasshouse-grown plants to solar UV radiation for up to 10 days.

5.2 Material and Methods

5.2.1 Plant Material

Tomato (*Solanum lycopersicum* cv. 'Money Maker') plants were propagated in the absence of UV-B radiation in a glasshouse at the Lancaster Environment Centre (Section 2.1) After 5 weeks of growth from seed, the 40 most uniform tomato plants were selected and transferred to the UV treatment polytunnels (10 plants per polytunnel), avoiding exposure to solar radiation during transfer by shielding the plants with UV-opaque plastic film. A leaflet from the most recent fully developed leaf pair on the 5th internode was used for the experiments.

5.2.2 Polytunnels and UV Radiation Treatments

Four consecutive experiments were conducted in four small polytunnel structures located at the Lancaster Environment Centre (Lancaster, UK; Fig. 5.1). These consisted of a metal frame (LxWxH: 3.0 x 1.5 m x 2.25 m) with an internal metallic mesh bench inside (LxW: 1.85 x 1.25 m) raised 0.75 m above the ground leaving space at each end for a user to work inside. Plastic cladding was only fitted down to the bench level to allow ventilation inside the polytunnels, along with a small opening at the top of the north-facing end (Fig. 5.1). Two polytunnels were clad with

UV-transparent plastic film (Lightworks Sun Smart: Arid Agritec Ltd.; referred to here as “UV+”) that transmitted 73% of solar UV radiation, and two with UV-opaque plastic film (Lightworks Sun Master: Arid Agritec Ltd.; referred to as “UV-”) that transmitted 2% of solar UV radiation. The spectral transmission of the plastics was measured in the laboratory (Section 2.3; Fig. 5.2).



Figure 5.1: The four small polytunnel structures located at the Lancaster Environment Centre at Lancaster University, Lancaster, UK.

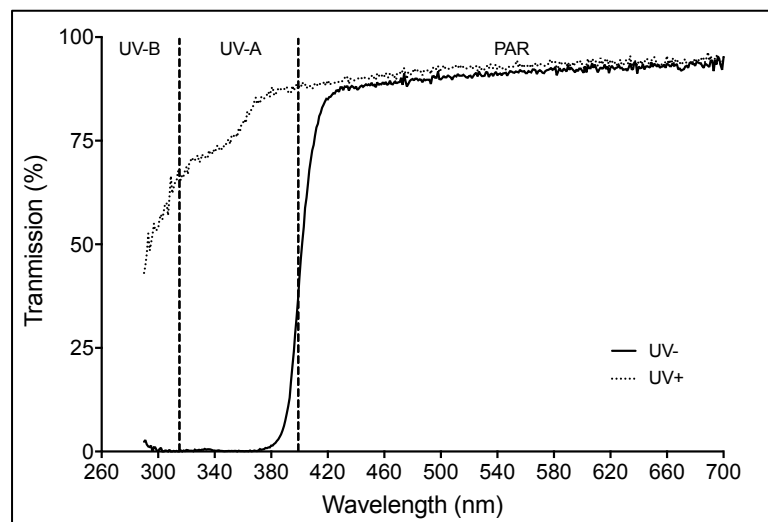


Figure 5.2: Spectral transmission (260-700 nm) of the UV-transparent (UV+; Lightworks Sun Smart) and UV-opaque (UV-; Lightworks Sun Master: Arid Agritec, Lancaster UK) plastic films when first exposed to solar radiation on the polytunnel structures. UV-B, UV-A and photosynthetically active radiation (PAR) wavelength ranges are highlighted.

UV, photosynthetically active radiation (PAR) and short-wave infrared radiation (700-800 nm) inside the polytunnels was quantified with a spectroradiometer (Section 2.2)

on a clear sunny day during the experimental period. It provided the spectral transmission (260-800 nm) of solar radiation within each polytunnel, from which mean maximum irradiances were calculated. Daily UV radiation doses were calculated from UV irradiances measured hourly from 09:00-17:00 (Tab. 5.1). A typical UV radiation profile under each type of plastic on a clear sunny day is provided as an example (Fig. 5.3). UV treatments are expressed unweighted, and weighted by the PGIAS and GPAS biological spectral weighting functions (Section 2.5; Tab. 5.1).

Table 5.1: Maximum irradiances and daily doses applicable to the UV+ and UV- polytunnels, consisting of: unweighted, GPAS weighted (Caldwell, 1971; Caldwell *et al.*, 1986) and PGIAS weighted (Flint and Caldwell, 2003) values.

UV Treatment	Unweighted Irradiance 280-400 nm (W m^{-2})	Unweighted Dose 280-400 nm (kJ m^{-2})	GPAS Weighted UV Irradiance (W m^{-2})	GPAS Weighted UV Dose (kJ m^{-2})	PGIAS Weighted UV Irradiance (W m^{-2})	PGIAS Weighted UV Dose (kJ m^{-2})
UV+	23.54	640	0.050	1.1	0.476	12.8
UV-	0.93	28	0.001	0.01	0.014	0.4

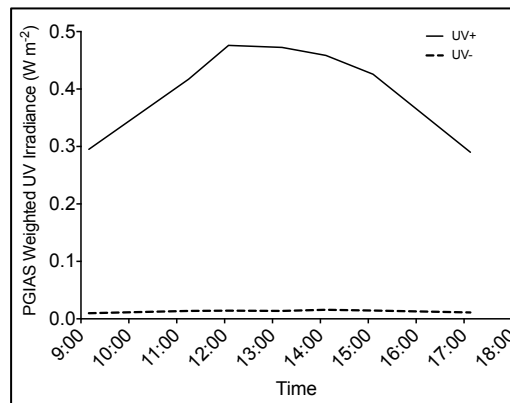


Figure 5.3: Typical PGIAS weighted UV irradiance under the UV-transparent (UV+; Lightworks Sun Smart) and UV-opaque (UV-; Lightworks Sun Master: Arid Agritec Ltd., Lancaster UK) plastic films on a cloudless day on 30 June 2018 in Lancaster, UK.

Four consecutive multi-day experiments were conducted from 21 June until 25 July 2018. Each experiment consisted of two UV treatments after transfer from the glasshouse: UV+ and UV- (Tab. 5.1; Fig. 5.2; Fig. 5.3). However, the UV irradiances and doses of the UV+ treatment were dependent on the weather conditions. Without

continuous UV irradiance measurements throughout the experimental period, solar irradiance was used as a proxy for UV irradiance, which highlights any variation during and between the four experiments. There were 20 plants per UV treatment (10 plants per polytunnel). The plants remained in the treatment polytunnels for 7-10 days depending on the experiment.

5.2.3 Leaf Gas Exchange and Temperature Measurements

Leaf gas exchange and leaf temperature measurements were made with an AP4 leaf porometer (Delta T Devices Ltd, Cambridge, UK) and infrared thermometer (WZ-39755-10 Deluxe, Cole-Parmer Instrument Company Ltd., St. Neots, UK), to collect stomatal conductance and leaf temperature data respectively. The leaf gas exchange analyser (LI-6400XT), which would have provided more data (see Chapters 3, 4 and 6), was not available at the time. Measurements were centred around solar noon, from 11:00 until 15:00, alternating daily the first treatment polytunnel in which data was collected to minimise diurnal effects confounding UV impacts on the measured variables.

5.2.4 Polytunnel Air Temperature

Air temperature was continuously logged with a TinyTag Ultra 2 data logger (TGU-4017: TinyTag, Gemini Data Loggers, Chichester, UK) hung centrally in each polytunnel 0.3 m above the plants. To determine whether air temperature varied between the differently clad polytunnels, the mean air temperature at the time of leaf temperature measurements was calculated for each polytunnel. From these data the mean air temperature for each treatment (UV+/UV-) was calculated for 12 consecutive days when solar irradiance was near to the maximum in its annual cycle.

This provided the mean air temperature of each UV treatment polytunnel at the time that leaf temperature was simultaneously measured with the infrared thermometer.

The same air temperature data was used to calculate the mean difference between UV+/UV- polytunnels on a daily basis (ΔT_{air}). The same calculations were performed for leaf temperature to determine the daily difference of mean leaf temperature between UV+/UV- polytunnels (ΔT_{leaf}). These data were analysed with a linear regression to determine whether polytunnel air temperature and leaf temperature were correlated.

5.2.5 Weather Data

Throughout the experimental period, sensors attached to a 1 m high mast on the roof of the Lancaster Environment Centre measured outside air temperature with a Hortimax TEMP Pt1000 (Hortisystems UK Ltd, Pulborough, UK) and solar irradiance with a Hortimax GRAD photodiode (400-800 nm range: Hortisystems UK Ltd). Solar irradiance was used as a proxy for UV irradiance throughout the experimental period because it was not possible to measure UV irradiance continuously. This allowed any UV induced leaf responses to be compared with changing UV irradiance on a daily basis. Whole experiment and daily cumulative solar radiation were determined in GraphPad Prism version 7.0d for Mac OS X (GraphPad Software, La Jolla California USA, www.graphpad.com) by calculating the area under the curve of the solar irradiance data for each experiment or day of treatment.

5.2.6 Statistical Analysis

Data from the four sequential multi-day experiments were tested for normal distribution and equal variances in SPSS version 18 (SPSS Inc. Chicago, USA). These

data were statistically analysed for differences between the UV treatments (UV+ / UV-) using a repeated measures ANOVA in SPSS, with UV treatment and experiment as the main factors, and day as the repeated measure. The experiments were analysed as a combined data set initially but when a significant experiment x UV treatment interaction was identified, the experiments were also analysed separately. To determine daily differences between UV radiation treatments, unpaired t-tests were performed for each day (corrected for multiple comparisons) using the Sidak-Bonferroni method, in GraphPad Prism version 7.0d for Mac OS X (GraphPad Software, La Jolla California USA, www.graphpad.com).

5.3 Results

Each treatment period began when plants were transferred from the glasshouse to the UV treatment polytunnels (day zero). Solar irradiance, a proxy for UV irradiance, is summarised for each treatment day (including day zero, the day of transfer). Data could not always be collected on each day due to problems with equipment, resulting in data gaps on occasional days.

5.3.1 All Experiments Combined

When the four experiments were combined and analysed as a single data set, leaf temperature varied significantly between the four experiments ($P < 0.001$; Tab. 5.2), due to variations in ambient air temperature (apparent in the 16-36°C range of mean leaf temperatures) and solar irradiance (Tab. 5.3). However, the UV effect was consistent (no significant treatment x experiment interaction: $P = 0.131$; Tab. 5.2) meaning data from all experiments can be pooled for analysis. There was also a significant effect of polytunnel on leaf temperature ($P = 0.045$; Tab. 5.2) but not for

stomatal conductance ($P=0.833$; Tab. 5.2) but this did not interact with the difference between treatments for both parameters (treatment x polytunnel: $P>0.05$; Tab. 5.2).

Table 5.2: Summary of P values for each factor and factor interaction from the repeated measures ANOVA analysis for leaf temperature (T_{leaf}) and stomatal conductance (g_s) for the four experiments combined together as one data set. The asterisks highlight the statistically significant ANOVA results (*: $P<0.05$; **: $P<0.01$; ***: $P<0.001$).

ANOVA Factors	T_{leaf}	g_s
Experiment	<0.001***	<0.001***
Treatment	<0.001***	0.003**
Day	<0.001***	<0.001***
Polytunnel	0.045*	0.833
Treatment x Experiment	0.131	0.001**
Treatment x Polytunnel	0.306	0.435
Experiment x Polytunnel	0.271	0.211
Treatment x Day	0.436	0.188
Experiment x Day	<0.001***	<0.001***
Polytunnel x Day	0.141	0.041
Treatment x Experiment x Polytunnel	0.001**	0.544
Treatment x Experiment x Day	0.030*	0.010*
Experiment x Polytunnel x Day	<0.001***	0.337
Treatment x Polytunnel x Day	0.002**	0.128
Treatment x Experiment x Polytunnel x Day	<0.001***	0.164

The UV+ treatment significantly ($P<0.001$; Tab. 5.2) increased leaf temperature by up to $2.2\pm 1.6^\circ\text{C}$. Leaf temperature varied between days ($P<0.001$; Tab. 5.2) but again there was no interaction with the treatment effect (treatment x day: $P=0.436$; Tab. 5.2) indicating a consistent response across each day. However, this variation between days differed between experiments (experiment x day: $P<0.001$; Tab. 5.2). There was also a 3-way interaction between treatment, experiment and day ($P=0.030$; Tab. 5.2) meaning the leaf temperature response to UV radiation was affected by the interaction

of variable leaf temperature between days and experiments. When all experimental data were pooled, UV+ polytunnels consistently increased leaf temperature.

Table 5.3: Summary of daily cumulative solar radiation and cumulative totals ($W\ m^{-2}$) for each experiment. N/A means data were not applicable due to the different durations of experiments.

Treatment Day	Experiment 1	Experiment 2	Experiment 3	Experiment 4
Day 0	6526	6922	6171	4390
Day 1	7122	6469	6921	6291
Day 2	5580	6840	6880	1652
Day 3	7040	6922	6833	2523
Day 4	6922	6785	6428	2784
Day 5	6469	7006	6692	2200
Day 6	6840	6390	6614	3011
Day 7	6924	6173	6270	5791
Day 8	N/A	6922	5563	N/A
Day 9	N/A	N/A	6330	N/A
Day 10	N/A	N/A	3028	N/A
Mean	6678	6714	6157	3580

Stomatal conductance also significantly differed between experiments ($P < 0.001$; Tab. 5.2) because stomatal conductance increased as ambient air temperature reduced over the experimental period, from $>30^{\circ}C$ in first two weeks. These experimental differences interacted with the UV treatment effect (treatment x experiment: $P = 0.001$; Tab. 5.2), meaning the experiments should be analysed separately. Experiments 1 and 2 were combined and analysed together because the solar radiation conditions across the two consecutive weeks were consistently good (Tab. 5.3) and there was no interaction of the experimental differences on the UV treatment effect within these two experiments (treatment x experiment: $P > 0.05$; Tab. 5.2). Experiments 3 and 4 are analysed separately because of differing weather conditions during each. Solar irradiance in Experiment 3 diminished from near maximal on day zero by $\sim 50\%$ 10

days later (Tab. 5.3), whereas solar irradiance was substantially reduced for much of Experiment 4 (Tab. 5.3), producing a different stomatal response to the previous three experiments.

5.3.2 Experiments 1 and 2 Combined

Taking Experiments 1 and 2 together (Section 5.3.1), stomatal conductance and leaf temperature both varied significantly between experiments ($P < 0.001$; Tab. 5.4), likely due to higher ambient air temperature in the first week. This resulted in very high air temperatures inside the poly tunnels ($>35^{\circ}\text{C}$), which appeared to lower stomatal conductance in all poly tunnels.

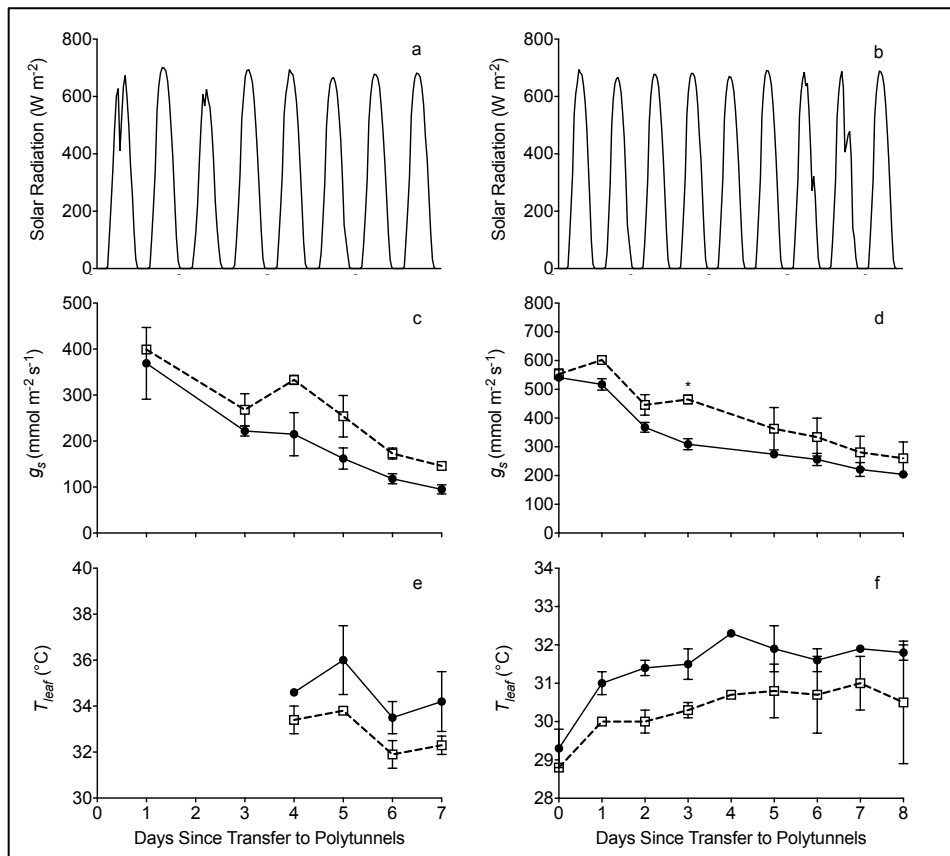


Figure 5.4: Time courses of (a,b) solar irradiance (400-800 nm) measured at the Lancaster Environment Centre during the period of data collection, (c,d) the daily stomatal conductance response (g_s), and (e,f) daily leaf temperature response (T_{leaf}), for Experiment 1 (a,c,e) and Experiment 2 (b,d,f) to UV+ (closed circles) and UV- (open squares) treatments. The asterisks highlight individual days where there was a significant difference between treatments (*: $P < 0.05$) corrected for multiple t-tests. Error bars represent ± 1 SE ($n=20$) but if not visible they were smaller than the symbol. See Table 5.4 for full ANOVA analysis.

Table 5.4: Summary of P values for each factor and factor interaction from the repeated measures ANOVA analysis for leaf temperature (T_{leaf}) and stomatal conductance (g_s) for Experiments 1 and 2 combined together as one data set. The asterisks highlight the statistically significant ANOVA results (*: $P < 0.05$; **: $P < 0.01$; ***: $P < 0.001$).

ANOVA Factors	T_{leaf}	g_s
Experiment	<0.001***	<0.001***
Treatment	<0.001***	0.001**
Day	<0.001***	<0.001***
Polytunnel	0.057	0.277
Treatment x Experiment	0.301	0.289
Treatment x Polytunnel	0.117	0.239
Experiment x Polytunnel	0.411	0.169
Treatment x Day	0.826	0.604
Experiment x Day	<0.001***	0.574
Polytunnel x Day	0.226	0.022*
Treatment x Experiment x Polytunnel	0.053	0.457
Treatment x Experiment x Day	0.319	0.595
Experiment x Polytunnel x Day	0.208	0.769
Treatment x Polytunnel x Day	0.135	0.331
Treatment x Experiment x Polytunnel x Day	0.023*	0.365

UV radiation significantly decreased stomatal conductance ($P=0.001$; Tab. 5.4) and significantly increased leaf temperature ($P < 0.001$; Tab. 5.4). Conductance was up to $156 \pm 88 \text{ mmol m}^{-2} \text{ s}^{-1}$ (34%; mean difference: $78 \pm 57 \text{ mmol m}^{-2} \text{ s}^{-1}$) lower and leaf temperature was up to $2.2 \pm 1.1^\circ\text{C}$ (mean difference: $1.3 \pm 0.9^\circ\text{C}$) greater (Fig. 5.4c,e). There was no effect of polytunnel ($P > 0.05$; Tab. 5.4) or interaction between polytunnel and treatment ($P > 0.05$; Tab. 5.4) for leaf temperature or stomatal conductance. There were significant variations between days for both parameters ($P < 0.001$; Tab. 5.4) but these differences did not affect the UV treatment response identified above for either leaf temperature or stomatal conductance (treatment x day: $P > 0.05$ for each; Tab. 5.4). Daily variations in stomatal conductance were consistent

across experiments (experiment x day: $P=0.574$; Tab. 5.4) but not so for leaf temperature (experiment x day: $P<0.001$; Tab. 5.4) meaning those daily variations were inconsistent across the two experiments. There was no interaction between treatment, experiment and day ($P>0.05$; Tab. 5.4) for both parameters. These results show that stomatal conductance was reduced, and leaf temperature increased, in UV+ poly tunnels across the two experiments conducted in similar weather conditions, even though the response varied between days and experiments.

5.3.3 Experiment 3

In analysing Experiment 3 individually (Section 5.3.1), stomatal conductance ($P=0.001$; Fig. 5.5b; Tab. 5.5) and leaf temperature ($P<0.001$; Fig. 5.5c; Tab. 5.5) both responded significantly to the UV+ treatment. Stomatal conductance was up to $236\pm 25 \text{ mmol m}^{-2} \text{ s}^{-1}$ (34%; mean difference: $112\pm 130 \text{ mmol m}^{-2} \text{ s}^{-1}$) lower in response to UV+ and leaf temperature was up to $1.7\pm 0.5^\circ\text{C}$ (mean difference: $0.9\pm 0.6^\circ\text{C}$) greater (Fig. 5.5b,c). There was an effect of poly tunnel on both parameters ($P<0.05$; Tab. 5.5) but this did not interact with the treatment effect for either ($P>0.05$; Tab. 5.5). Thus, the significant effect of UV treatment on both parameters was not affected by differences between poly tunnels.

There were variations between days in both parameters ($P<0.001$; Tab. 5.5) caused by the variable weather conditions towards the end of the week when ambient air temperature and solar irradiance reduced substantially (Fig. 5.5a). These daily variations had no effect on the UV treatment response observed for stomatal conductance (treatment x day: $P=0.064$; Tab. 5.5) but did interact with the effect of UV treatment on leaf temperature (treatment x day: $P=0.032$; Tab. 5.5). This is a result of the proportionally greater stomatal conductance differences between treatments

(but not always in the same direction of response), whereas the differences between treatments for leaf temperature were much smaller (but always had the same direction of response). The significant effect of polytunnel did vary between days (polytunnel x day: $P < 0.05$; Tab. 5.5) but the day did not interact with the effect of polytunnel on treatment (treatment x polytunnel x Day: $P > 0.05$; Tab. 5.5). The UV+ treatment significantly reduced stomatal conductance and increased leaf temperature but variable solar radiation conditions, particularly towards the end of the week, caused a reversal of the UV response in stomatal conductance that was less evident in the leaf temperature response.

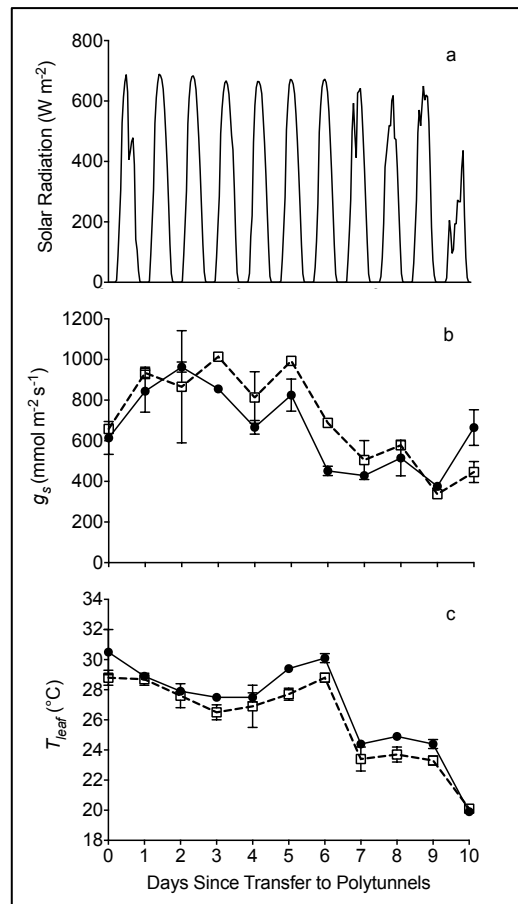


Figure 5.5: Time courses of (a) solar irradiance (400-800 nm) measured at the Lancaster Environment Centre during the period of data collection, (b) the stomatal conductance response (g_s), and (c) leaf temperature response (T_{leaf}), to UV+ (closed circles) and UV- (open squares) treatments of Experiment 3 plants. There were no individual days where there was a significant difference between treatments (corrected for multiple t-tests). Error bars represent ± 1 SE ($n=20$) but if not visible they were smaller than the symbol. See Table 5.5 for full ANOVA analysis.

From Day 7 onwards cloud cover increased, reducing solar irradiance (Fig. 5.5a). As a proxy for UV irradiance, this reduction in solar irradiance coincided with a gradual reversal of the direction of stomatal conductance response observed earlier in the week, with the UV- treated leaves exhibiting lower stomatal conductance than UV+ leaves on Days 9 and 10 (Fig. 5.5b). This indicates that leaves responded to UV radiation when solar irradiance was at or near maximum, but when this reduced from Day 7 onwards the response gradually diminished until it was clearly reversed on Day 10, when solar irradiance was ~50% lower than earlier in that week. This reversal of the UV radiation response was reflected in leaf temperature, which also diminished towards the end of the week, although the direction of response did not completely reverse in the same way as stomatal conductance (Fig. 5.5c). This sequence of events demonstrates a readily reversible response to UV radiation, dependent on solar and therefore UV irradiance.

Table 5.5: Summary of P values for each factor and factor interaction from the repeated measures ANOVA analysis for leaf temperature (T_{leaf}) and stomatal conductance (g_s) for Experiment 3. The asterisks highlight the statistically significant ANOVA results (*: $P < 0.05$; **: $P < 0.01$; ***: $P < 0.001$).

ANOVA Factors	T_{leaf}	g_s
Treatment	<0.001***	0.001**
Polytunnel	0.012*	0.037*
Day	<0.001***	<0.001***
Treatment x Polytunnel	0.052	0.102
Treatment x Day	0.032*	0.064
Polytunnel x Day	0.033*	0.001**
Treatment x Polytunnel x Day	0.662	0.072

5.3.4 Experiment 4

Ambient air temperature was extremely variable, which is clear from the range of leaf temperatures (16-33°C; Fig. 5.6c), with substantial cloud cover during Experiment 4 (Fig. 5.6a). The cloud reduced solar irradiance (Tab. 5.3), a good indicator for UV irradiance, which appeared to alter the direction of stomatal conductance response in contrast to Experiments 1 and 2. Stomatal conductance was significantly greater in response to UV+ (treatment: $P=0.048$; Fig. 5.6b; Tab. 5.6), up to $189\pm 88 \text{ mmol m}^{-2} \text{ s}^{-1}$ (28%; mean difference: $57\pm 60 \text{ mmol m}^{-2} \text{ s}^{-1}$), compared to the UV- treatment. However, leaf temperature was also significantly greater in response to UV+ ($P=0.006$; Tab. 5.6), by up to $1.4\pm 1.4^\circ\text{C}$ (mean difference: $0.4\pm 0.4^\circ\text{C}$), with the range (16.4 ± 0.3 to $33.2\pm 1.4^\circ\text{C}$; Fig. 5.6c) reflecting the variable ambient air temperature outside the polytunnels. The leaf temperature differences between treatments were smaller than observed in the other experiments, particularly Experiments 1 and 2, which is not surprising given that UV+ stomatal conductance was actually higher than UV-. There were significant differences in leaf temperature between the polytunnels ($P<0.001$; Tab. 5.6) but not for stomatal conductance ($P=0.329$; Tab. 5.6) but there was no interaction between the polytunnels differences and the treatment effect for both parameters (treatment x polytunnel: $P>0.05$; Tab. 5.6). Leaf temperature and stomatal conductance were both higher in UV+ polytunnels.

There was significant daily variation in both parameters ($P<0.001$; Fig. 5.6b,c; Tab. 5.6), which significantly affected the UV treatment response of both (treatment x day: $P<0.01$; Fig. 5.6b,c; Tab. 5.6), also evident as fluctuations in the magnitude, including reversal in the direction, of response of both parameters over the course of the week. The effect of day interacted with the effect of polytunnel for both parameters (day x polytunnel: $P<0.05$; Tab. 5.6) meaning the effect of polytunnels was not consistent

across each day. There was no significant interaction between treatment, polytunnel and day for leaf temperature ($P=0.098$; Tab. 5.6), but there was for stomatal conductance ($P=0.020$; Tab. 5.6), indicating the effect of polytunnel on treatments did vary with day. Reduced solar irradiance during this experiment meant stomatal conductance was actually greater in UV+ polytunnels, because of less UV radiation. Surprisingly, leaf temperature was also greater in those polytunnels, which indicates that leaf warming unrelated to stomatal conductance occurred.

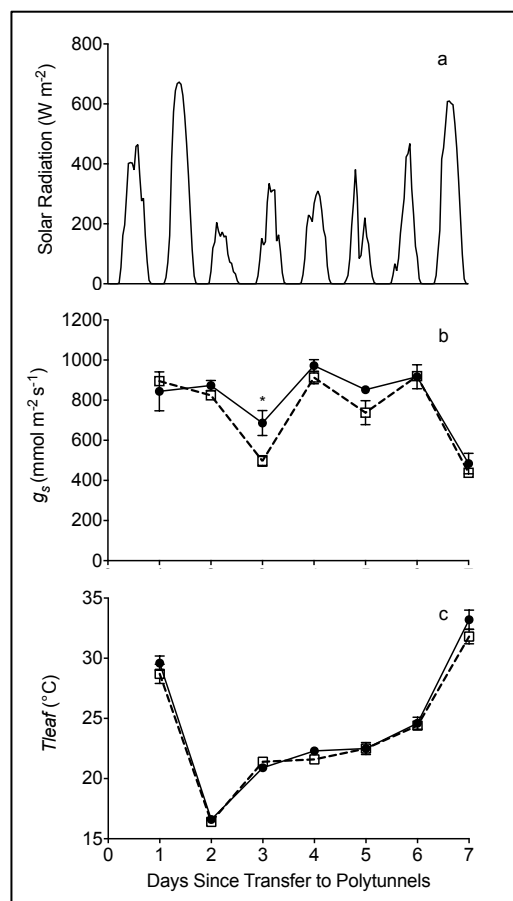


Figure 5.6: Time courses of (a) solar irradiance (400-800 nm) measured at the Lancaster Environment Centre during the period of data collection, (b) the stomatal conductance response (g_s), and (c) leaf temperature response (T_{leaf}), to UV+ (closed circles) and UV- (open squares) treatments of Experiment 4 plants. The asterisks represent individual days where there was a significant difference between treatments (*: $P<0.05$) corrected for multiple t-tests. Error bars represent ± 1 SE ($n=20$) but if not visible they were smaller than the symbol. See Table 5.6 for full ANOVA analysis.

Table 5.6: Summary of P values for each factor and factor interaction from the repeated measures ANOVA analysis for leaf temperature (T_{leaf}) and stomatal conductance (g_s) for Experiment 4. The asterisks highlight the statistically significant ANOVA results (*: $P < 0.05$; **: $P < 0.01$; ***: $P < 0.001$).

ANOVA Factors	T_{leaf}	g_s
Treatment	0.006**	0.048*
Polytunnel	<0.001***	0.329
Day	<0.001***	<0.001***
Treatment x Polytunnel	0.779	0.449
Treatment x Day	0.001**	0.002**
Polytunnel x Day	0.005**	0.034*
Treatment x Polytunnel x Day	0.098	0.020*

5.3.5 Relationship Between Stomatal Conductance and Leaf Temperature

Linear regression analysis indicated that leaf temperature of UV+ treated plants significantly increased ($P < 0.001$; Fig. 5.7) as stomatal conductance decreased. Stomatal conductance can explain 82% of the change in leaf temperature (R^2 : 0.82; Fig. 5.7), with the remaining response indicating leaf warming unrelated to stomatal conductance and therefore transpiration rate. The resulting equation for the linear regression shows leaf temperature increases by 1.13°C for each $100 \text{ mmol m}^{-2} \text{ s}^{-1}$ decrease in stomatal conductance. Thus reduced stomatal conductance caused leaf warming.

5.3.6 Leaf Warming Unrelated to Reduced Stomatal Conductance

Further linear regression analysis of stomatal conductance and leaf temperature for the different UV treatments across all four experiments indicates no significant difference in the slopes ($P = 0.071$) or Y intercepts ($P = 0.274$; Fig. 5.8). Similar Y intercepts indicate that leaf warming was solely related to changes in stomatal conductance. However, leaf temperature varied considerably ($16.4\text{--}36.0^\circ\text{C}$; Fig. 5.8) as ambient air

temperatures changed during the five week experiment campaign. This variance causes uncertainty in the difference between the Y intercepts of the individual linear regressions ($1.56 \pm 1.04^\circ\text{C}$; Fig. 5.8) with the large standard error clearly demonstrating the variation in the data. This analysis does not confirm that leaf warming unrelated to reduced stomatal conductance occurred, due to the variable leaf temperature data, but does indicate additional leaf warming may have occurred.

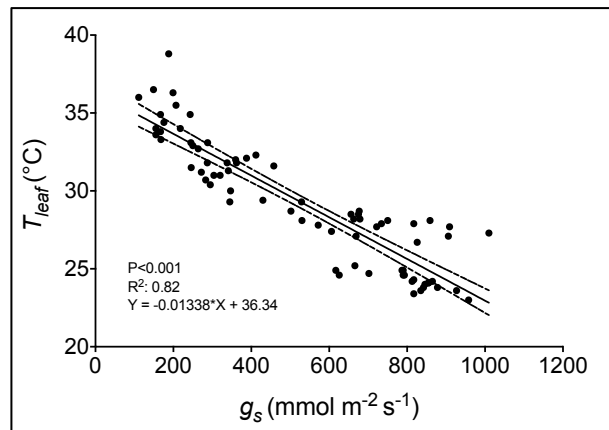


Figure 5.7: Linear regression analysis of daily stomatal conductance and leaf temperature of UV+ treated plants across all four experiments (UV- data are excluded in order to analyse the relationship when UV radiation is present). The results of linear regression analysis are summarised. The 95% confidence intervals are highlighted (dashed lines). Each data point represents an individual plant (n=80).

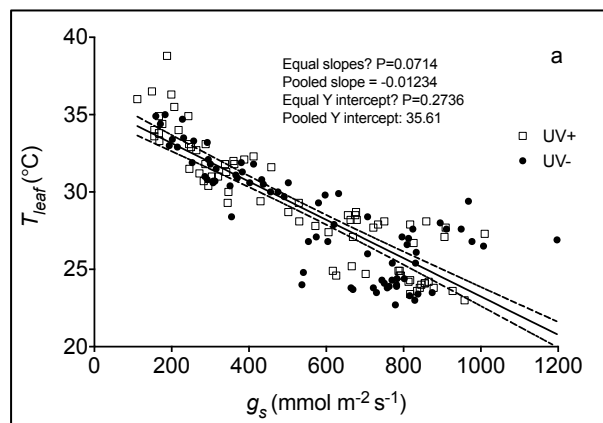


Figure 5.8: Stomatal conductance (g_s) plotted against leaf temperature (T_{leaf}) for all experiments. Summary of the linear regression analysis is summarised, because there was no significant difference between the slopes and Y intercepts of UV+ and UV- treatments the pooled regression line has been plotted (pooled linear regression: $P < 0.0001$; $R^2 = 0.74$). The 95% confidence intervals are highlighted (dashed lines). The slopes ($P = 0.0714$) and Y intercepts ($P = 0.2736$) were not significantly different for the two UV treatments (n=160). The horizontal displacement of the regression lines represents the UV-induced stomatal conductance reduction related to increased leaf temperature in UV+ plants. Vertical displacement of the slopes would indicate increased leaf temperature unrelated to stomatal conductance.

5.3.7 Relationship Between Solar Radiation and Stomatal Conductance and Leaf Temperature

Solar radiation (400-800 nm), measured continuously throughout the experiments, can be used as a proxy for UV radiation to indicate how it affected stomatal conductance and leaf temperature (Fig. 5.9). Regression analysis indicates a significant relationship exists ($P < 0.001$) for both parameters with daily cumulative solar radiation explaining 48% of the variation in stomatal conductance and 47% of the variation in leaf temperature (Fig. 5.9). Treatment differences in stomatal conductance (-97 to 236 $\text{mmol m}^{-2} \text{s}^{-1}$; Fig. 5.9a) and leaf temperature (-0.2 to -2.2 $^{\circ}\text{C}$; Fig. 5.9b) varied substantially between days when daily cumulative solar radiation is at or near maximal (6000 - 7000 W m^{-2} ; Fig. 5.9), which reduces the R^2 value. Ambient air temperature varied considerably between the different experiments, thereby affecting stomatal conductance. Lower stomatal conductances in Experiment 1 coincided with mean leaf temperatures of 32 - 36°C (Fig. 5.4c), whereas much higher conductances occurred when leaf temperature was 16 - 33°C (Fig. 5.6c). As increased cloud cover reduced solar (and therefore UV) radiation, stomatal conductance and leaf temperature responded quickly, on a daily basis.

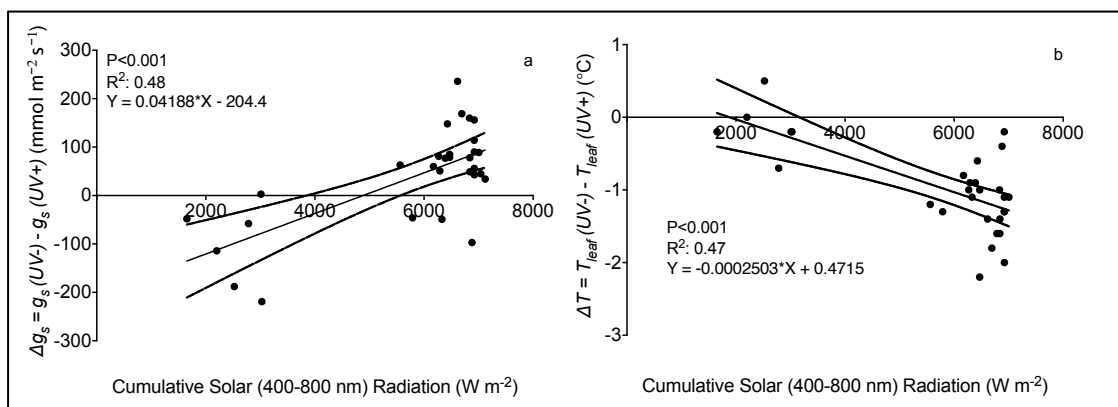


Figure 5.9: Linear regression analysis of daily cumulative solar radiation (400-800 nm) and (a) the daily difference in stomatal conductance between UV+ and UV- ($\Delta g_s = g_s(\text{UV-}) - g_s(\text{UV+})$) treated plants, and (b) the daily difference in leaf temperature between UV+ and UV- ($\Delta T = T_{\text{leaf}}(\text{UV-}) - T_{\text{leaf}}(\text{UV+})$) treated plants across all four experiments ($n=80$). The results of linear regression analysis are summarised. The 95% confidence intervals are highlighted (dashed lines).

5.3.8 Relationship Between Polytunnel Air Temperature and Leaf Temperature

It was important to assess whether differences in air temperature between the UV treatment polytunnels (UV+ / UV-) affected leaf temperature measurements with the infrared thermometer. Air temperature measured at the time of leaf temperature measurements, averaged over 12 consecutive days, indicates no significant difference between UV+ ($23.92 \pm 1.39^\circ\text{C}$) and UV- ($23.72 \pm 1.36^\circ\text{C}$) treatments (t-test: $P=0.93$). Linear regression analysis of the difference in air temperature between UV+/UV- polytunnels at the time of leaf temperature measurements (ΔT_{air}) and the difference in leaf temperature between UV+/UV- polytunnels (ΔT_{leaf}) demonstrate that no relationship exists ($P=0.75$; $R^2: 0.003$; Fig. 5.10). Thus air temperature did not cause treatment differences in leaf temperature. Together the two methods of analysis demonstrate that air temperature was similar between the differently clad polytunnels and on days that air temperature differed it did not affect leaf temperature

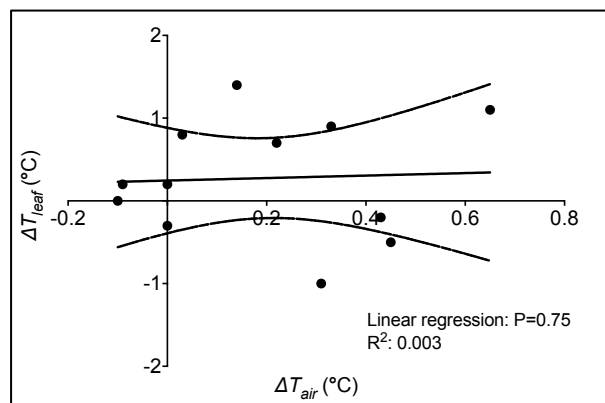


Figure 5.10: Linear regression analysis of the differences in air temperature (ΔT_{air}) between UV+ and UV- polytunnels at the time of leaf temperature measurements ($n=3$) with the infrared thermometer, and the difference in leaf temperatures (ΔT_{leaf}) between those polytunnels ($n=20$), for 12 consecutive days. Each data point represents an individual day. The 95% confidence intervals (dashed lines) and results of linear regression analysis are highlighted.

5.3.9 Total and Photosynthetically Active Radiation (PAR)

PAR and total radiation were both significantly ($P<0.01$) higher in UV+ polytunnels than UV-. PAR (400-700 nm) was up to 17% ($203 \pm 19 \mu\text{mol m}^{-2} \text{s}^{-1}$; Fig. 5.11a)

greater, averaging 9.3% ($102 \pm 32 \mu\text{mol m}^{-2} \text{s}^{-1}$) greater between 09:00-17:00. Total radiation (290-800 nm) was up to 23% ($78 \pm 6 \text{ W m}^{-2}$; Fig. 5.11b) greater in UV+ polytunnels compared to UV-, averaging 15% ($47 \pm 9 \text{ W m}^{-2}$) greater between 09:00-17:00. Both varied significantly diurnally (time: $P < 0.001$; Fig. 5.11) and, as expected, there was a significant interaction between treatment and time ($P < 0.01$; Fig. 5.11). These data clearly demonstrate that PAR and total radiation transmission was greater through the UV-transparent plastic causing higher radiation loading in the UV+ polytunnels.

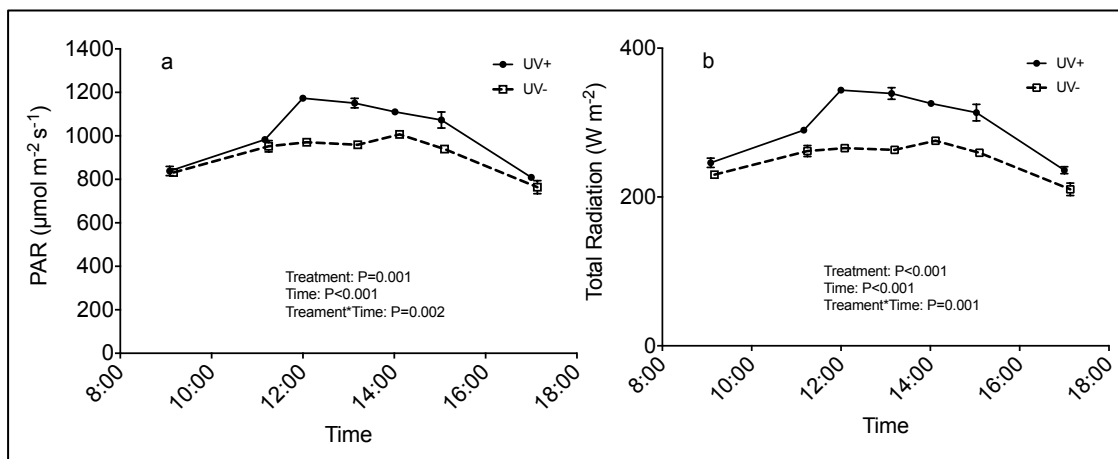


Figure 5.11: Time courses of (a) Photosynthetically active radiation (PAR: 400-700 nm) and (b) total radiation (290-800 nm) inside the UV+ (black circles and solid line) and UV- (open squares and dashed line) polytunnels on a cloudless day on 30 June 2018. Summary of repeated measures ANOVA analysis highlighted. Error bars represent ± 1 SE ($n=3$) but if not visible they were smaller than the symbol.

5.4 Discussion

5.4.1 Leaf Warming Caused by Partial Stomatal Closure

Leaf temperature was significantly warmer in UV+ polytunnels across all four experiments (Figs. 5.4-5.6). This is consistent with the leaf temperature responses to UV radiation observed in the climate cabinet (Chapter 3) and the controlled environment room (Chapter 4) experiments. The leaf temperature difference between treatments was up to $2.2 \pm 1.6^\circ\text{C}$, similar to that originally reported from UV-transparent polytunnels at a commercial tomato farm in Antalya, Turkey

($1.9 \pm 1.3^\circ\text{C}$; Williams *et al.*, 2020) and in a UV exclusion study of a mountain grassland in the Czech Republic, which inferred partial stomatal closure as the cause ($\sim 2^\circ\text{C}$; Novotná *et al.*, 2016). However, it is considerably higher than the observed leaf temperature increases in the climate cabinet (up to $0.72 \pm 0.16^\circ\text{C}$: Chapter 3) and the controlled environment room (up to $0.23 \pm 0.10^\circ\text{C}$: Chapter 4). There are two possible causes for these discrepancies in leaf temperature response to UV radiation: differences in the UV irradiance or dose, and / or differences in radiation loading between the field and the laboratory.

The maximum UV irradiance in this study was 0.476 W m^{-2} (PGIAS; Tab. 5.1) whereas in the controlled environment (CE) room it was 0.354 W m^{-2} (PGIAS; Tab. 3.1) and in the climate cabinet the closest comparable treatment was 0.297 W m^{-2} (PGIAS; Tab. 4.1). This greater UV irradiance in the polytunnels at Lancaster can partly explain why stomatal conductance was reduced more (-34%, -21% and -27% respectively) although the differences are not substantial. Radiation loading, measured as total radiation, appears to have had a greater effect on increasing leaf temperature in UV+ treatments. There was no difference in radiation loading between measurements of UV+ and UV- leaves in the CE room, because the method was identical for both (Chapter 4), so that leaf temperature increase observed there was caused only by reduced stomatal conductance. There was an effect of radiation loading in the climate cabinet experiments, identified as $0.16 \pm 0.09^\circ\text{C}$ (Chapter 3), which is the main reason why leaf temperature increase was greater there than it was in the CE room (Chapter 4), when UV irradiances were similar. The difference in total radiation (310-2800 nm) between control (zero UV radiation) and that UV treatment was 53.6 W m^{-2} (Chapter 3). In the polytunnels at Lancaster the difference in total radiation between UV+ and UV- polytunnels was 155 W m^{-2} , 3x greater than the

difference in the climate cabinet, which can partly explain why difference in leaf temperature between UV treatments was 1.5°C greater in the polytunnels at Lancaster compared to that observed in the climate cabinet in response to a marginally greater UV irradiance. This demonstrates that increased radiation loading enhances leaf temperature, and how it has varied between the experiments conducted so far.

Stomatal conductance was significantly reduced in UV+ polytunnels in Experiments 1-3 (Figs. 5.4-5.5). These reductions occurred when solar irradiance, a proxy for UV irradiance, was at or near maximal for most of that time (Fig. 5.9a). The consistent direction of response, and statistical significance, of reduced stomatal conductance and increased leaf temperature (Fig. 5.9b) in UV+ polytunnels compared to UV- on each day of treatment during Experiments 1 and 2 (Fig. 5.4), and for the majority of Experiment 3 (Fig. 5.5) demonstrates that reduced stomatal conductance causes increased leaf temperature. This is corroborated by the strong relationship between stomatal conductance and leaf temperature (Fig. 5.7). Partial stomatal closure is inferred as the cause of reduced stomatal conductance since measurements occurred on fully expanded leaves that could not have altered their stomatal distribution.

The maximum absolute decrease in stomatal conductance in Experiments 1 and 2 ($-156 \pm 88 \text{ mmol m}^{-2} \text{ s}^{-1}$; Fig. 5.4) was similar to the observed decrease in the controlled environment room experiments ($-118 \pm 87 \text{ mmol m}^{-2} \text{ s}^{-1}$; Chapter 4) but the percentage changes were further apart (-34% and -21% respectively). The UV doses were similar when weighted by GPAS (1.1 and 13.0 $\text{kJ m}^{-2} \text{ s}^{-1}$ respectively) but quite different when weighted by PGIAS (12.8 and 17.8 $\text{kJ m}^{-2} \text{ s}^{-1}$ respectively), due to its inclusion of UV-A, so the choice of applied BSWF determines whether these were similar UV

treatments, or quite different, which is dependent on whether UV-A actually affects stomatal closure in these experiments.

There was a greater maximum stomatal conductance reduction in Experiments 1 and 2 of the polytunnels at Lancaster (Fig. 5.4) than in the climate cabinet experiments ($-112 \pm 47 \text{ mmol m}^{-2} \text{ s}^{-1}$; -27% ; Chapter 3). When comparing the UV irradiances rather than doses (because a dose is not particularly applicable to a 90 minute treatment), the maximum UV+ polytunnel irradiance was 0.476 W m^{-2} (PGIAS), greater than the comparable irradiance in the climate cabinet (0.297 W m^{-2} PGIAS), which can explain the greater stomatal conductance reduction in the polytunnels. This demonstrates the consistent UV-induced stomatal conductance reductions across the three experimental campaigns so far, in different experimental conditions, and that the absolute reductions are similar. It also highlights the effect that BSWF weighting has on interpreting the similarity of the UV doses for comparative purposes.

Previous UV exclusion studies have generally reported stomatal conductance increases. A UV radiation exclusion study in India, using wavelength selective filters, found a general increase in stomatal conductance in the absence of UV radiation over 3 months (Kataria *et al.*, 2013). The stomatal conductance of cotton, sorghum (*Sorghum bicolor*) and amaranthus (*Amaranthus tricolor*) increased significantly when UV radiation was excluded but the increase in wheat was not significant, the cause of the response is not suggested (Kataria *et al.*, 2013). Very similar studies of cotton, amaranthus and wheat, with the same experimental setup, also found stomatal conductance was significantly enhanced when UV radiation was excluded in the field (Dehariya *et al.*, 2012; Kataria *et al.*, 2014) but none investigated the cause, whereas Kataria and Guruprasad (2015) indicated it may relate to aperture. Another UV

exclusion study in poplar found enhanced stomatal conductance in mature leaves compared to those irradiated with $12 \text{ kJ m}^{-2} \text{ d}^{-1}$ (GPAS weighted) but did not suggest a cause, it could relate to stomatal aperture or changes in stomatal frequency because the experiment was conducted over a full growing season (Schumaker *et al.*, 1997). Whatever the cause of UV-exclusion stomatal conductance increases, such changes would clearly be expected to reduce leaf temperature and vice versa, as observed here (Figs. 5.4-5.6).

UV-induced stomatal conductance increases have also been observed. An ambient UV exclusion study found variable responses of soybean, with increases and decreases in two cultivars each (Gitz III *et al.*, 2013). Both responses were associated with changes in stomatal density rather than aperture (Gitz III *et al.*, 2013). This demonstrates that UV radiation can decrease stomatal conductance via different mechanisms and different species show variable direction of response in UV exclusion studies. It is apparent that UV radiation generally decreases stomatal conductance in different species, but the cause may relate to stomatal closure or reduced density. Regardless of the cause, any reduction in stomatal conductance would decrease transpiration rate and increase leaf temperature, as observed in this study (Figs. 5.4-5.6).

5.4.2 Leaf Warming Unrelated to Partial Stomatal Closure

Although it is clear that UV-induced partial stomatal closure that reduces stomatal conductance and increases leaf temperature occurs in UV+ polytunnels, there is also evidence that non-stomatal leaf warming is also present. An example occurred at the end of Experiment 3, when solar irradiance and therefore UV was reduced (Days 7-10; Fig. 5.5). The difference in stomatal conductance between treatments gradually reduced over days 7-9 eventually leading to a reversal of the response culminating in

stomatal conductance being greater in UV+ poly tunnels than UV-. At the same time leaf temperature remained higher in UV+ poly tunnels, clearly demonstrating a decoupling from stomatal conductance. An even clearer example of the decoupling of stomatal conductance and leaf temperature was the simultaneous significant increases in both during Experiment 4 when cloud cover substantially reduced solar radiation (Figs. 5.6 and 5.9). The only evidence that does not fully support the occurrence of leaf warming unrelated to stomatal closure was the difference in the Y intercepts ($1.56 \pm 1.04^\circ\text{C}$; Fig. 5.8) that was not significant. That may be partly explained by the variance of the data caused by variable ambient air temperatures over the four weeks of experimentation, as the absolute difference was relatively large but so was the standard error. These discrepancies between stomatal conductance and leaf temperature, in two separate experiments, demonstrates that leaves were warmed by a mechanism not related to stomatal closure.

The decoupling of stomatal conductance and leaf temperature may be explained by two factors. Firstly, reduced UV radiation meant there was limited, if any, UV+ induced stomatal closure. Secondly, the difference in the transmission of PAR and total radiation would induce stomatal opening and increase leaf radiation loading in UV+ poly tunnels respectively. PAR was significantly greater in UV+ poly tunnels (Fig. 5.11a). Two of the main components of PAR, red and blue light, both stimulate stomatal opening (Shimazaki *et al.*, 2007), counteracting any UV-induced stomatal closure. Additionally, an increase in PAR can enhance photosynthesis causing stomatal opening to facilitate greater CO₂ uptake (Ballarè, 2014). Thus, these two mechanisms of stomatal opening, in addition to reduced UV radiation that limited UV-induced stomatal closure, act to increase stomatal conductance in UV+ poly tunnels compared to UV-. Furthermore, a greater radiation loading would enhance

leaf temperature, in conjunction with reduced stomatal closure, which can therefore explain why leaf temperature was significantly warmer in UV+ treated plants even when this was not consistent with stomatal conductance. This cannot be related to higher air temperature within UV+ polytunnels compared to UV- because air temperature did not differ when leaf temperature was measured (Fig. 5.10). These mechanisms, acting in different directions, can decouple stomatal conductance and leaf temperature.

Leaf warming unrelated to reduced stomatal conductance was observed in the climate cabinet experiments (Chapter 3). The mechanism had similarities to that observed in the polytunnels but the source was entirely different. In the climate cabinet experiments, direct radiative heating from the UV lamps caused leaf warming, which was evident when the UV lamp was switched on. The lamp acted similarly to the effect of greater PAR and total radiation observed in UV+ polytunnels compared to UV-. When the lamp was switched on, plants were irradiated not only with UV radiation, but also additional PAR and infrared radiation that heated the leaves in addition to the effect of UV-induced partial stomatal closure (Chapter 3). This was not observed in the controlled environment room experiments (Chapter 4) due to the different methodology of leaf temperature measurement (inside an environmentally controlled cuvette) minimising differences in radiation loading when UV+ and UV- treated plants were measured. This indicates that the effect of radiative heating observed in the climate cabinet also occurs when comparing leaf temperature between UV+ and UV- polytunnels.

Total radiation, which constitutes radiation loading, was significantly greater in UV+ polytunnels than UV- (Fig. 5.11b). However, the total radiation measured only

included 290-800 nm whereas in reality infrared radiation extends much further upwards, and the 700-1200 nm portion is largely reflected or transmitted through the leaf, meaning this ‘total radiation’ does not include the portion of infrared radiation >1200 nm that is absorbed by water in the leaf (Lambers *et. al.*, 2008). This will be investigated further by assessing net radiation under the same plastics in poly tunnels in Turkey (Chapter 6).

5.4.3 Reversible Partial Stomatal Closure in Response to Changing UV Irradiance

The variation in solar irradiance, a proxy for UV irradiance, between and within the separate experiments, facilitated analysis of the stomatal response to changing UV radiation. As discussed above, there are elements of solar radiation (PAR) that act to open stomata, but it is clear from the results that UV treatments caused partial stomatal closure, therefore these mechanisms were outweighed by the effect of UV radiation on stomatal closure (Section 5.3). When solar irradiance was not substantially affected by cloud in Experiments 1 and 2, stomatal conductance was clearly and consistently decreased (Figs. 5.4 and 5.9a). When solar irradiance was substantially reduced by cloud during Experiment 4, the difference between treatments reversed, with higher stomatal conductance in response to UV+ compared to UV- (Fig. 5.6 and 5.9a). This demonstrates a readily reversible response of stomata to UV radiation dependent on the UV irradiance or dose.

Although neither UV irradiance or dose were directly measured during each experiment, the solar irradiance data acts as a proxy of UV irradiance, which shows that UV irradiance affected by cloud cover reduced by >50% during Experiment 4 compared to Experiments 1 and 2 (Fig. 5.4 and 5.6). Mean daily solar irradiance (total

radiation: 400-800 nm) in Experiment 4 was 3580 W m^{-2} (Tab. 5.3), only 54% of the solar radiation during Experiment 1 (6678 W m^{-2} daily mean; Tab. 5.3) and 53% of solar radiation during Experiment 2 (6714 W m^{-2} daily mean; Tab. 5.3). This demonstrates that solar irradiance, and therefore UV radiation, caused UV+ treated leaves to exhibit reduced stomatal conductance in Experiments 1 and 2 but the opposite response occurred in Experiment 4 when it was reduced by cloud. This interpretation of these data is substantiated by the sequence of results during Experiment 3. As solar radiation was reduced by cloud cover towards the end of the week, the difference in stomatal conductance between treatments gradually diminished until it had reversed on the final day, whereas leaf temperature did not, as these parameters decoupled (Section 5.3.3; Fig. 5.5).

Regression analysis of daily cumulative solar radiation and the difference in stomatal conductance between UV+ and UV- polytunnels demonstrates a significant negative relationship exists where increasing solar radiation can explain 48% of the decrease in stomatal conductance when all experiments were combined (Fig. 5.9a). The R^2 may have been considerably higher if variation in ambient air temperature had not affected stomatal conductance between each experiment. Under similar solar radiation conditions ($\sim 7000 \text{ W m}^{-2}$) stomatal conductance ranged $95\text{-}963 \text{ mmol m}^{-2} \text{ s}^{-1}$ (Fig. 5.9a), the lower conductances were observed during Experiment 1 when mean leaf temperatures were $32\text{-}36^\circ\text{C}$ and the higher conductances occurred during Experiment 4 when mean leaf temperature was $16\text{-}33^\circ\text{C}$. Leaf temperature broadly followed stomatal conductance (Fig. 5.9b), in a positive relationship with solar radiation, but rather than completely reverse the response when solar radiation reduced the difference between treatments only narrowed, remaining higher in UV+ polytunnels in an example of the decoupling of stomatal conductance and leaf temperature.

There are no apparent previous reports of solar UV-induced reversible stomatal responses on these timescales (days), perhaps because most UV exclusion studies operate over longer timescales (weeks or months) measuring leaf gas exchange parameters at the end of the treatment period, or weekly at most, and very few do this on a daily basis. Equally, such UV exclusion studies often occur in locations where conditions do not vary much, making it difficult to evaluate. A glasshouse experiment using supplemental UV-B lighting found that plants previously exposed to UV-B and transferred to a zero UV-B environment increased stomatal conductance significantly after 24 hours, a similar timescale to this study (Noguès *et al.*, 1999). However, over the following 4 days, conductance reverted back to that previously observed when exposed to UV-B (Noguès *et al.*, 1999), which was not apparent in this study. Perhaps that difference is a result of the UV doses applied: $32 \text{ kJ m}^{-2} \text{ d}^{-1}$ (GPAS; Noguès *et al.*, 1999) which is very high, and $11.3 \text{ kJ m}^{-2} \text{ d}^{-1}$ (GPAS) in this study (Tab. 5.1), but the observed recovery over 24 hours, and the apparent stomatal opening and closing within the same experiments in this study (Figs. 5.5-5.6), indicates there was no irreparable damage to stomatal guard cell functioning allowing a variable temporal response to changing UV radiation.

5.5 Conclusions

Enhanced leaf temperature in UV+ poly tunnels compared to UV- was partly caused by reduced stomatal conductance. This was evident when solar irradiance, and therefore UV irradiance, was at or near maximum but not so when it was substantially reduced. UV-induced partial stomatal closure was inferred as the cause of reduced stomatal conductance because experiments were conducted on fully expanded leaves over a duration that was insufficient to allow changes in stomatal frequency. UV-

induced partial stomatal closure causing increased leaf temperature has been consistently observed in the three experimental campaigns conducted so far (Chapters 3, 4 and current) in different experimental environments and timescales. Maximum leaf temperature increases were consistent with previous reports, both commercial and scientific, but were considerably greater than observed in the experiments conducted in controlled environments (Chapters 3 and 4), which probably reflects differences in the radiation loading that exist between artificial and solar radiation conditions.

Changeable solar and UV radiation conditions appeared to induce a readily reversible stomatal conductance response. When solar radiation and thus UV radiation was decreased by cloud the direction of stomatal conductance response reversed, decoupling from leaf temperature that remained greater in UV+ polytunnels. This decoupling of leaf temperature and stomatal conductance indicated leaf warming unrelated to stomatal closure. This was caused by greater PAR and total radiation transmission in UV+ polytunnels compared to UV-, which enhanced radiation loading and leaf temperature as the UV effect of stomatal closure diminished. These radiation transmission differences between the plastic claddings require further investigation in both scientific studies and commercial protected cultivation of crops. This will be undertaken in polytunnel experiments in Antalya (Turkey; Chapters 6 and 7) where the effect of radiation loading is likely to be greater than in the UK, and is a location where commercial protected cultivation is prevalent.

6 Antalya (Turkey) Part A: Leaf Temperature and Gas Exchange Responses to Ultraviolet Radiation in Polytunnels

6.1 Introduction

This chapter builds on the work undertaken in polytunnels at Lancaster by applying similar UV treatments in a location where commercial protected crop cultivation in polytunnels is extensive. This finalises the link from understanding the fundamental leaf responses to UV radiation (Chapter 3), the bridge from those acute UV treatments to longer term 6-day experiments (Chapter 4), to the multi-day experiments in small polytunnels at Lancaster (UK; Chapter 5) and Antalya (current chapter).

In the polytunnels at Lancaster, UV radiation induced partial stomatal closure that enhanced leaf temperature, corroborating the findings of the controlled environment experiments (Chapter 3 and 4) and those from commercial growers (Chapter 1). The

observed maximum leaf temperature increase of 2.2°C was similar to the report from commercial growers in Turkey (1.9°C; Williams *et al.*, 2020) and a study in the Czech Republic (~2°C: Novotná *et al.*, 2016), demonstrating a consistent response of leaf temperature to UV radiation in the field under plastics. Various studies have shown that stomatal conductance increases when UV radiation is excluded (e.g. Kataria *et al.*, 2014), because of stomatal opening (Kataria and Guruprasad, 2015), but these studies generally occur over multiple weeks and even months compared to the duration of UV exclusion experiments in this thesis (Chapter 5 and current). Together with the results thus far in this thesis, these findings demonstrate UV radiation causes partial stomatal closure that would be expected, or has been observed, to increase leaf temperature.

A readily reversible UV radiation response was also observed in the polytunnels at Lancaster (Chapter 5), caused by variable cloud cover and thus solar irradiance. Stomata re-opened after initial UV-induced closure while leaf temperature remained higher in those leaves, in an apparent decoupling of stomatal conductance and leaf temperature. This indicated leaf warming unrelated to stomatal closure also occurred. Radiation measurements showed that PAR and total radiation transmission was significantly greater through the UV-transparent plastic cladding (UV+) than the UV-opaque cladding (UV-), which probably caused leaf warming unrelated to stomatal closure, which will be investigated further in Antalya.

The ultimate aim of this project was to test the findings gleaned in controlled environment settings in the ‘real world’ of polytunnels in a location where protected cultivation is prevalent. The work in this chapter is similar to that of the last (Chapter 5) in that the small polytunnel structures are almost identical (purpose-built in Turkey with equal dimensions) to those used in Lancaster. The differences between

experiments were the climate (hotter), radiation loading (greater due to lower latitude), tomato cultivar (unfortunately the 'Money Maker' cultivar was not adapted to the extremely hot conditions of Turkey, so a local Turkish cultivar was used) and the method of data collection.

Only leaf temperature and stomatal conductance data were obtained in Lancaster due to unavailability of the leaf gas exchange analyser (Chapter 5), thus in Antalya it was used to allow simultaneous measurements of transpiration and assimilation rate to assess water use efficiency, following a similar method to the controlled environment experiments (Chapters 3 and 4). Additionally, extensive radiation measurements were undertaken to detect differences in the transmission properties of the UV-transparent and opaque plastic claddings to determine whether the differences observed in Lancaster were consistent, and the repercussions for leaf temperature. Radiation was measured with two separate methods: with the same PAR and total radiation sensors as used in Lancaster for direct comparison (current chapter), and with a 4-way net radiometer that has a 300-42000 nm range to understand downwelling and upwelling of short and longwave radiation balance within the polytunnels (Chapter 7), important components of leaf energy balance (Eq. 1.1). The plant and radiation data from Antalya are presented in two separate chapters.

Based on the work already conducted (Chapters 3-5), it was predicted that partial stomatal closure would reduce stomatal conductance and transpiration rate causing an increase in leaf temperature. Photosynthesis and water use efficiency will also be investigated to determine how each is affected in comparison to the previous inconclusive work (Chapters 3 and 4). Following the results observed in Lancaster (Chapter 5), it was hypothesised that transmission of PAR and total radiation would be

greater in UV+ polytunnels compared to UV-, contributing to enhanced leaf temperature in those polytunnels.

6.2 Materials and Methods

Two separate experiments were conducted in Antalya (Turkey). The first between 15-21 October 2018 (Appendix 2) and the second from 27 June until 2 July 2019. The location, polytunnels, plastics, plant materials, leaf gas exchange measurements and statistical analyses were identical in each, as described below. The only differences between the experiments were the duration (6 days in 2018 and 5 days in 2019) and the UV irradiances and doses (due to time of year). In 2018, the UV irradiances were 77%, and doses 63%, of those present in 2019 due to lower ambient UV irradiance and shorter day length.

6.2.1 Poly tunnels and UV Radiation Treatments

The experimental setup was designed to replicate that used in Lancaster (Chapter 5) as closely as possible, but with two additional polytunnels for greater replication. The experiments were conducted in six small polytunnel structures located at the premises of Arideyilik Teknoloji Tarım, Antalya, Turkey (36.942754 N, 30.815311 E). The polytunnels were purpose built in Turkey to replicate the polytunnels used in Lancaster (UK; Chapter 5; Fig. 6.1). These consisted of a metal frame (LxWxH: 3.0 x 1.5 m x 2.25 m) with an internal metallic mesh bench inside (LxW: 1.85 x 1.25 m) raised 0.75 m above the ground leaving space at each end for a user to work inside. Plastic cladding was only fitted down to the bench level to allow ventilation inside the polytunnels, along with a small opening at the top of the north-facing end.



Figure 6.1: The six small polytunnel structures located at the premises of Arideyilik Teknoloji Tarım, Antalya, Turkey (left) and the inside of one of those polytunnels showing the internal metallic mesh bench (right).

The polytunnels were clad with the same plastics as those used in Lancaster (Chapter 5). Three polytunnels were clad with UV-transparent plastic film (UV+; Lightworks Sun Smart: Arid Agritec, Lancaster, UK; Fig. 6.2) that transmitted 48% of solar UV radiation, and three with UV-opaque plastic film (UV-; Lightworks Sun Master: Arid Agritec, Lancaster, UK; Fig. 6.2) that transmitted 3% of solar UV radiation. The spectral transmission of the plastics was measured in the laboratory (Section 2.3; Fig. 6.2).

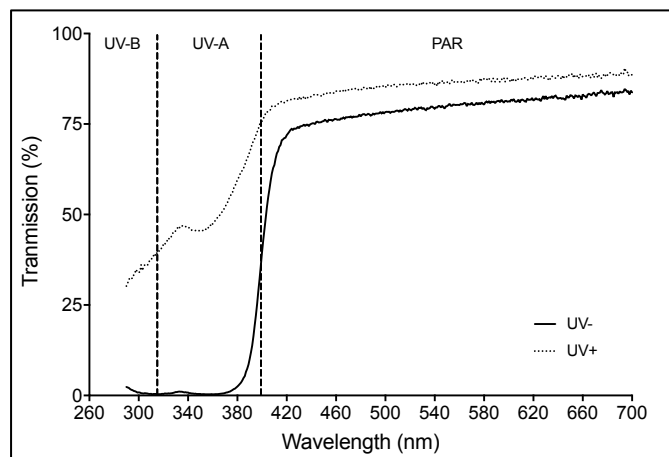


Figure 6.2: Spectral transmission (260-700 nm) of the UV-transparent (UV+; Lightworks Sun Smart) and UV-opaque (UV-; Lightworks Sun Master: Arid Agritec, Lancaster UK) plastic films when first exposed to solar radiation on the polytunnel structures. UV-B, UV-A and photosynthetically active radiation (PAR) wavelength ranges are highlighted.

The UV radiation transmission of the UV+ plastic was considerably lower (-25%) than for the same plastics used in Lancaster (Chapter 5). The same manufacturer

produced the plastics but information supplied (Sobeih, W., Arid Agritec Ltd., personal communication) confirms there is a 5-7% tolerance for the transmission for plastics produced by the same machine (as was the case). The polytunnels were clad with these plastics 8 months earlier and thus were not entirely clean, and accumulated dust can reduce transmission by ~10% (Sobeih, W., Arid Agritec Ltd., personal communication). Plastic ageing will also have altered the optical properties to a small extent. There is also the measurement uncertainty associated with the sensors used for transmission measurement. Clearly there are various reasons for the difference in UV transmission between essentially the same plastics.

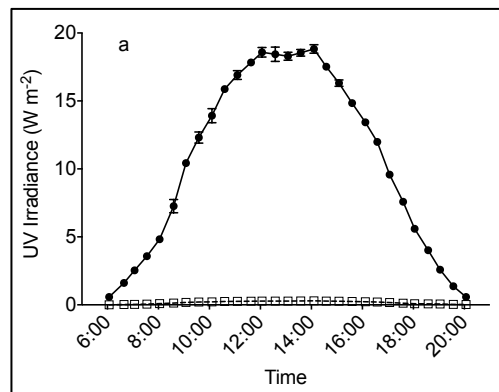


Figure 6.3: Typical unweighted UV (280-400 nm) irradiance under the UV-transparent (UV+; Lightworks Sun Smart; closed circles) and UV-opaque (UV-; Lightworks Sun Master; Arid Agritec Ltd., Lancaster UK; open squares) plastic films on a clear sunny day during the experimental period in Antalya, Turkey. Error bars represent ± 1 SE ($n=3$) but if not visible they were smaller than the symbol.

Solar radiation transmission was quantified on a clear sunny day immediately prior to the experimental period with broadband radiation sensors (Section 2.2). A typical UV radiation profile under each type of plastic on a clear sunny day is provided as an example (Fig. 6.3), with additional daily UV irradiances and doses (Tab. 6.1). UV treatments are expressed as mean unweighted irradiances and doses of total UV (280-400 nm), UV-A (315-400 nm) and UV-B (280-315 nm). It was not possible to calculate weighted UV irradiances and doses from the broadband data. However, the

unweighted values may be compared with the unweighted values referenced in other chapters.

Table 6.1: Unweighted maximum irradiances and daily doses applicable to the UV+ and UV- poly tunnels consisting of total UV, UV-A and UV-B radiation.

UV Treatment	Unweighted UV Irradiance 280-400 nm ($W m^{-2}$)	Unweighted UV Dose 280-400 nm ($kJ m^{-2}$)	Unweighted UV-A Irradiance ($W m^{-2}$)	Unweighted UV-A Dose ($kJ m^{-2}$)	Unweighted UV-B Irradiance ($W m^{-2}$)	Unweighted UV-B Dose ($kJ m^{-2}$)
UV+	18.8	551	17.6	519	1.2	32
UV-	0.294	9.0	0.287	8.9	0.007	0.1

6.2.2 Plant Material

Two tomato cultivars were envisaged, ‘Money Maker’ because it was used in the previous chapters and a commercially produced Turkish cultivar to provide a direct link to the original reports from commercial growers of UV-induced increased leaf temperature that instigated this project. However, the ‘Money Maker’ plants grew very slowly compared to the Turkish variety, with a stomatal conductance $<100 \text{ mmol m}^{-2} \text{ s}^{-1}$. This was probably a result of heat stress caused by high temperatures within the poly tunnels (up to 50°C) that the Turkish cultivar was accustomed to. Therefore, only the Turkish cultivar was used (*Solanum lycopersicum* cv. ‘STILL F 41’) for experimentation.

The plants were propagated in the absence of UV-B radiation in a poly tunnel clad with standard plastic (transmittance of PAR: 93%, UV-A: 33%, UV-B: $<1\%$) at a local seedling nursery (Lider Fide, Altiyak Mah, 8275 Sokak, No. 34 Kepez, Antalya, Turkey). Seeds sown in modular tray inserts containing a peat-based substrate (Greenterra Professional, Greenterra Ltd., Riga, Latvia) were at the 3-leaf stage (~ 3 weeks old depending on the season) when they were transplanted individually into 2 L pots (150 mm diameter) containing the same substrate. At the 4-

leaf stage (after ~4 weeks of growth from seed), the 36 most uniform plants were selected and distributed evenly between the six polytunnels with different UV treatments. Each polytunnel received 6 plants, based on their physiological properties (leaf temperature, transpiration rate, stomatal conductance, assimilation rate and instantaneous water use efficiency) measured in the absence of UV-B radiation, to ensure any subsequent differences resulted from UV radiation and not pre-treatment physiology. A leaflet from the most recent fully developed leaf pair on the 3rd internode was used for the experiments. Plant positions on the bench were rotated daily to eliminate any positional effects of variation in radiation.

6.2.3 Leaf Gas Exchange and Temperature Measurements

Leaf gas exchange and temperature measurements were made using a LI-6400XT (LI-COR Inc., Lincoln, NE, USA). The LI-6400XT light emitting diode (LED) cuvette attachment provided the specified PAR ($1600 \mu\text{mol m}^{-2} \text{s}^{-1}$), without any UV radiation, to the experimental leaf enclosed inside. To avoid any effect of spatial heterogeneity in temperature or radiation loading inside the polytunnels on leaf temperature measurements, the LED cuvette attachment provided air temperature control and constant radiation. Once a leaf was enclosed inside the cuvette, the internal environment (cuvette block temperature: 40°C , relative humidity: 20-30%, CO_2 : 400 ppm, flow rate: $500 \mu\text{mol s}^{-1}$) was allowed to stabilise (1-2 minutes) before data was recorded. These settings were selected because they closely matched the conditions inside the polytunnels. All leaf gas exchange measurements were centred around solar noon to minimise effects of diurnal variation in stomatal conductance. Since leaf gas exchange and temperature measurements occurred inside an environmentally controlled cuvette, any differences in polytunnel air temperature could not affect leaf temperature during measurement.

6.2.4 Data Analysis

The results are presented as the absolute post-UV treatment values for each parameter, except leaf temperature where the absolute change in ($T_{leaf}-T_{air}$) (see Section 2.6 for explanation) was used to account for any variations in air temperature that could swamp the small leaf temperature changes expected, based on the previous experiments (Chapters 3-5).

6.2.5 Statistical Analysis

These data were tested for normal distribution and equal variances in SPSS version 18 (SPSS Inc. Chicago, USA). The plant data were statistically analysed for differences between the UV treatments (UV+ / UV-) using a repeated measures ANOVA in SPSS, with UV treatment and polytunnel as the main factors, and day as the repeated measure. The PAR and total radiation data were also analysed in SPSS using a repeated measures ANOVA with treatment (plastic type) as the main factor and time of day as the repeated measure. To determine daily differences between UV radiation treatments, unpaired t-tests were performed for each day (corrected for multiple comparisons) using the Sidak-Bonferroni method, in GraphPad Prism version 7.0d for Mac OS X (GraphPad Software, La Jolla California USA, www.graphpad.com).

6.3 Results

The results from 2018 (October) are summarised separately because there was very little difference between UV treatments due to the substantially lower UV irradiances and doses caused by the difference in season to the 2019 experiment (June/July; Section 6.2; Appendix 2). The following results relate solely to the experiment conducted in 2019.

6.3.1 Plant Responses to UV Radiation Treatments

Although there was a significant effect of polytunnel for all parameters ($P < 0.01$; Tab. 6.2) except transpiration rate ($P = 0.485$; Tab. 6.2) this did not interact with the treatment response ($P > 0.05$; Tab. 6.2). Leaf temperature, relative to air temperature ($T_{leaf} - T_{air}$), was significantly higher in UV+ polytunnels compared to UV- ($P < 0.001$; Fig. 6.4a) over the 5 days of treatment. Leaf temperature varied between days ($P < 0.001$; Fig. 6.4a) due to daily variations in ambient air temperature. The treatment response also varied between days ($P < 0.001$; Fig. 6.4a) with the magnitude of difference between treatments (up to $0.65 \pm 0.21^\circ\text{C}$; Fig. 6.4a) fluctuating daily, with little difference between treatments on days 1 and 4. This in part caused the significant interaction between treatment, polytunnel and day ($P = 0.011$; Tab. 6.2), which was caused by leaf temperature that was greater in two UV- polytunnels than UV+ on day 1 only. The lack of difference between treatments on day 1 appears to be caused by a delay on the response to UV radiation, but there is no apparent explanation for the similarity between treatments on day 4 as temperature and solar conditions were consistent. This demonstrates that UV radiation increased leaf temperature but the difference between treatments varied daily.

This leaf temperature response coincided with significantly reduced transpiration rate ($P = 0.036$; Fig. 6.4b) in UV+ treated plants that was up to $1.31 \pm 0.64 \text{ mmol m}^{-2} \text{ s}^{-1}$ lower (16%; mean: $0.76 \pm 0.56 \text{ mmol m}^{-2} \text{ s}^{-1}$) than UV- treated plants. Transpiration rate fluctuations were significant from day to day ($P = 0.094$; Fig. 6.4b), but this did not interact with the treatment effect ($P = 0.085$; Fig. 6.4b), as the daily fluctuations in the treatments differences were not as clear as they were for leaf temperature. Stomatal conductance was also significantly enhanced by UV exclusion (treatment: $P = 0.010$; Fig. 6.4c) by up to $34 \pm 18 \text{ mmol m}^{-2} \text{ s}^{-1}$ (19%; mean: $15 \pm 15 \text{ mmol m}^{-2} \text{ s}^{-1}$). There were

fluctuations between days ($P < 0.001$; Fig. 6.4c) that, unlike transpiration rate, interacted with the effect of treatment ($P = 0.004$; Fig. 6.4c), perhaps reflecting the response on day 1. UV radiation reduced transpiration rate and stomatal conductance in UV+ polytunnels.

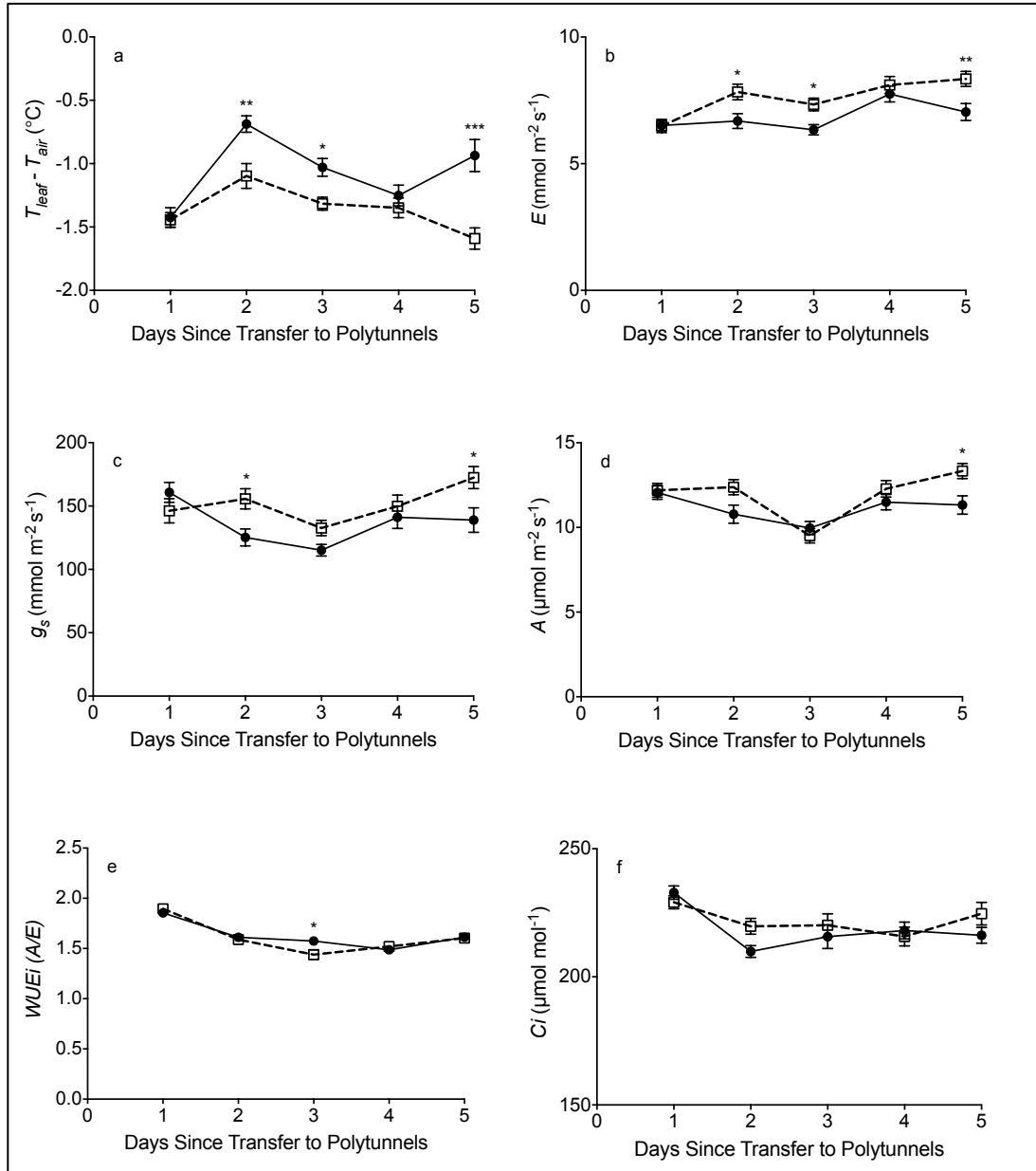


Figure 6.4: Antalya 2019: The response to UV+ (black circles and solid line) and UV- (open squares and dashed line) treatments of (a) leaf temperature ($T_{leaf} - T_{air}$), (b) transpiration rate (E), (c) stomatal conductance (g_s), (d) assimilation rate (A), (e) instantaneous water use efficiency (WUE_i), and (f) intracellular CO₂ (C_i). The asterisks represent individual days where there was a significant difference between treatments (*: $P < 0.05$; **: $P < 0.01$; ***: $P < 0.001$) corrected for multiple t-tests. Summary of repeated measures ANOVA analysis of the whole treatment period are highlighted. Cuvette temperature was 40°C during measurements. Error bars represent ± 1 SE ($n = 18$) but if not visible they were smaller than the symbol. See Table 6.2 for full ANOVA analysis.

UV radiation (UV+) significantly reduced assimilation rate ($P=0.009$; Fig. 6.4d) by up to $2.01 \mu\text{mol m}^{-2} \text{s}^{-1}$ (15%; mean: $0.82 \pm 0.91 \mu\text{mol m}^{-2} \text{s}^{-1}$). There were also daily fluctuations ($P < 0.001$; Fig. 6.4d) that affected the magnitude and even direction (day 3) of the treatment response ($P=0.011$; Fig. 6.4d). The simultaneous reductions in transpiration and assimilation rates resulted in no significant effect of UV radiation on instantaneous water use efficiency (WUE_i ; $P=0.350$; Fig. 6.4e). The maximum difference in WUE_i was $0.13 \mu\text{mol CO}_2 / \text{mmol H}_2\text{O}$ greater in UV+ treated plants (9%; mean: $0.02 \pm 0.07 \mu\text{mol CO}_2 / \text{mmol H}_2\text{O}$). This indicates that these transpiration and assimilation rates reduced proportionally. Even so, WUE_i fluctuated between days ($P < 0.001$; Fig. 6.4e) but this did cause significant fluctuations in the treatment response ($P=0.028$; Fig. 6.4e). Intracellular CO_2 was not significantly affected by the UV treatments ($P=0.178$; Fig. 6.4f) although could be up to $10 \mu\text{mol mol}^{-1}$ lower in UV+ polytunnels (5%; mean: $3 \pm 7 \mu\text{mol mol}^{-1}$). Again, C_i fluctuated from day to day ($P < 0.001$; Fig. 6.4f), and did significantly affect the treatment response to UV radiation ($P=0.038$; Fig. 6.4f). Simultaneous UV-induced reductions in assimilation rate and transpiration rate led to no substantial change in WUE_i .

Table 6.2: Summary of P values for each factor and factor interaction from the repeated measures ANOVA analysis for leaf temperature ($T_{leaf} - T_{air}$), transpiration rate (E), stomatal conductance (g_s), assimilation rate (A), intracellular CO_2 (C_i) and instantaneous water use efficiency (WUE_i) for the experiment in 2019.

ANOVA Factors	$T_{leaf} - T_{air}$	E	g_s	A	C_i	WUE_i
Treatment	<0.001***	0.036*	0.010*	0.009**	0.178	0.350
Polytunnel	0.006**	0.485	0.001**	<0.001***	<0.001***	0.002**
Day	<0.001***	<0.001***	<0.001***	<0.001***	<0.001***	<0.001***
Treatment x Polytunnel	0.124	0.219	0.220	0.529	0.832	0.404
Treatment x Day	<0.001***	0.085	0.004**	0.011*	0.038*	0.028*
Polytunnel x Day	<0.001***	<0.001***	<0.001***	<0.001***	<0.001***	<0.001***
Treatment x Polytunnel x Day	0.011*	0.532	0.053	0.317	0.413	0.073

6.3.2 Relationship Between Stomatal Conductance and Leaf Temperature

Linear regression analysis demonstrated leaf temperature (T_{leaf} and $T_{leaf} - T_{air}$) of UV+ treated plants significantly ($P < 0.001$; Fig. 6.5) increased as stomatal conductance decreased. Stomatal conductance explained 85% of $T_{leaf} - T_{air}$ and 80% of T_{leaf} increases (Fig. 6.5). The slopes of the relationship for each were very similar, indicating that leaf temperature would increase 0.7-0.8°C for each 100 $\text{mmol m}^{-2} \text{s}^{-1}$ decrease in stomatal conductance. (Fig. 6.5). Thus UV-induced stomatal closure caused leaf warming.

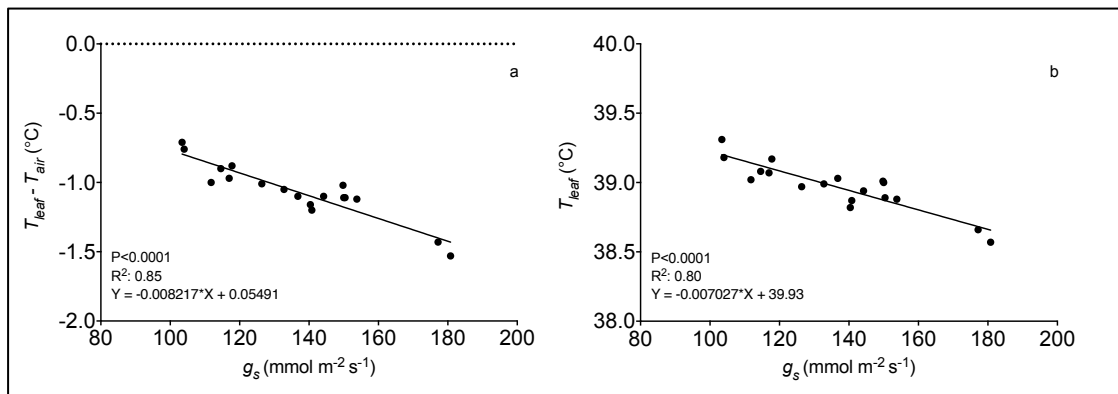


Figure 6.5: Linear regression analysis of daily (a) stomatal conductance and leaf temperature ($T_{leaf} - T_{air}$), and (b) stomatal conductance and leaf temperature (T_{leaf}), of UV+ treated plants only (UV- data are excluded in order to analyse the relationship when UV radiation is present). The results of linear regression analysis are summarised. Each data point represents an individual plant ($n=18$).

6.3.3 Total and Photosynthetically Active Radiation Transmission

Photosynthetically active radiation (PAR: 400-700 nm) was significantly greater ($P=0.002$; Fig. 6.6a) in UV+ poly tunnels than UV-. PAR varied significantly diurnally (time: $P < 0.001$; Fig. 6.6a) as expected. There was a significant interaction between treatment and time ($P < 0.001$; Fig. 6.6a) because the difference between poly tunnels predominantly occurred between 10:00–16:30, with the greatest difference occurring around solar noon (up to $350 \pm 107 \mu\text{mol m}^{-2} \text{s}^{-1}$; 22%; Fig. 6.6a). This demonstrates

that PAR was substantially greater in UV+ polytunnels for ~6.5 hours around solar noon when PAR was greatest.

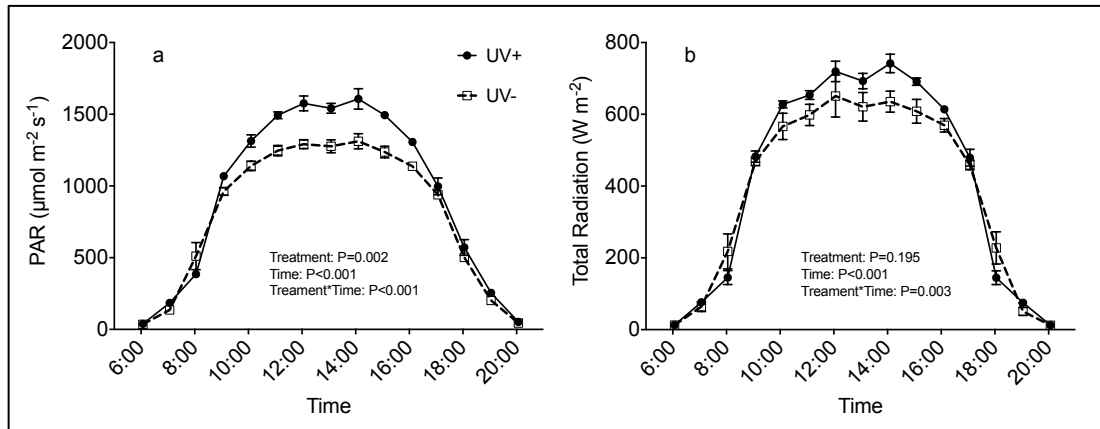


Figure 6.6: Time courses of (a) Photosynthetically active radiation (PAR: 400-700 nm) and (b) total radiation (310-2800 nm) inside the UV+ (black circles and solid line) and UV- (open squares and dashed line) polytunnels. Summary of repeated measures ANOVA analyses are highlighted. Error bars represent ± 1 SE (n=3) but if not visible they were smaller than the symbol.

Total (solar) radiation (310-2800 nm) did not significantly differ between the differently clad polytunnels ($P=0.195$; Fig. 6.6b). Total radiation varied significantly with time ($P<0.001$; Fig. 6.6b), as expected with solar radiation. There was a significant interaction between treatment and time ($P=0.003$; Fig. 6.6b), reflecting the consistently greater total radiation in UV+ polytunnels between 10:00–16:30 (up to $107 \pm 41 \text{ W m}^{-2}$; 20%; Fig. 6.6b) whereas it was marginally lower in UV+ polytunnels in the morning and evening (Fig. 6.6b). Although total radiation was not significantly greater in UV+ polytunnels, it was consistently higher for ~6.5 hours around solar noon when total radiation peaks.

6.4 Discussion

As in previous chapters, exposing leaves to UV radiation decreased stomatal conductance and transpiration rate, which contributed to the increase in leaf temperature (Fig. 6.4abc). This can be inferred as UV-induced partial stomatal closure due to the duration of UV exposure in fully mature leaves. These findings corroborate

the results derived in a range of different experimental locations and with different methodologies (Chapters 3-5). It also corroborates the original reports from commercial growers in Turkey of higher leaf temperature under UV-transparent plastic cladding (Williams *et al.*, 2020) and the only scientific report that relates UV radiation to leaf warming (Novotná *et al.*, 2016). Stomatal conductance and leaf temperature were strongly inversely correlated (Fig. 6.5), with reduced conductance explaining a similar proportion of the leaf temperature increase as observed in the poly tunnels at Lancaster (~80%; Fig. 5.7). It is therefore clear from the leaf temperature and gas exchange responses to UV radiation that partial stomatal closure contributes to an increase in leaf temperature in UV+ poly tunnels compared to UV-.

When the season substantially reduced (maximum irradiance: -37%, daily dose: -57%; Appendix 2) UV radiation in the experiments at Antalya in October 2018, there were no significant differences between UV+ and UV- treatments for all measured parameters measured within the LI-6400XT cuvette. This demonstrates that a certain threshold of UV radiation is required to stimulate stomatal closure, so does not occur all year round, even at latitudes as far south as southern Turkey. That threshold may well be different under solar radiation compared to the artificial radiation in the climate cabinet experiments, due to differences in the spectral composition of the radiation applied (solar or lamps).

Perhaps even more interesting was the significant leaf temperature increase that was measured with the infrared thermometer, at the same time, in UV+ poly tunnels compared to UV- (Appendix 2). The LI-6400XT detected only a 0.08°C increase in UV+ poly tunnels but a 0.29°C increase when measured with the infrared thermometer. This indicates that leaf warming attributable to radiative heating caused

by greater radiation loading in the UV+ polytunnels was 0.21°C (Fig. 6.8), in the absence of significant UV-induced stomatal closure. This demonstrates that radiative heating occurs even when UV radiation is insufficient to cause stomatal closure.

The UV-induced leaf temperature increase observed here ($0.65\pm 0.21^{\circ}\text{C}$; Fig. 6.4) was considerably lower than observed in polytunnels at Lancaster ($2.2\pm 1.6^{\circ}\text{C}$; Chapter 5) for two reasons. Firstly, the magnitude of stomatal conductance reductions, which is used as a proxy for transpiration rate because that is not available for the Lancaster work, varied between the two data sets. In this study stomatal conductance was up to $34\pm 18\text{ mmol m}^{-2}\text{ s}^{-1}$ (19%; mean: $15\pm 15\text{ mmol m}^{-2}\text{ s}^{-1}$) lower in response to UV radiation but in Lancaster it was up to $156\pm 88\text{ mmol m}^{-2}\text{ s}^{-1}$ lower (34%; mean: $108\pm 63\text{ mmol m}^{-2}\text{ s}^{-1}$). Such variability was attributed to differences in ambient UV radiation transmitted into the UV+ polytunnels in each location. Unweighted UV radiation in UV+ polytunnels in Antalya was $551\text{ kJ m}^{-2}\text{ d}^{-1}$ (Tab. 6.1) but the greater transmission of UV-transparent cladding in Lancaster (72% compared to 43%) meant the unweighted UV dose was $640\text{ kJ m}^{-2}\text{ d}^{-1}$ (Section 5.2.2; Tab. 5.1). These absolute and percentage differences are proportionally very large which can partially explain the difference in leaf temperature increase between the two locations.

Secondly, although PAR and total radiation transmission in UV+ polytunnels in Antalya (Fig. 6.6) was very similar to that observed in the polytunnel experiments at Lancaster (Fig. 5.11), the method of measuring leaf temperature differed. In Antalya, leaves were enclosed within the cuvette of the leaf gas exchange analyser using the LED attachment, thus eliminating differences in radiation loading between treatments during measurements. In Lancaster, remote measurements with an infrared thermometer allowed exposure of leaves to solar radiation throughout measurement,

with a radiation loading difference between UV+ and UV- polytunnels causing additional leaf warming beyond that caused by stomatal closure alone. Combined UV-induced stomatal closure and differences in radiation loading between polytunnels / plastics can also explain why the originally reported leaf temperature increases observed in Turkey (1.9°C: Williams *et al.*, 2020) and the Czech Republic field experiment (Novotná *et al.*, 2016) were similarly high compared to the work in Antalya 2019. UV-induced partial stomatal closure coupled with a greater radiation loading at the time of leaf temperature measurements, explains why observed leaf warming was greater in polytunnels at Lancaster than in Antalya. This demonstrates that the amount of leaf temperature increase depends on the degree of stomatal closure (dependent on the UV irradiance) and the radiation loading (dependent on the location / method of leaf temperature measurement). Together, UV-induced stomatal closure, that limits transpirational leaf cooling thus increasing leaf temperature, acts in conjunction with the direct radiative heating effect from the difference in PAR and possibly total radiation conditions between UV+ and UV- polytunnels, enhancing the overall leaf temperature warming in UV+ polytunnels.

6.5 Conclusions

This work corroborates the findings in previous chapters: that UV radiation increases leaf temperature by reducing transpiration rate as a result of partial stomatal closure. This response occurred in different experimental conditions and field locations, durations of UV radiation exposure, and using both artificial light and solar radiation. UV radiation substantially decreased photosynthesis in UV+ polytunnels even though greater PAR should enhance photosynthesis. The combined reductions in transpiration rate and assimilation rate caused no change in water use efficiency, also corroborating

the finding in Chapters 4 and 5 where UV application lasted 5-6 days rather than 90 minutes (Chapter 3). Identifying that UV+ polytunnels transmit more PAR, and to some extent total radiation, has not been reported previously. This indicates that UV-induced stomatal closure, enhanced PAR, and possibly total radiation, act together to increase leaf temperature in UV+ polytunnels in the field compared to UV- polytunnels. This is corroborated by evidence that leaf temperature was greater in UV+ polytunnels than UV- in Antalya in October (2018) even though UV-induced stomatal closure was minimal due to seasonally low UV radiation levels. Therefore, further investigation of both downwelling and upwelling components of solar and far infrared radiation in these differently clad polytunnels will help understand the radiation balance under each type of plastic cladding.

7 Antalya (Turkey) Part B: Radiation Balance in UV+ and UV- Polytunnels

7.1 Introduction

In the experimental work already presented the role of “radiation loading” in leaf temperature increases, in association with partial stomatal closure, has been referred to numerous times:

- Direct radiative heating was found to increase leaf temperature as a result of additional radiation transmission into the gas exchange analyser cuvette (Chapter 3).
- The effect of radiation loading on leaves explained differences in the reported UV-induced leaf warming, depending on the method used to measure leaf temperature (Chapters 4 and 5).
- The effect of differences between artificial lights and solar radiation on radiation loading (Chapter 5).

- A factor in decoupling leaf temperature from stomatal conductance when UV radiation was naturally reduced by cloud (Chapter 5).
- Identification of greater PAR and total radiation transmission into UV+ polytunnels (Chapters 5 and 6).

Evidence of a difference in non-UV radiation transmission between UV+ and UV- polytunnels was discovered during the first outdoor polytunnel experimental campaign (Chapter 5) and was subsequently observed in polytunnels at Antalya (Chapter 6). A difference in total radiation transmission between the UV+ and UV- polytunnels would affect radiation loading on leaves inside polytunnels. Thus radiation loading may contribute to leaf temperature differences. However, only measurement of UV, PAR and infrared radiation up to 2800 nm had been possible (Chapter 6). Therefore, prior to the work in Antalya, a 4-way net radiometer was purchased capable of measuring downwelling and upwelling total radiation (300-42000 nm; Fig. 7.1), to determine any differences in radiation balance between UV-transparent (UV+) and UV-opaque (UV-) polytunnels.

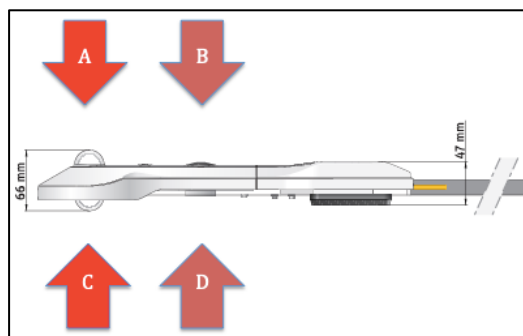


Figure 7.1: An image of the 4-way net radiometer (CNR4, Kipp and Zonen) demonstrating downwelling solar radiation (A), downwelling far infrared radiation (from sky: B), upwelling solar radiation (reflected from ground: C) and upwelling far infrared radiation (emitted by ground: D)

Total radiation is conventionally measured in two parts: (i) solar radiation (290-3000 nm) that comprises UV, PAR and near infrared radiation, and (ii) far infrared radiation (3000-42000 nm) that is effectively heat transfer (Lambers *et. al.*, 2008). Each part

affects temperature differently. Solar radiation is absorbed by black bodies (idealised physical bodies that absorb 100% of incident solar radiation due to lack of reflection) that increases temperature directly (Lambers *et. al.*, 2008). In reality bodies (objects) vary in their absorption dependent on their reflective properties. Differences in spatial heterogeneity of incident solar radiation, caused by glasshouse structure, has reportedly caused leaf temperature differences (Kaukoranta *et al.*, 2005) demonstrating the effect that differences in downwelling solar radiation may have on leaf temperature. Far infrared radiation is heat transfer that excites gaseous molecules in the air, warming it, which indirectly heats objects in contact with that air provided they are cooler (Lambers *et. al.*, 2008; Liang, 2013). Thus each element of total radiation affects leaf temperature, directly or indirectly, and the net balance of each equates to net (total) radiation, which indicates where radiation loading is greatest. Any effect of cladding on any element will determine which polytunnel leaves should be warmer if transpirational cooling is ignored.

Based on the discussion in previous chapters of radiation loading affecting leaf temperature, it was expected that:

- Downwelling solar radiation would be greater in UV+ polytunnels.
- This would proportionally enhance reflected upwelling solar radiation in UV+ polytunnels, as a result of ground albedo (consistent beneath the polytunnels).
- Net solar radiation would therefore be greater in UV+ polytunnels.
- Absorption of the greater downwelling solar radiation would enhance ground temperature beneath the UV+ polytunnels.
- Greater ground temperature would lead to enhanced upwelling far infrared radiation in UV+ polytunnels.

- Differences in the transmission (and so absorption) of upwelling far infrared radiation out of the polytunnels were not expected (and therefore).
- Differences in plastic temperature were not expected (and therefore).
- Differences in downwelling far infrared were not expected.
- Net far radiation was predicted to be greater in UV+ polytunnels due to the greater upwelling element.
- This would cause greater air temperature in UV+ polytunnels.
- It was predicted that greater net (total) radiation in UV+ polytunnels would increase the temperature of small pieces of black card (basic analogues of non-transpiring leaves) located in the polytunnels.

7.2 Material and Methods

7.2.1 Poly tunnels and UV radiation

The 4 day experiment was conducted in the same six small polytunnel structures as used for the plant experiment (Section 6.2.1). The polytunnels were clad with exactly the same plastics (UV+ / UV-) that exhibited equal radiation transmission described previously (Section 6.2.1).

7.2.2 Poly tunnel Radiation Balance

Total radiation inside the polytunnels was measured with a 4-way net radiometer (CNR4, Kipp and Zonen B. V., Delft, Netherlands; Fig. 7.2). The CNR4 radiometer has four sensors: two pyranometers measuring solar radiation (300-2800 nm) and two pyrgeometers measuring far infrared radiation (4500-42000 nm), with one of each sensor facing upwards to measure downwelling radiation, and downwards to measure upwelling radiation (Fig. 7.1). Total radiation was measured in the day and at night to determine how the net radiation balance differed when solar radiation was absent but

residual heat (ground) from the day remained. Day time radiation data was obtained between 12:15-13:45 for four consecutive days. Night time data was collected 00:30-01:30 for the three consecutive nights within these days. Each time the net radiometer was moved between polytunnels it was re-levelled. With only a single net radiometer available, the order of measurements in each polytunnel (UV+1, UV-1, UV+2, UV-2, UV+3, UV-3) was reversed each day to avoid any diurnal effect on results. Each data point for each polytunnel was the mean of two repeat measurements that were the mean of 1 minute of continuous data logging.



Figure 7.2: The inside of a polytunnel showing the internal metallic mesh bench, the Skye radiation sensors (left hand side) and the CNR4 net radiometer (right hand side).

The output from the pyrgeometer required a correction for pyrgeometer sensor surface temperature (Kipp & Zonen B. V., 2014),

$$E_{\text{corrected}} = E_{\text{uncorrected}} + 5.67 \times 10^{-8} * T^4 \quad (7.1)$$

Where the output E is the irradiance of downwelling far infrared and T (Kelvin) is the pyrgeometer sensor temperature. During the experimental field campaign in Antalya the internal temperature sensor was found to have failed but temperature of the pyrgeometer sensor was recorded with an infrared temperature meter (MI-220, Apogee Instruments, Logan, USA) pointed at the upper pyrgeometer sensor of the

CNR4. Subsequent discussion with the manufacturer confirmed that these data could be used in place of the internal temperature measurement (Clive Lee, Technical Sales and Services Manager, Kipp and Zonen). Net solar radiation was calculated as (Kipp & Zonen B. V., 2014),

$$\text{Net solar radiation} = (E \text{ upper pyranometer}) - (E \text{ lower pyranometer}). \quad (7.2)$$

Net far infrared radiation was calculated as,

$$\text{Net far infrared radiation} = (E \text{ upper pyrgeometer}) - (E \text{ lower pyrgeometer}). \quad (7.3)$$

The net (total) radiation (NR) balance was calculated as,

$$\text{NR} = (E \text{ upper pyranometer}) + (E \text{ upper pyrgeometer}) - (E \text{ lower pyranometer}) - (E \text{ lower pyrgeometer}). \quad (7.4)$$

The irradiance of downwelling far infrared radiation (E) measured with the upward facing pyrgeometer is the irradiance of the plastic with the sky behind it (hereafter referred to as ‘plastic temperature’). The irradiance of upwelling far infrared radiation (E) measured with the downward facing pyrgeometer is the irradiance of the ground. Assuming that these behave like perfect black bodies (an approximation; Kipp & Zonen B. V., 2014), the effective ‘plastic temperature’ and ‘ground temperature’ can be calculated.

$$\text{Plastic temperature} = ((E \text{ upper pyrgeometer}) / 5.67 \times 10^{-8})^{1/4} \quad (7.5)$$

$$\text{Ground temperature} = ((E \text{ lower pyrgeometer}) / 5.67 \times 10^{-8})^{1/4} \quad (7.6)$$

7.2.3 Surface Temperatures

To investigate any difference in surface temperatures between UV+ and UV- polytunnels resulting from differences in radiation transmission small pieces of black card (0.1 x 0.1 m) were fixed to the benches horizontal to the ground inside each polytunnel to act as analogues for non-transpiring leaves. The temperature of the card, plastic, and ground beneath each polytunnel, were measured with the infrared temperature meter (MI-220) simultaneously to radiation balance with the net radiometer. This allowed plastic and ground temperatures calculated from the far infrared radiation data (Section 7.3.2) to be compared with measured plastic and ground temperature to ground truth the data.

7.2.4 Poly tunnel Air Temperature

Air temperature was continuously logged with TinyTag Ultra 2 data loggers (TGU-4500: TinyTag, Gemini Data Loggers, Chichester, UK) hung centrally inside each polytunnel 0.3 m above the plants, and one outside, without additional shading. To determine whether there were any differences in air temperature between the differently clad polytunnels the mean air temperature was calculated for day (04:00-22:00) and night (22:00-04:00) for each polytunnel type over the 5 full days of available data. The difference between the differently clad polytunnels was calculated to give a $\Delta T (T_{air}(UV-) - T_{air}(UV+))$ for day and night where a positive value indicates temperature was higher inside the UV- polytunnel.

7.2.5 Statistical Analysis

These data were tested for normal distribution and equal variances in SPSS version 18 (SPSS Inc. Chicago, USA). The polytunnel radiation balance data were statistically analysed for differences between the UV treatment polytunnels (UV+ / UV-) using a

repeated measures ANOVA in SPSS, with UV treatment as the main factor and day as the repeated measure. Polytunnel air temperature data was also analysed, separately for day and night, using a repeated measures ANOVA in SPSS, but with UV treatment as the main factor, and time as the repeated measure. To determine daily differences between UV radiation treatments, unpaired t-tests were performed for each day (corrected for multiple comparisons) using the Sidak-Bonferroni method, in GraphPad Prism version 7.0d for Mac OS X (GraphPad Software, La Jolla California USA, www.graphpad.com).

7.3 Results

7.3.1 Polytunnel Day Time Radiation Balance

Downwelling solar radiation was significantly ($P < 0.001$; Fig. 7.3a) greater in UV+ polytunnels (mean difference: $159 \pm 34 \text{ W m}^{-2}$; 24%) than UV- polytunnels. There was no significant variation between days ($P = 0.485$; Fig. 7.3a) and no significant interaction between treatment and day ($P = 0.901$; Fig. 7.3a). Upwelling (reflected) solar radiation was not significantly different between treatments ($P = 0.863$; Fig. 7.3b) with UV+ polytunnels marginally lower (mean difference: $-2 \pm 12 \text{ W m}^{-2}$; -1%). There was a significant variation between days ($P = 0.034$; Fig. 7.3b) and also a significant interaction between treatment and days in the magnitude and even direction of the difference between polytunnels (treatment x day: $P = 0.012$; Fig. 7.3b). It is not entirely clear why this variation occurred, perhaps because the magnitude of the difference between UV+ and UV- polytunnels was very low allowing noise to have an effect on measurements. Downwelling solar radiation was greater in UV+ polytunnels but there was little difference in upwelling solar radiation.

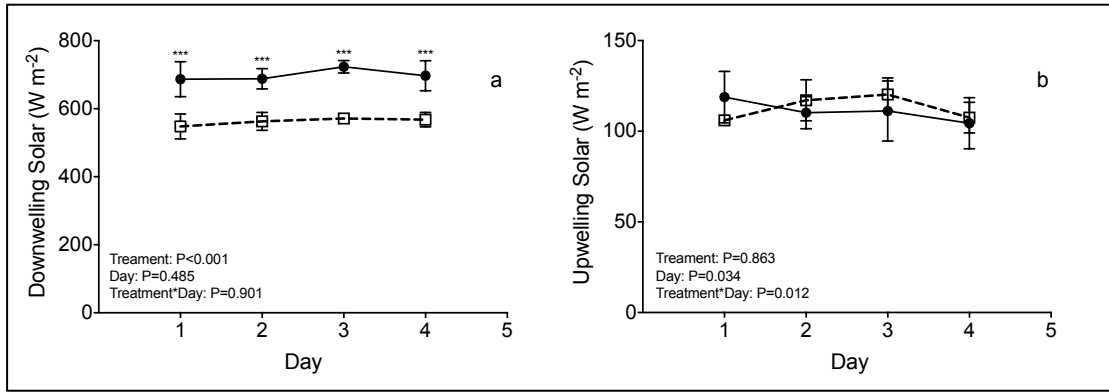


Figure 7.3: The day time response to UV+ (black circles and solid line) and UV- (open squares and dashed line) treatments of (a) downwelling solar radiation, and (b) upwelling solar radiation. Repeated measures ANOVA analysis of the whole treatment period is summarised. The asterisks represent individual days where there was a significant difference between treatments (*: $P < 0.05$; **: $P < 0.01$; ***: $P < 0.001$) corrected for multiple t-tests. Error bars represent ± 1 SE ($n=3$) but if not visible they were smaller than the symbol.

The combined effects of downwelling and upwelling solar radiation resulted in significantly greater ($P < 0.001$; Fig. 7.4) net (solar) radiation in UV+ poly tunnels (mean difference: 138 ± 36 W m⁻²; 31%). There was no significant variation between days ($P = 0.520$; Fig. 7.4) or interaction between treatment and day ($P = 0.812$; Fig. 7.4). Net solar radiation was significantly higher in UV- poly tunnels.

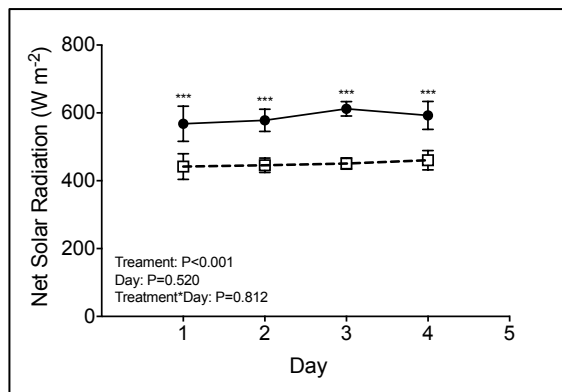


Figure 7.4: The day time response to UV+ (black circles and solid line) and UV- (open squares and dashed line) treatments of net solar radiation. Repeated measures ANOVA analysis of the whole treatment period is summarised. The asterisks represent individual days where there was a significant difference between treatments (*: $P < 0.05$; **: $P < 0.01$; ***: $P < 0.001$) corrected for multiple t-tests. Error bars represent ± 1 SE ($n=3$) but if not visible they were smaller than the symbol.

Downwelling far infrared radiation was significantly ($P = 0.022$; Fig. 7.5a) lower (mean difference: -17 ± 8 W m⁻²; -3%) in UV+ poly tunnels than UV- poly tunnels. There was a significant variation between days ($P < 0.001$; Fig. 7.5a), down-welling far infrared

radiation decreased between days 1 and 2 but then increased again on days 3 and 4. There was no significant interaction between treatments and day ($P=0.766$; Fig. 7.5a) as the difference between polytunnel types remained consistent across all four days. There was very little difference in upwelling far infrared radiation between the polytunnels (mean difference: $0\pm 6 \text{ W m}^{-2}$; $P=0.940$; Fig. 7.5b). There was a significant variation between days ($P<0.001$; Fig. 7.5b) mirroring the variation in downwelling far infrared radiation but no interaction with the effect of plastic on upwelling far infrared radiation (treatment x day: $P=0.138$; Fig. 7.5b). Downwelling far infrared radiation was greater in UV+ polytunnels but there was little difference in the upwelling component.

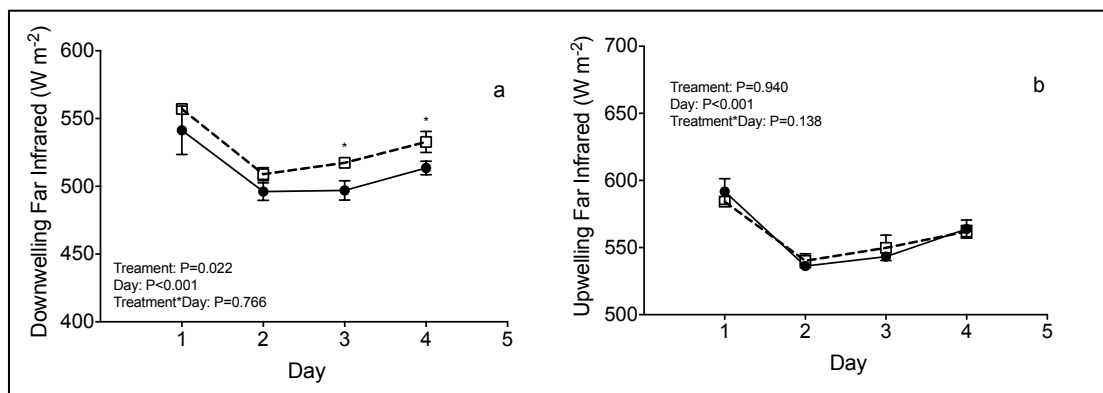


Figure 7.5: The day time response to UV+ (black circles and solid line) and UV- (open squares and dashed line) treatments of (a) downwelling far infrared radiation, and (b) upwelling far infrared radiation. Repeated measures ANOVA analysis of the whole treatment period is summarised. The asterisks represent individual days where there was a significant difference between treatments (*: $P<0.05$; **: $P<0.01$; ***: $P<0.001$) corrected for multiple t-tests. Error bars represent $\pm 1 \text{ SE}$ ($n=3$) but if not visible they were smaller than the symbol.

The combined effects of downwelling and upwelling far infrared radiation resulted in significantly lower ($P=0.035$; Fig. 7.6) net far infrared radiation in UV+ polytunnels (mean difference: $-27\pm 13 \text{ W m}^{-2}$; -91%). The negative values are a result of greater upwelling than downwelling radiation, indicating heat transfer out of the polytunnels, but more so from UV+ polytunnels (a greater negative). There was no significant variation between days ($P=0.576$; Fig. 7.6) or interaction between treatment and day

($P=0.433$; Fig. 7.6). Net far infrared radiation was significantly higher in UV- polytunnels.

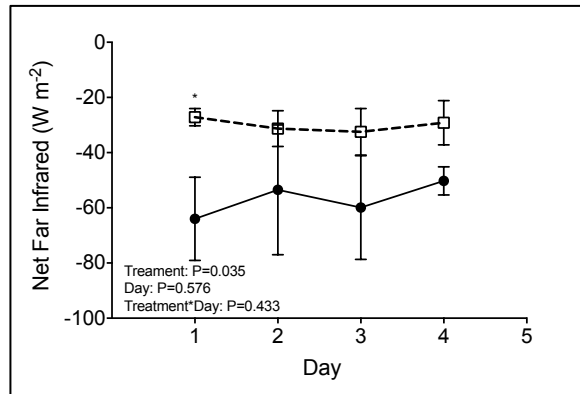


Figure 7.6: The day time response to UV+ (black circles and solid line) and UV- (open squares and dashed line) treatments of net far infrared radiation. Repeated measures ANOVA analysis of the whole treatment period is summarised. The asterisks represent individual days where there was a significant difference between treatments (*: $P<0.05$; **: $P<0.01$; ***: $P<0.001$) corrected for multiple t-tests. Error bars represent ± 1 SE ($n=3$) but if not visible they were smaller than the symbol.

The combined effects of solar and far infrared radiation balances give an overall net (total) radiation balance that was significantly ($P=0.001$; Fig. 7.7) greater (mean difference: 121 ± 37 $W\ m^{-2}$; 29%) in UV+ polytunnels than UV- polytunnels. There was no significant variation between days ($P=0.601$; Fig. 7.7) or interaction between treatment and day ($P=0.720$; Fig. 7.7) for net (total) radiation. Thus net (total) radiation balance was greater in UV+ polytunnels.

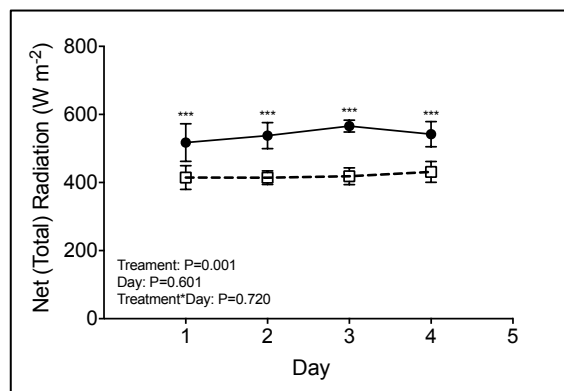


Figure 7.7: The day time response to UV+ (black circles and solid line) and UV- (open squares and dashed line) treatments of net (total) radiation. Repeated measures ANOVA analysis of the whole treatment period is summarised. The asterisks represent individual days where there was a significant difference between treatments (*: $P<0.05$; **: $P<0.01$; ***: $P<0.001$) corrected for multiple t-tests. Error bars represent ± 1 SE ($n=3$) but if not visible they were smaller than the symbol.

There were no significant (treatment: $P=0.996$; Fig. 7.8) or mean differences in black card temperature (mean difference: $0.0\pm 3.0^{\circ}\text{C}$) between UV+ and UV- polytunnels over the four days. There was a significant variation between days ($P<0.001$; Fig. 7.8), caused by differences in ambient air temperature rather than incident solar radiation. There was no interaction between treatment and day ($P=0.313$; Fig. 7.8) even though on each day there was a difference of $>1.5^{\circ}\text{C}$, but this alternated between treatments over the 4 days from UV- to UV+ (Fig. 7.8) resulting in no overall mean difference. The net (total) radiation balance was greater in UV+ polytunnels but this was not reflected in higher black card temperature inside those polytunnels.

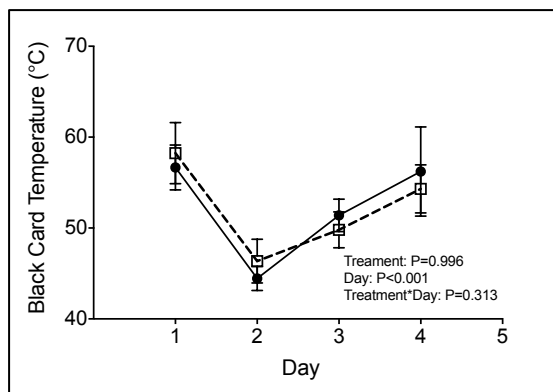


Figure 7.8: The day time response to UV+ (black circles and solid line) and UV- (open squares and dashed line) treatments of the temperature of black card located in the polytunnels. Repeated measures ANOVA analysis of the whole treatment period is summarised. The asterisks represent individual days where there was a significant difference between treatments (*: $P<0.05$; **: $P<0.01$; ***: $P<0.001$) corrected for multiple t-tests. Error bars represent ± 1 SE ($n=3$) but if not visible they were smaller than the symbol.

The calculated plastic temperature was significantly lower (treatment: $P=0.037$; Fig. 7.9a) in UV+ polytunnels than UV- (mean difference: $-1.8\pm 1.1^{\circ}\text{C}$; -4.8%). There were variations between days in the plastic temperature ($P<0.001$; Fig. 7.9a) but these did not affect the differences between the plastic types (treatment x day: $P=0.095$; Fig. 7.9a). The measured plastic temperature was also significantly lower (treatment: $P<0.001$; Fig. 7.9b) in UV+ polytunnels but the difference between polytunnels was much greater (mean difference: $-6.1\pm 0.9^{\circ}\text{C}$; -16.1%) than observed with the calculated

plastic temperature. Similar to calculated temperature, there were variations between days ($P < 0.001$; Fig. 7.9b) that did not interact with the treatment effect ($P = 0.476$; Fig. 7.9b). Both methods produced the same pattern of reduced temperature on days 2 and 3 (day: $P < 0.001$; Fig. 7.9), caused by the combined variations in ambient air temperature, solar radiation and far infrared radiation, reflecting the consistency between the methods. Plastic temperature was higher in UV- polytunnels than UV+.

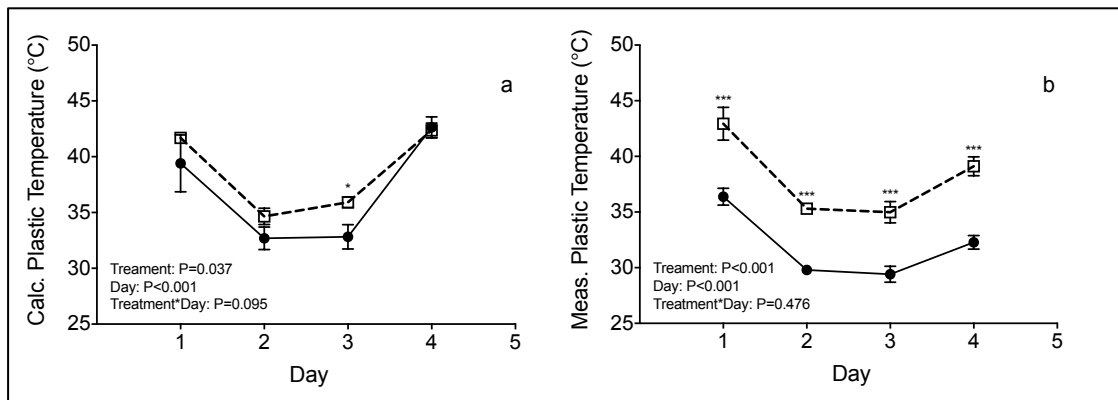


Figure 7.9: The day time response to UV+ (black circles and solid line) and UV- (open squares and dashed line) treatments of (a) plastic temperature calculated from downwelling far infrared radiation, and (b) plastic temperature directly measured. Repeated measures ANOVA analysis of the whole treatment period is summarised. The asterisks represent individual days where there was a significant difference between treatments (*: $P < 0.05$; **: $P < 0.01$; ***: $P < 0.001$) corrected for multiple t-tests. Error bars represent ± 1 SE (n=3) but if not visible they were smaller than the symbol.

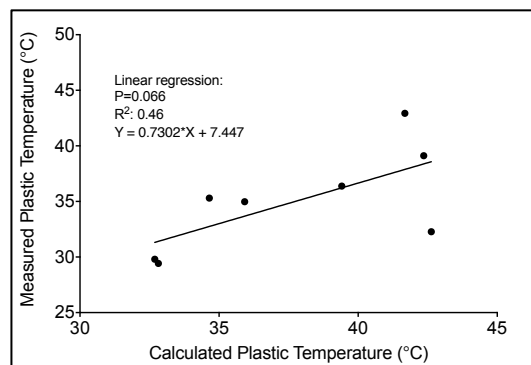


Figure 7.10: Linear regression analysis (summarised) of calculated and measured plastic temperature. Error bars represent ± 1 SE (n=3) but if not visible they were smaller than the symbol.

Linear regression analysis of the calculated and measured plastic temperatures indicate the relationship was not quite significant ($P = 0.066$; Fig. 7.10) but could explain 46% of the change in each (R^2 : 0.46; Fig. 7.10), though not a 1:1 relationship.

Comparing calculated and measured plastic temperatures corroborates that the plastic was warmer in UV- polytunnels, consistent with downwelling far infrared radiation being greater in these polytunnels.

Calculated ground temperature beneath UV+ polytunnels was marginally warmer (0.25°C; treatment: P=0.913; Fig. 7.11a). There were significant daily variations in ground temperature (day: P<0.001; Fig. 7.11a), caused by variable air temperature and differences in radiation balance under the different plastics, but these variations did not interact with the effect of the plastics on ground temperature (treatment x day: P=0.141; Fig. 7.11a). There was also no significant (treatment: P=0.323; Fig. 7.11b) difference in measured ground temperature between the polytunnels although it was consistently warmer under UV+ over the four days (mean difference: 2.1±2.6°C; 5.0%), which wasn't detected with calculated ground temperature. Ground temperature varied significantly between days (day: P<0.001; Fig. 7.11b) but this did not interact with the effect of the plastics (treatment x day: P=0.901; Fig. 7.11b). The comparison of calculated and measured ground temperature hints that ground temperature was warmer but the data is not conclusive.

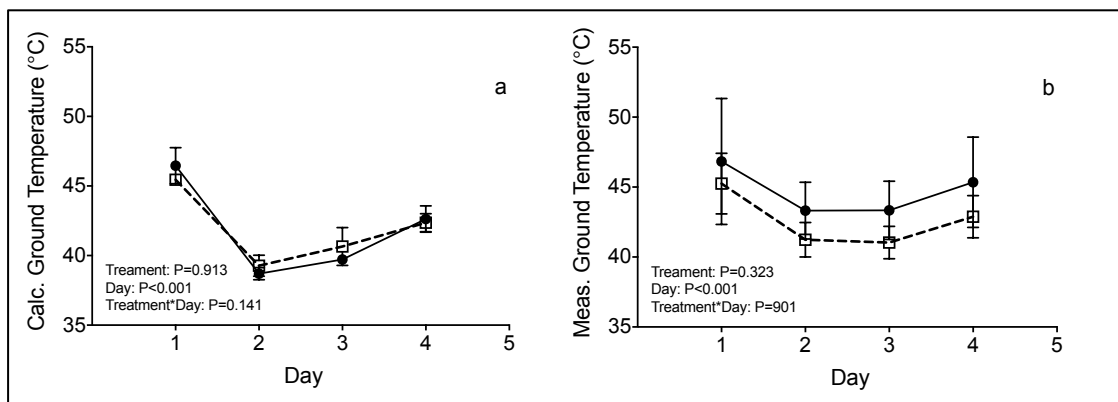


Figure 7.11: The day time response to UV+ (black circles and solid line) and UV- (open squares and dashed line) treatments of (a) plastic temperature calculated from downwelling far infrared radiation, and (b) plastic temperature directly measured. Repeated measures ANOVA analysis of the whole treatment period is summarised. The asterisks represent individual days where there was a significant difference between treatments (*: P<0.05; **: P<0.01; ***: P<0.001) corrected for multiple t-tests. Error bars represent ± 1 SE (n=3) but if not visible they were smaller than the symbol.

Calculated and measured ground temperatures were significantly ($P=0.019$; Fig. 7.12) linearly related, explaining a good proportion of the change in each ($R^2: 0.63$; Fig. 7.12). Although ground temperature was not significantly different between polytunnel claddings, the direct measurements did indicate ground temperature was warmer in UV+ polytunnels.

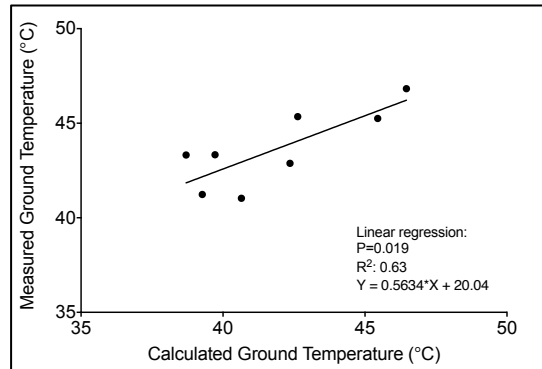


Figure 7.12: Linear regression analysis (summarised) of calculated and measured ground temperature. Error bars represent ± 1 SE ($n=3$) but if not visible they were smaller than the symbol.

7.3.2 Poly tunnel Night Time Radiation Balance

As expected downwelling solar radiation at night was very low, with no sun. Values centred around zero ($\pm 6 \text{ W m}^{-2}$), within the uncertainty associated for the net radiometer, so is not presented.

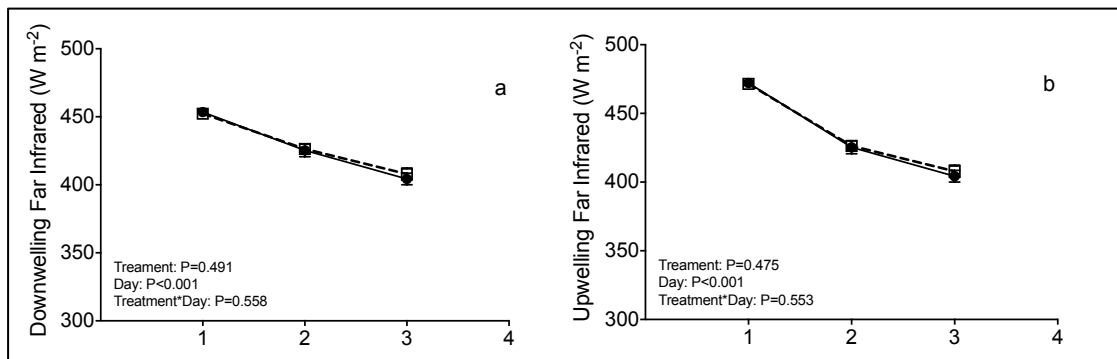


Figure 7.13: The night time response to UV+ (black circles and solid line) and UV- (open squares and dashed line) treatments of (a) downwelling far infrared radiation and (b) upwelling far infrared radiation. Repeated measures ANOVA analysis of the whole treatment period is summarised. Error bars represent ± 1 SE ($n=3$) but if not visible they were smaller than the symbol.

There were no significant ($P>0.05$; Fig. 7.13) differences in downwelling far infrared radiation (mean difference: $-1.2\pm 3.9 \text{ W m}^{-2}$; -0.3% ; Fig. 7.13a) or upwelling far infrared radiation (mean difference: $-1.4\pm 3.6 \text{ W m}^{-2}$; -0.3% ; Fig. 7.13b) between UV+ and UV- polytunnels. Both parameters significantly reduced from day 1 to day 3 ($P<0.001$; Fig. 7.13), but this did not interact with the effect of treatment for either parameter ($P>0.05$; Fig. 7.13). Far infrared radiation was reduced by $\sim 20\%$ from day time levels but remained substantial, compared to solar radiation, due to the residual heat in the ground from the day.

Net far infrared radiation was not significantly ($P>0.05$; Fig. 7.14) different between the differently clad polytunnels (mean difference: $0.3\pm 1.8 \text{ W m}^{-2}$; 1.4%). Net far infrared radiation in both sets of polytunnels was significantly reduced from day 1 to 3 ($P<0.001$; Fig. 7.14) but that did not interact with the treatment effect ($P>0.05$; Fig. 7.14). Net far infrared radiation was negative indicating the overall direction of heat transfer was upwards out of the polytunnels (Fig. 7.14), as expected at night with falling ambient air temperatures as the polytunnels cool down from their day time maximums.

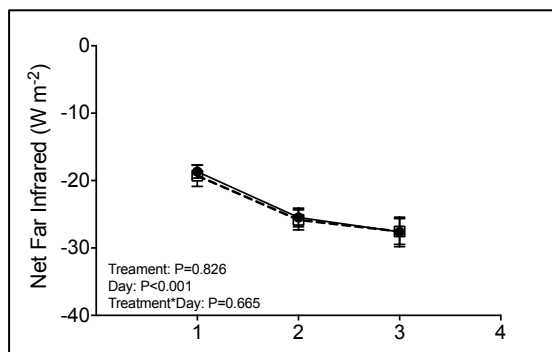


Figure 7.14: The night time response to UV+ (black circles and solid line) and UV- (open squares and dashed line) treatments of net far infrared radiation. Repeated measures ANOVA analysis of the whole treatment period is summarised. Error bars represent $\pm 1 \text{ SE}$ ($n=3$) but if not visible they were smaller than the symbol.

There were no significant ($P=0.938$; Fig. 7.15) differences in net (total) radiation between UV+ and UV- polytunnels (mean difference: $0.1\pm 2.1 \text{ W m}^{-2}$; 0.6%). The

same reduction from days 1-3 occurred ($P < 0.001$; Fig. 7.15) that also did not interact with the treatment effect ($P = 0.274$; Fig. 7.15). The result of absent solar radiation and negative far infrared radiation was negative net (total) radiation (Fig. 7.15) demonstrating that the balance of radiation transfer at night, predominantly heat, was out of the polytunnels. There were no net radiation differences between the differently clad polytunnels at night.

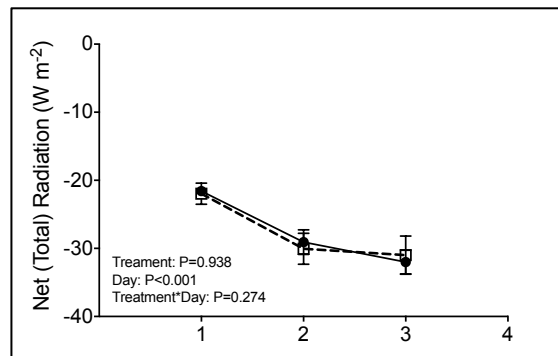


Figure 7.15: The night time response to UV+ (black circles and solid line) and UV- (open squares and dashed line) treatments of net (total) radiation. Repeated measures ANOVA analysis of the whole treatment period is summarised. Error bars represent ± 1 SE ($n=3$) but if not visible they were smaller than the symbol.

The absence of a difference in net radiation between the differently clad polytunnels during the night was consistent with there being no significant ($P = 0.858$; Fig. 7.16) difference in card temperature between UV+ and UV- polytunnels (mean difference: $0.0 \pm 0.4^\circ\text{C}$). There was a significant reduction between days 1-3 ($P < 0.001$; Fig. 7.16) but this did not interact with the treatment effect.

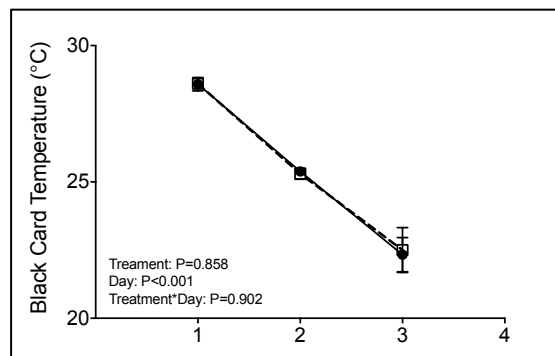


Figure 7.16: The night time response to UV+ (black circles and solid line) and UV- (open squares and dashed line) treatments of black card temperature. Repeated measures ANOVA analysis of the whole treatment period is summarised. Error bars represent ± 1 SE ($n=3$) but if not visible they were smaller than the symbol.

There were no significant ($P=0.484$; Fig. 7.17a) differences between the plastic temperatures of UV+ and UV- polytunnels calculated from the far infrared radiation data (mean difference $0.2\pm0.7^{\circ}\text{C}$; Fig. 7.17a). However, there was a significant ($P=0.027$; Fig. 7.17b) difference between treatments when plastic temperature was directly measured (mean difference $1.1\pm0.5^{\circ}\text{C}$; Fig. 7.17b). There was a significant reduction from days 1-3 ($P<0.001$; Fig. 7.17) for both calculated and measured plastic temperature. This did not interact with the treatment effect for calculated plastic temperature ($P=0.548$; Fig. 7.17a) but it did interact with the measured temperature ($P=0.009$; Fig. 7.17b) as the difference between treatments widened between days 1-3 (the days where there was a significant difference between treatments are highlighted; Fig. 7.17). This calculated plastic temperature indicates there was no difference between treatments but measured temperature indicates there was, although this was not consistent across all three days.

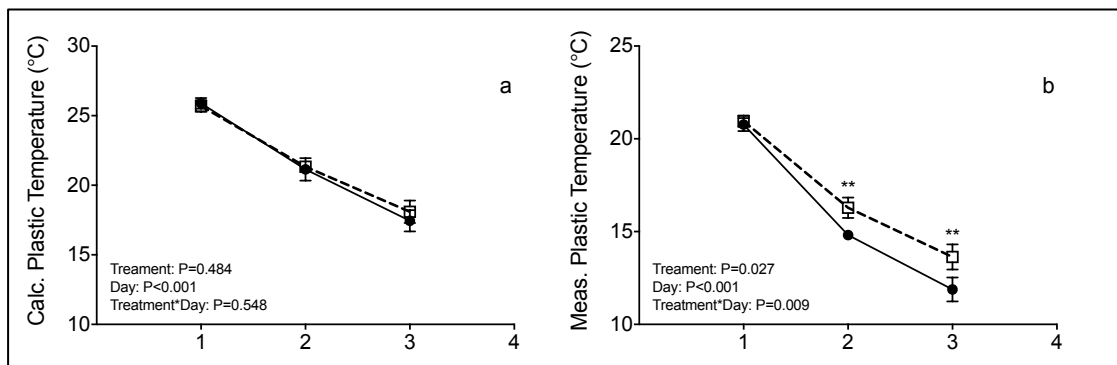


Figure 7.17: The night time response to UV+ (black circles and solid line) and UV- (open squares and dashed line) treatments of (a) plastic temperature calculated from downwelling far infrared radiation and (b) measured plastic temperature. Repeated measures ANOVA analysis of the whole treatment period is summarised. The asterisks represent individual days where there was a significant ($P<0.01$) difference between treatments corrected for multiple t-tests. Error bars represent ± 1 SE (n=3) but if not visible they were smaller than the symbol.

There were no significant ($P=0.584$; Fig. 7.18a) differences between the ground temperatures of UV+ and UV- polytunnels calculated from the far infrared radiation data (mean difference $0.3\pm0.8^{\circ}\text{C}$; Fig. 7.18a). Neither were there any significant ($P=0.436$; Fig. 7.18b) differences between the ground temperatures of UV+ and UV-

directly measured (mean difference $0.9 \pm 1.4^\circ\text{C}$; Fig. 7.18b). There was a significant reduction from days 1-3 ($P < 0.001$; Fig. 7.18) for both methods of determining ground temperature but this did not interact with the treatment effect for either method ($P > 0.05$; Fig. 7.18). There is no evidence that ground temperature was different between UV+ and UV- polytunnels.

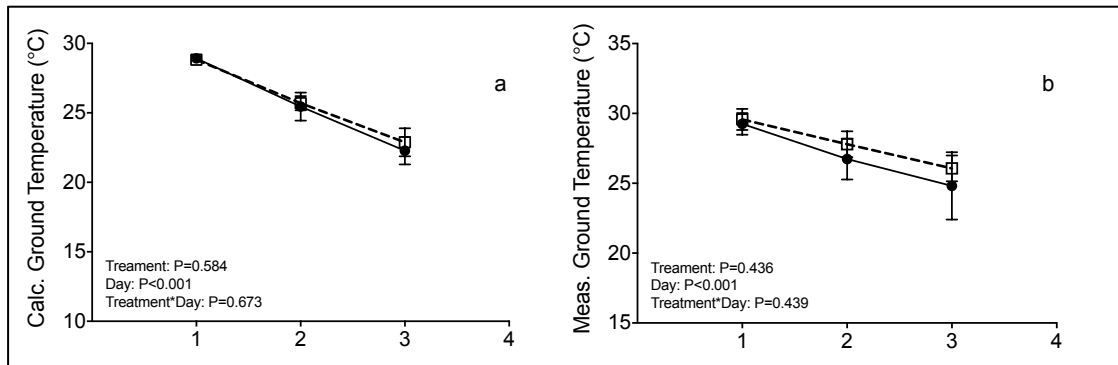


Figure 7.18: The night time response to UV+ (black circles and solid line) and UV- (open squares and dashed line) treatments of (a) ground temperature calculated from downwelling far infrared radiation and (b) measured ground temperature. Repeated measures ANOVA analysis of the whole treatment period is summarised. Error bars represent ± 1 SE (n=3) but if not visible they were smaller than the symbol.

Linear regression analysis of calculated and measured plastic temperature, demonstrate a significant relationship ($P < 0.001$; Fig. 7.19a) with good correlation (R^2 : 0.97; Fig. 7.19a). A similar correlation exists between calculated and measured ground temperatures ($P < 0.001$; R^2 : 0.95; Fig. 7.19b). These relationships demonstrate that the separate methods of measuring plastic and ground temperature are well correlated but not on a 1:1 basis.

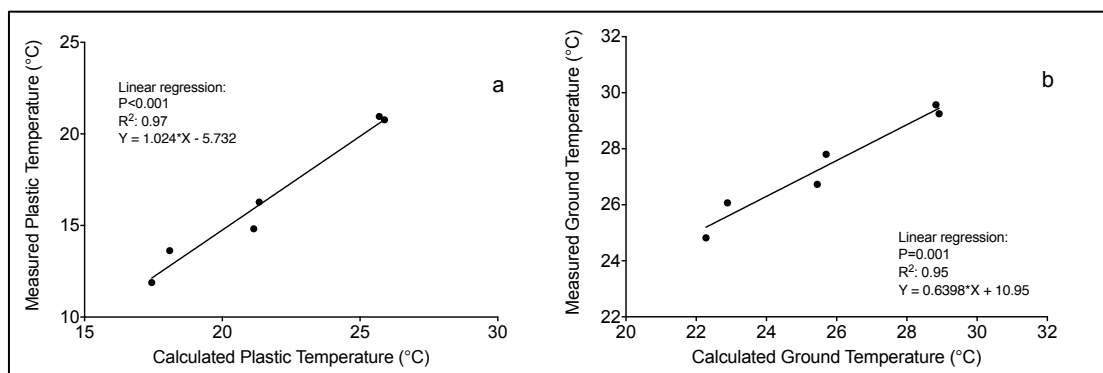


Figure 7.19: Linear regression analysis (summarised) of (a) calculated and measured plastic temperature and (b) calculated and measured ground temperature. Error bars represent ± 1 SE (n=3) but if not visible they were smaller than the symbol.

7.3.3 Polytunnel Air Temperature

There was no significant ($P=0.125$; Fig. 7.20) difference in polytunnel air temperature between treatments during the day (04:00-22:00) although air temperature was a mean 0.5°C (Tab. 7.1) greater, and up to $\sim 1^{\circ}\text{C}$ greater around solar noon (Fig. 7.20), in UV- polytunnels compared to UV+. Air temperature fluctuated from day to day ($P<0.001$; Fig. 7.20) following changes in ambient air temperature but this did not interact with the treatment effect ($P=0.173$; Fig. 7.20).

Table 7.1: Day time (04:00-22:00) and night time (22:00-04:00) mean air temperatures ($^{\circ}\text{C}$) inside the differently clad polytunnels (UV+ / UV-) for the period of radiation data collection (27 June – 2 July 2019). The differences between polytunnels were not statistically significant for day or night (repeated measures ANOVA).

Time	Outside	UV-	UV+	$\Delta T = T_{air}(UV-) - T_{air}(UV+)$
Day (04:00-22:00)	34.81	37.60	37.10	0.50
Night (22:00-04:00)	23.76	24.46	24.41	0.05

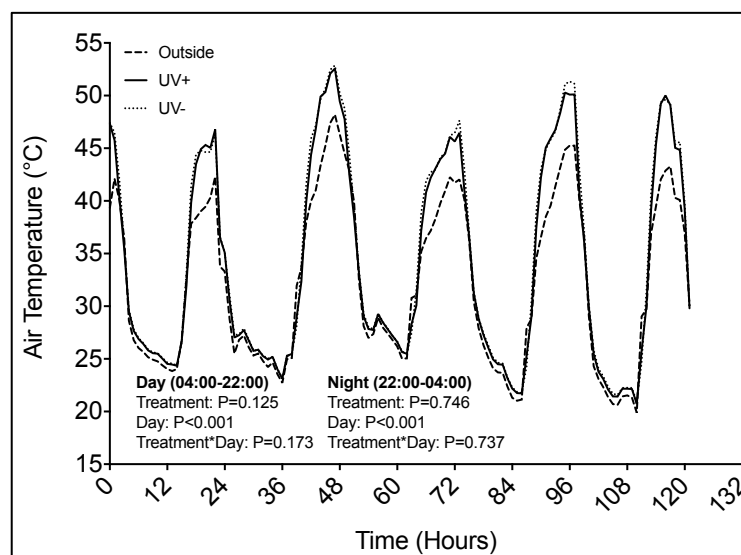


Figure 7.20: Time course of air temperature outside and inside each type of polytunnel (UV+ / UV-). Summary of repeated measures ANOVA analysing the difference between UV+ and UV- polytunnels (not including outside air temperature) are highlighted ($n=3$).

There was no significant ($P=0.746$; Fig. 7.20) difference between treatments in night time (22:00-04:00) air temperature (Tab. 7.1) There were significant variations between nights ($P<0.001$; Fig. 7.20) following variation in ambient air temperature

between nights but there was no interaction with the treatment effect on air temperature at night ($P=0.737$; Fig. 7.20). Although UV- polytunnels were marginally warmer in general than UV+, particularly during the day, the differences were not significant but could have biological importance.

7.4 Discussion

7.4.1 Implications of Greater Day Time Downwelling and Net (Solar) Radiation in UV+ Poly tunnels

Day time downwelling solar radiation was substantially greater inside UV+ poly tunnels than UV- poly tunnels (Fig. 7.3a), corroborating the significantly greater PAR and total radiation detected in UV+ poly tunnels at Lancaster (Chapter 5). It also substantiates the significantly greater PAR, and total radiation (not significant), in UV+ poly tunnels in Antalya (Chapter 6). In each case different equipment (spectroradiometer: Chapter 5; Broadband PAR and total radiation sensors: Chapter 6; net radiometer: current Chapter) was used in these measurements, which corroborates these findings. This greater downwelling solar radiation within UV+ poly tunnels compared to UV-, in two separate locations, measured with three different devices, demonstrates a consistent difference between these plastics in PAR and total radiation, even though UV radiation transmission varied considerably between them (Lancaster: 72%; Antalya: 43%) for various reasons (Section 6.2.1).

Downwelling solar radiation detected with the pyranometer comprises longwave UV-A, PAR and near infrared radiation. A very small proportion (<7%) is UV-A, most of which is absorbed by the leaf (Lambers *et al.*, 2008) contributing to warming. About 50% is PAR of which 85% is absorbed by the leaf (Lambers *et al.*, 2008). The remaining downwelling solar radiation, infrared radiation, can be divided into two

parts, 700-1200 nm that is largely reflected or transmitted through the leaf that does not directly affect leaf temperature, and 1200-3000 nm that is absorbed by water within leaves, resulting in ~50% infrared radiation being absorbed which directly heats leaves (Lambers *et al.*, 2008). All of the other surfaces within the polytunnels exposed to the sun also absorb solar radiation, but at different wavelengths dependent on their reflective and transmission properties, ultimately increasing temperature is dependent on the magnitude of absorption. However, near solar radiation has little direct effect on air temperature because absorption by atmospheric gases is far lower than for idealised black bodies (that absorb 100% of incident solar radiation; Liang, 2013). Therefore, greater downwelling solar radiation should cause greater surface temperatures in UV+ polytunnels than in UV- polytunnels, but not air temperature.

It was therefore predicted that black card located parallel to the ground on the internal polytunnel benches, analogues for non-transpiring leaves, would be warmer in UV+ polytunnels. The differences in downwelling solar radiation between the differently clad polytunnels would have the same effect on leaf temperature within each polytunnel type. Thus, the greater downwelling solar radiation should cause a similar response in black card and leaves, with the additional solar radiation absorbed by the black card causing those inside the UV+ polytunnels to be warmer, but there was no mean difference over the four days (Fig. 7.8). There were daily differences $>1.5^{\circ}\text{C}$ but UV+ polytunnels were warmer on two days and likewise for UV- polytunnels, resulting in no overall or consistent differences in card warming (Fig. 7.8). This was unexpected given the substantial difference in downwelling and net solar radiation balance between the differently clad polytunnels. However, the calibration uncertainty of the infrared temperature meter is $\pm 0.5^{\circ}\text{C}$ and the measurement repeatability uncertainty $\pm 1.0^{\circ}\text{C}$, which can account for much of the variation between UV+ and

UV- polytunnels over the four days. It has previously been reported that any leaf temperature changes caused by abiotic factors, such as wind speed, are enhanced by stomatal closure that magnifies the effect on leaf temperature (De Boeck *et al.*, 2012). It may be that a similar enhancement of radiation-induced leaf temperature differences occurs between UV+ and UV-, and the absence of transpirational cooling resulted in inconsistent differences in card temperature in the differently clad polytunnels, in addition to the measurements uncertainties highlighted.

Substantially greater day time downwelling solar radiation in UV+ polytunnels was expected to increase upwelling solar radiation. Upwelling solar radiation is reflected downwelling solar radiation, the extent of reflected radiation is determined by the albedo of the ground. However this was not the case, with the differently clad polytunnels differing by 1% in upwelling solar radiation (Fig. 7.3b), compared to 24% greater downwelling solar radiation in UV+ polytunnels (Fig. 7.3a). This may be caused by the polytunnel structures themselves, being open around the lower 0.75 m of each polytunnel allowing ventilation but also reflected solar radiation from the adjacent ground to enter into the polytunnels affecting these measurements. The resulting balance of downwelling and upwelling (reflected solar) radiation was a substantially greater net solar radiation balance within the UV+ polytunnels (Fig. 7.4), a result of the differences in downwelling incident solar radiation, the consequences of which were greater energy input and temperature increase to all surfaces inside, including plants.

7.4.2 Implications of Greater Day Time Downwelling and Net Far Infrared Radiation in UV- Polytunnels

Substantially greater day time downwelling solar radiation transmitted by the UV+ cladding would be expected to increase the ground temperature beneath the UV+

polytunnels. The ground, similar to the black card, absorbs incident solar radiation, heating it, which is then emitted as longwave infrared radiation (heat) that is measured as far infrared radiation (4500-42000 nm). Therefore, upwelling of far infrared radiation was expected to be greater in UV+ polytunnels but no significant differences were observed between the differently clad polytunnels (Fig. 7.5b). This was possibly for the same reasons discussed previously relating to a lack of upwelling solar radiation: open polytunnels beneath the bench level (0.75 m). Neither was there a significant difference in directly measured ground temperature between the differently clad polytunnels, which corroborates the temperatures calculated from upwelling far infrared radiation (Fig. 7.11). The small (not significant) difference observed in the measured ground temperature is probably a result of the narrower field of view of the infrared thermometer (18° encompassing only ground directly beneath the polytunnel) which would limit the inclusion of “leaked” radiation from the ground adjacent to the polytunnels, compared to the 180° field of view of the net radiometer sensors. Temperature correction of the far infrared data from the pyrgeometer sensor with external temperature measurement (7.2.2), prior to calculation of ground temperature, may also have had an impact on the calculated temperature affecting the difference when compared to the measured temperature. The evidence indicates that there is little difference in ground temperature beneath the differently clad polytunnels but this may have been easier to analyse in a larger polytunnel, minimising the effects of polytunnels contents and side leakage.

Day time downwelling far infrared radiation was significantly greater in UV-polytunnels (Fig. 7.5a), which is the effective plastic temperature of the polytunnel. This was corroborated by the significantly greater measured plastic temperature (Fig. 7.9). This is partly caused by absorption of the downwelling solar radiation by the

plastic, but more importantly trapping (and re-emitted after absorption) of upwelling far infrared radiation. Therefore the difference is a result of the reduced upward transmission of far infrared radiation in UV- polytunnels compared to UV+, the greenhouse effect. Far infrared radiation warms air temperature, in contrast to solar radiation that increases surface temperature, thus air temperature should have been greater in UV- polytunnels.

The greater day time net balance of far infrared radiation (Fig. 7.6) in UV- polytunnels would be expected to increase air temperature. However, air temperature was only marginally (0.5°C) higher, and not significantly, in the UV- polytunnels compared to UV+ (Tab. 7.1; Fig. 7.20). This indicates that the significant difference in the net balance of far infrared radiation was not sufficient to raise air temperature significantly. If transpiration rates were equal, a difference in air temperature would cause a similar difference in leaf temperature, as when thermal imaging was used to detect drought stress in glasshouses with spatial heterogeneity in air temperature (Grant *et al.*, 2006). However, there is no firm evidence that the greater far infrared radiation in UV- polytunnels increased air temperature.

7.4.3 Implications of Net (Total) Radiation Balance

The results discussed above demonstrate that the significant differences in day time radiation inside the differently clad polytunnels are greater downwelling solar radiation in UV+ polytunnels but greater downwelling far infrared radiation in the UV- polytunnels. Each affects temperature inside the polytunnels differently: increased surface temperature in UV+ polytunnels and increased air temperature inside UV- polytunnels, but which has the greatest effect on leaf temperature of crops inside? Net (total) radiation is a good indicator.

Net (total) radiation was significantly greater in UV+ polytunnels (Fig. 7.7) and the absolute differences in net far infrared radiation and net solar radiation are the key to understanding the net radiation balance. The absolute differences were much greater for net solar radiation (138 W m^{-2}) than net far infrared radiation (27 W m^{-2}) resulting in much greater net (total) radiation within UV+ polytunnels. Thus the differences between the differently clad polytunnels in solar radiation would be expected to outweigh those in far infrared radiation, so that the effect of direct heating by incident solar radiation in UV+ polytunnels would be expected to be greater than that of indirect heating caused by the greater air temperature within the UV- polytunnels. Mean day time air temperature was 0.5°C greater in UV- polytunnels, and around solar noon this was up to $\sim 1^{\circ}\text{C}$ (Tab. 7.1; Fig. 7.20). On this basis, the greater leaf warming ($\sim 2^{\circ}\text{C}$) in UV+ treatments in the field (Novotná *et al.*, 2016; Williams *et al.*, 2020; Chapter 5) would be consistent with the effect of absorbed incident solar radiation and partial stomatal closure (Chapters 3-6) overcoming the air temperature influence on leaf temperature.

The occurrence of direct radiative heating from solar radiation in UV+ polytunnels exceeding the effect of greater air temperature in UV- polytunnels may be partly caused by decoupling of leaf temperature from air temperature. A study of mountain plants showed a capacity for leaves to decouple from atmospheric air temperature, with leaves up to 10°C warmer or cooler than air dependent on the functioning of their heat dissipation mechanisms (Section 1.3; Scherrer & Körner, 2010). This demonstrates that leaves can decouple from air temperature thus limiting its effect on leaf temperature. This may partly explain why the greater air temperature in UV- polytunnels does not cause leaves in those polytunnels to be warmer than in UV+.

Modelling of the response of leaf temperature between outside and enclosed conditions, such as glasshouses and open top chambers, indicated the difference in windspeed between the enclosed and outdoor environments had more effect on leaf temperature than differences in solar or far infrared radiation balance (De Boeck *et al.*, 2012). In a modelling comparison of glasshouse and outside leaf temperatures the warmer 'sky' (glass in that case and plastic in the case of polytunnels) and differences in solar radiation caused only small differences in leaf temperature (De Boeck *et al.*, 2012). Their report indicates that the differences in day time net solar and far infrared radiation observed in this study (Fig. 7.4 and 7.6) would not necessarily have a great impact on leaf temperatures in the differently clad polytunnels when compared to another abiotic factor such as UV-induced partial stomatal closure. The modelling (De Boeck *et al.*, 2012) also suggests that partial stomatal closure exacerbates any environmentally induced leaf temperature differences. This indicates that the difference in leaf temperature observed between UV+ and UV- polytunnels in the previous two chapters (Chapters 5 and 6) are predominantly caused by UV-induced partial stomatal closure, to a lesser extent incident solar radiation, and least of all air temperature differences resulting from variations in far infrared radiation between the differently clad polytunnels.

7.5 Conclusions

Day time downwelling solar radiation was substantially greater in UV+ polytunnels. This corroborates the greater downwelling solar radiation detected in Lancaster (Chapter 5) with a spectroradiometer, and greater PAR and total radiation in Antalya (Chapter 6) with broadband sensors, demonstrating the consistency of these results. Greater net solar radiation in UV+ polytunnels would be expected to increase surface temperatures within those polytunnels. Day time downwelling far infrared radiation

was significantly lower in UV+ polytunnels, which decreased air temperature within them compared to UV- polytunnels. The balance of solar and far infrared radiation resulted in a greater day time net (total) radiation balance within UV+ polytunnels because the absolute difference in net solar radiation was much greater than that for net far infrared radiation. Surprisingly this greater downwelling solar and net radiation balance within UV+ polytunnels was not evident in the temperature of black card located inside each polytunnel. The measured differences in downwelling far infrared radiation were corroborated by direct measurements of the plastic temperature. There were barely any differences in the measured and calculated parameters at night. These radiation data indicate an additional cause of the increased leaf temperatures observed within UV+ polytunnels in Lancaster (Chapter 5) compared to Antalya (Chapter 6). Analysis of the relative effects of partial stomatal closure and net radiation balance on leaf temperature in UV+ polytunnels will be addressed in the General Discussion.

It is clear that significant and substantial differences exist between these ‘UV-transparent’ and ‘UV-opaque’ plastics in terms of PAR, infrared and total radiation transmission. Many different plastic polytunnel claddings are available on the market. Understanding the effects of the transmission of these different elements of the electromagnetic spectrum is important for crop cultivation and experiments that use wavelength selective filters in UV exclusion studies, in terms of leaf temperature. This also applies to photosynthetic performance where PAR transmission varies substantially between plastics. Much of this work has been completed already (Paul *et al.*, in prep.) but due to time and space constraints has not been included in the thesis.

8 General Discussion

8.1 The Difficulties of Measuring UV-Induced Leaf Temperature Increases

At the beginning of this project, the absence of peer reviewed literature on UV-induced leaf temperature increases was striking. The general consensus from the literature was that UV radiation decreases stomatal conductance (Kakani *et al.*, 2003b; Tab. 1.2, p. 16), which would be expected to increase leaf temperature. So why not include leaf temperature measurements in such studies? The only explanation is the difficulty of detecting small changes in leaf temperature amongst the noise of a variable environmental background in the field. However, there was no evidence of laboratory experiments that could limit background noise either.

Apart from my own preliminary data (Williams *et al.*, 2020) a single report of UV radiation related leaf temperature increase now exists (Novotná *et al.*, 2016) with partial stomatal closure inferred as the cause, but this was not a direct investigation of leaf temperature. A 2°C leaf temperature increase was detected but was not significant (Novotná *et al.*, 2016; Tab. 1.2, p. 16) demonstrating the difficulty of detecting significant effects of UV radiation on leaf temperature, particularly in the field. Thus,

this project began by first establishing that UV radiation increased leaf temperature and that the cause was partial stomatal closure.

To limit the problems associated with uncontrollable variables in the field, this work began by using a porometer and thermocouples in a controlled climate cabinet, but it was difficult to ensure good contact between thermocouples and leaves throughout UV exposure, especially when air flow moved the leaves. Air flow, with fans, was introduced to increase transpirational cooling of leaves with stomata open and thus enhance leaf temperature differences with leaves that exhibited UV-induced partial stomatal closure. Together these methods did not detect any clear difference between UV radiation and control (zero UV radiation) treatments.

Eventually I turned to the LI-6400XT for a number of reasons. It has reliable temperature measurement with a thermocouple (the cuvette enables the thermocouple to be held in continuous contact with the leaf without the problems encountered previously). It provides a greater range of leaf physiological data compared to the previously employed methods (including photosynthesis from which instantaneous water use efficiency could be analysed). It also provided an additional level of environmental control around the subject leaf that enhanced the environmental control provided by the climate cabinet, dampening the effect of air temperature fluctuations that are inherent to most controlled environments, reducing the variability in leaf temperature thus making it easier to detect consistently. It also allowed application of UV radiation through the clear window cuvette attachment (UV-transparent 'Teflon' window). This enabled the method ultimately employed in the climate cabinet experiments (Chapter 3), where a leaf was enclosed inside the cuvette. Data logging was started in the absence of UV radiation, the cuvette conditions allowed to stabilise

with the leaf inside, after which the UV radiation source was switched on and the UV transmitted into the cuvette onto the leaf while measurements were continuously logged (Fig. 3.3, p. 40). Clearly only a single leaf could be experimented with at a time so a high throughput system was developed by applying UV radiation for only 90 minutes, enabling four leaves a day to be analysed centred around the middle of the photoperiod (Fig. 3.3, p. 40). The method also allowed the UV irradiance to be changed easily, unlike in the field, by varying the distance between leaf and UV source, providing a range of UV irradiances from which a dose, or irradiance, response could be determined.

Although this method produced reliable and consistent results, it was apparent from post-treatment analysis that direct radiative heating from the UV lamp enhanced any leaf warming caused by partial stomatal closure (Fig. 3.12, p. 53). UV lamps emit infrared radiation, which was transmitted by the Teflon window onto the leaf enhancing warming (Fig. 3.13, p. 54). There was also PAR emitted by the UV lamp that it was not possible to block, thus when the lamp was switched on during data logging additional PAR to that provided by the climate cabinet was applied to the leaf inside the cuvette (Fig. 3.8, p. 48), which would also increase the energy input to, and temperature of, the leaf. Initially this appeared to complicate identification of the UV-induced leaf temperature increase resulting from partial stomatal closure, although it was possible to dissect the individual warming effects related to stomatal closure and direct radiative heating (Fig. 3.12, p. 53). Only later, during the polytunnel experiments at Lancaster, it became apparent that differences in radiation (not just UV) transmission between UV-opaque (UV-) and UV-transparent (UV+) plastics existed and that the radiative heating effect observed in the climate cabinet may actually occur between the differently clad polytunnels in the field (Fig. 5.11, p. 107).

Thus for the first time I began thinking about the presence of the combined effects of UV-induced stomatal closure and radiative heating resulting from the different transmission of PAR and infrared radiation through these plastics.

This LI-6400XT method was also adaptable with the LED attachment. To eliminate the radiative heating effect from the UV source (lamps in the controlled environment experiments and sun in the field) and ensure equal radiation loading for both treatments during measurements, and to ensure constant PAR and infrared radiation when outside under solar conditions that can be affected by cloud, the clear window attachment was replaced with the LED attachment (Section 4.2.3, p. 68). This method was used for all plant measurements thereafter (Chapters 4 and 6), except in the polytunnels at Lancaster (Chapter 5) when the equipment was not available. Ultimately this has been advantageous because it has allowed comparison of UV-induced leaf temperature increases where the UV treatments differed in radiation loading when measured, and those where there were no differences.

8.2 Leaf Warming in Polytunnels

When the project was instigated by reports from commercial growers that leaf temperature was greater under UV-transparent cladding compared to UV-opaque cladding (Tab. 1.1, p. 3), UV-induced stomatal response was hypothesised. However, as discussed in the last section, radiative heating associated with a radiation imbalance between the differently clad polytunnels became apparent as the project progressed (Chapter 5). It was clear from the work in the controlled environments (Chapters 3 and 4) that UV-induced partial stomatal closure occurred. As discussed, the effect of radiative heating in the climate cabinet experiments was accounted for (Section 3.3.8, p. 53). This effect was eliminated in the controlled environment room by using the

LED cuvette attachment (Section 4.2.3, p. 68), meaning there were no radiation differences between treatments during measurement. When the effect of radiative heating was deducted from the climate cabinet results, the remaining leaf warming attributable to stomatal closure was very similar in both experimental environments, corroborating that UV-induced stomatal related leaf temperature increase occurs when other environmental factors are eliminated or accounted for.

The polytunnel experiments conducted at Lancaster demonstrated that leaf warming unrelated to stomatal closure occurred in polytunnels in the field (Chapter 5). This understanding emerged from varied radiation conditions caused by cloud cover over four consecutive experiments (Figs. 5.4-5.6, p. 96, 99, 101). In the first two experiments (Fig. 5.4, p. 96), solar radiation was scarcely affected by cloud resulting in consistently lower stomatal conductance and greater leaf temperature in UV+ polytunnels. In the third week (Fig. 5.5, p. 99) the same response was observed until the latter days of the experiment when cloud cover reduced solar (and thus UV) radiation, causing the stomatal response to reverse while leaf temperature did not reverse. This decoupling of stomatal conductance and leaf temperature was confirmed in the fourth experiment when cloud cover was substantial for most of the week during which stomatal conductance and leaf temperature were both significantly greater in UV+ polytunnels compared to UV- polytunnels (Figure 5.6, p. 101). The only plausible cause of this decoupling of stomatal conductance and leaf temperature were differences in radiation transmission through the different plastics and therefore radiation loading on UV+ treated leaves. Solar radiation was measured continuously throughout the experiments at Lancaster but only in the wavelength range of 400-800 nm, which did reliably indicate infrared radiation transmission, particularly in the range that directly heats leaves (1200-3000 nm). Thus, the data indicated that solar

radiation transmission into UV+ polytunnels was significantly greater than UV- polytunnels but more detailed measurements were required, which became an objective for the experimental work in polytunnels at Antalya (Chapter 7).

In Antalya, UV+ polytunnels transmitted significantly more PAR than UV- polytunnels (Fig. 6.6, p. 131). It seemed plausible that this difference might also occur in the infrared radiation range too. A 4-way net radiometer allowed full quantification of differences in solar and far infrared radiation transmission and balances within the differently clad polytunnels. These data clearly demonstrated that transmission of solar radiation was significantly greater (24%; Fig. 7.3a, p. 147) in UV+ polytunnels resulting in a net solar radiation balance that was 31% (Fig. 7.4, p. 147) greater in those polytunnels. This would be expected to enhance leaf temperature in UV+ polytunnels. However, greater downwelling (Fig. 7.5a, p. 148) and net far infrared radiation balance (Fig. 7.6, p. 149) were identified in UV- polytunnels, unexpectedly enhancing air temperature (not significantly; Tab. 7.1; Fig. 7.20, p. 158-159) in those polytunnels thus partially offsetting the effects of greater solar radiation balance in UV+ polytunnels. Ultimately, with decoupling of stomatal conductance and leaf temperature, and the greater net (total) radiation balance in UV+ polytunnels (Fig. 7.7, p. 150), it is clear that the enhanced solar radiation in UV+ polytunnels outweighed enhanced far infrared radiation in UV- polytunnels, otherwise net radiation and leaf temperature would be greater in UV- polytunnels. Thus, the radiative heating effect identified in the climate cabinet experiments (Fig. 3.12, p. 53) was not entirely different to the effect of differences in net (total) radiation balance between UV+ and UV- polytunnels. The initial discovery of greater radiation transmission in UV+ polytunnels at Lancaster (Fig. 5.11, p. 107) was corroborated by the net radiation measurements in Antalya (Chapter 7). However, there is no doubt that UV-induced

partial stomatal closure occurs, increasing leaf temperature, so the balance between the mechanisms regulating leaf temperature need elucidating.

8.3 The Relative and Absolute Effects of Partial Stomatal Closure and Radiation Loading on Leaf Temperature

Three possible methods exist for analysing the separate effects of UV-induced partial stomatal closure and differences in radiation loading on leaf temperature increases.

8.3.1 Method 1: Relationships Between Stomatal Conductance and Leaf Temperature

Comparing relationships between stomatal conductance and leaf temperature in the separate experimental campaigns (each with differing levels of radiation loading) demonstrates the effect that radiation loading has on leaf temperature increases in combination with UV-induced partial stomatal closure. Stomatal conductance is used instead of transpiration rate because transpiration data are not available for the Lancaster polytunnel experiments, so this enables comparison of all plant related experiments. The slopes of the relationships between stomatal conductance and leaf temperature identify the degree of leaf warming that would result from an equal reduction in stomatal conductance, with temperature increases varying between experiments depending on the radiation loading in the environment in which measurements were conducted.

Of the four experimental campaigns, leaf measurements in the climate cabinets were conducted within the environmentally controlled LI-6400XT cuvette with the clear window attachment, that allowed radiation from the climate cabinet to be transmitted into the cuvette creating a difference in total radiation between the UV treatments and control (zero UV; Chapter 3). Measurements in the controlled environment (CE) room

and polytunnels at Antalya (2019) were also conducted within the environmentally controlled LI-6400XT cuvette but with the LED attachment rather than the clear window, with equal radiation loading between UV+ and UV- treatments during measurements (Chapters 4 and 6). Measurements in the polytunnels at Lancaster were conducted with an infrared thermometer under solar conditions without environmental control with different plastic transmission creating greater radiation loading in UV+ than in UV- polytunnels (Chapter 6). Thus, three distinct radiation loading environments are compared.

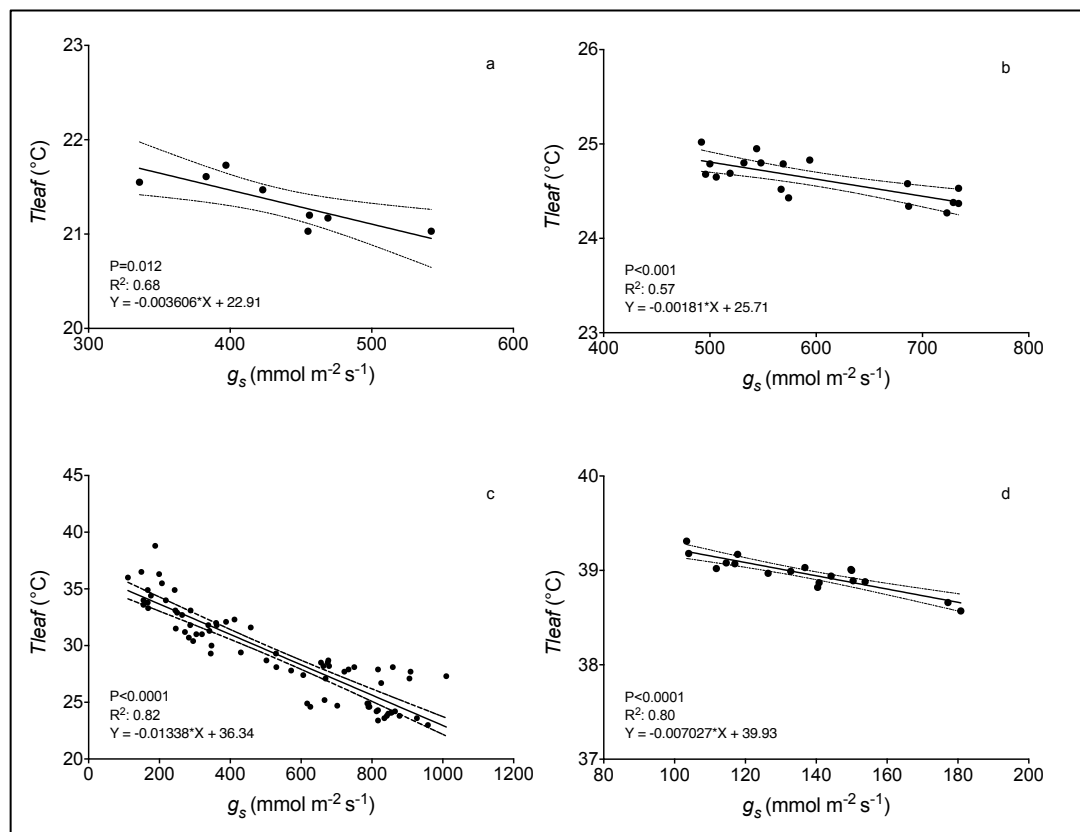


Figure 8.1: Linear regression analysis of the relationship between stomatal conductance and leaf temperature for each UV+ treated plant (UV- data are excluded in order to analyse the relationship when UV radiation is present) for (a) the climate cabinet experiment that applied cellulose acetate filtered 0.297 W m^{-2} PGIAS, (b) the three controlled environment room experiments, (c) the four polytunnel experiments at Lancaster, and (d) the polytunnel experiment at Antalya 2019. The results of linear regression analysis are summarised. The 95% confidence intervals are highlighted (dashed lines). Each data point represents an individual plant (n varies between experiment location, see individual chapters).

In all experiments there was a significant ($P<0.05$; Fig. 8.1) relationship between stomatal conductance and leaf temperature, as expected. Comparing the lowest leaf

temperature increase (CE room: 0.0018°C; Fig. 8.1b) with the other experiments demonstrates that the leaf temperature increases caused by the differences in radiation loading lies between 200-700% (0.0036-0.0134°C). Exploring how these different slopes relate to total radiation, and thus radiation loading, indicates an exponential increase in leaf temperature with enhanced total radiation (R^2 : 0.68; Fig. 8.2). This reveals that leaf temperature increases will vary considerably depending on the radiation loading, dependent on total radiation, which will vary subject to latitude, season and weather conditions. However, as observed in this thesis (Chapters 3-6), UV radiation caused partial stomatal closure which increases leaf temperature, therefore leaf temperature will increase in response to UV radiation but the magnitude of increase is driven by the radiation load.

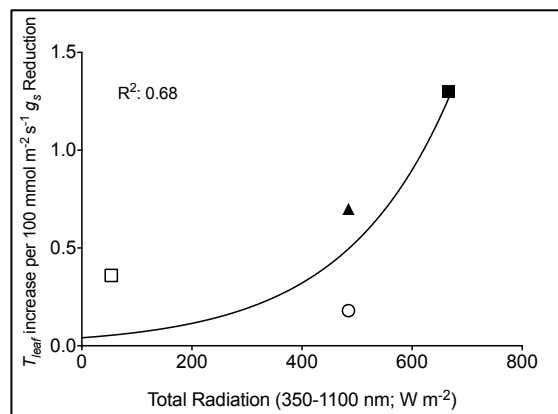


Figure 8.2: Non-linear regression analysis (exponential increase) of total radiation (350-1100 nm) and the increase in leaf temperature (T_{leaf}) for each 100 mmol m⁻² s⁻¹ reduction in stomatal conductance. The symbols represent separate experiments: (open square) the climate cabinet experiment that applied cellulose acetate filtered 0.297 W m⁻² PGIAS, (open circle) the three controlled environment room experiments, (closed square) experiments 1 and 2 at Lancaster, and (closed triangle) the polytunnel experiment at Antalya 2019.

8.3.2 Method 2: Radiative Heating in a Low Total Radiation Environment

The second method of quantifying the absolute effect of radiation loading on leaf temperature increase is to compare leaf temperature measurements that were conducted in the first experiment at Antalya in 2018 (Fig. 6.8, p. 138). Leaf

temperature was measured with two separate methods: the LI-6400XT and the infrared temperature meter. Stomatal conductance and transpiration rate hardly changed across the experiment (Fig. 6.7, p. 137) but mean leaf temperature differed depending on the method of measurement. Mean leaf temperature was only 0.08°C higher in UV+ polytunnels when measured with the LI-6400XT, with zero difference in radiation loading during measurement because total radiation was equal. However, the difference was 0.29°C higher when measured with the infrared temperature meter (Fig. 6.8, p. 138), and so was affected by differences in radiation loading, resulting from a difference in total radiation transmission between UV+ and UV- polytunnels, which was 67 W m⁻². This demonstrates that leaf warming caused by a difference in total radiation of 67 W m⁻² due to downwelling solar radiation imbalance between the differently clad polytunnels was 0.21°C. The difference in total radiation in Antalya in the summer (2019) was up to 107 W m⁻² indicating leaf warming resulting from that, and on the basis of exponential leaf temperature increase (Fig. 8.2) would be much greater. Analysing the difference in radiation loading between treatments for each experiment location, rather than the absolute radiation loading for each of those experiment locations, leads to the third method of quantifying the relative effects of stomatal closure and radiation loading on UV-induced leaf temperature increases.

8.3.3 Method 3: Comparing Experiments Under Different Radiation Loading Environments

The third method analyses the differences in radiation loading between UV+ and UV- treatments when leaf temperature measurements occur, rather than absolute total radiation. Firstly, by taking the known difference in total radiation (radiation loading) between treatments when leaf temperature was measured and analysing it with the known leaf temperature increase attributable to differences in total radiation

demonstrates the relationship between each (Fig 8.3). The relationship indicates an exponential increase in leaf temperature as the difference in radiation loading increases ($R^2: 0.997$; Fig. 8.3), similar to the relationship between the leaf temperature increase for each $100 \text{ mmol m}^{-2} \text{ s}^{-1}$ reduction in stomatal conductance and absolute total radiation (Fig. 8.2). This substantiates that the general relationship between total radiation and leaf temperature is an exponential increase.

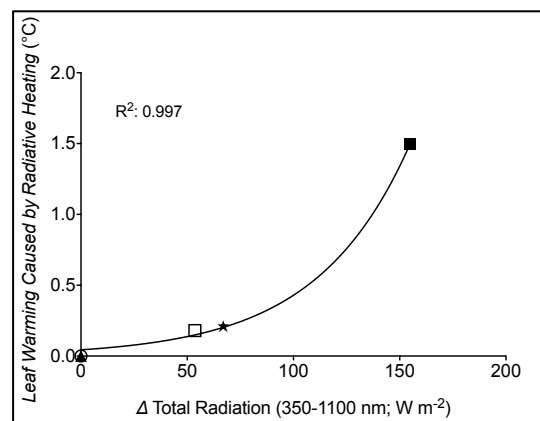


Figure 8.3: Non-linear regression analysis (exponential increase) of the difference in total radiation (Δ Total Radiation (350-1100 nm) between UV+ and UV- treated leaves during measurements and the leaf warming caused by radiative heating alone. The symbols represent separate experiments: (open square) the climate cabinet experiment that applied cellulose acetate filtered 0.297 W m^{-2} PGIAS, (open circle) the three controlled environment room experiments, which is overlapped by (closed triangle) the polytunnel experiment at Antalya 2019, (closed square) experiments 1 and 2 at Lancaster, and, (star) the polytunnel experiment at Antalya 2018.

Secondly, comparison of experiments where the LI-6400XT LED attachment was used for measurements, with zero total radiation differences between treatments (‘no radiative heating’; Tab. 8.1) with results arising from measurements under maximal solar radiation conditions (with high total radiation differences between treatments, ‘solar’; Tab. 8.1) can identify the individual absolute contributions to leaf warming of stomatal closure and radiative heating. The reduction in stomatal conductance is not known for the reports from commercial growers (Williams *et al.*, 2020) or the work in the Czech Republic (Novotná *et al.*, 2016) but radiation loading at those latitudes in summer would be at least equal to that in Lancaster, and at or near maximum.

Table 8.1: A summary and comparison of maximum leaf temperature increase (T_{leaf}), stomatal conductance decrease (g_s) and transpiration rate decrease (E) between UV+ and UV- treatments in measurements made with the LI-6400XT ('no radiative heating') with zero difference in radiation loading between treatments when measured, and those made under 'solar' conditions where radiation loading differences were much greater.

Experimental Campaign	T_{leaf} Increase (°C)	g_s Reduction (mmol m ⁻² s ⁻¹)	E Reduction (mmol m ⁻² s ⁻¹)	Δ Total Radiation (W m ⁻²)	UV Radiation
CE Room (Chapter 4)	0.23±0.10	-118±43 (-21%)	-0.85±0.25 (-13%)	0	0.35 W m ⁻² / 17.8 kJ m ⁻² d ⁻¹ (PGIAS) 6.57 W m ⁻² / 346 kJ m ⁻² d ⁻¹ (unweighted)
Antalya 2019 (Chapter 6)	0.65±0.21	-34±19 (-19%)	-1.31±0.64 (-16%)	0	18.8 W m ⁻² / 551 kJ m ⁻² d ⁻¹ (unweighted)
Mean (no radiative heating)	0.56	-76 (-20%)	-1.03 (-15%)	0	
Lancaster Poly tunnels (Chapter 5)	2.2±1.6	-156±88 (-34%)	Not available	155	0.476 W m ⁻² / 12.8 kJ m ⁻² d ⁻¹ (PGIAS) 23.5 W m ⁻² / 640 kJ m ⁻² d ⁻¹ (unweighted)
Turkey (Williams <i>et al.</i> , 2020)	1.9±1.3	Not available	Not available	Not available	Not available
Czech Republic (Novotná <i>et al.</i> , 2016)	~2.0	Not available	Not available	Not available	Not available
Mean (solar)	2.0	-156±88 (-34%)	Not available	155	

The 'no radiative heating' experiments demonstrate that leaf temperature increase resulting from UV-induced stomatal closure alone (mean stomatal conductance reduction: 76 mmol m⁻² s⁻¹ / 20%) is 0.56°C (Tab. 8.1). The stomatal conductance reduction at Lancaster was 14% greater than the mean for those with 'no radiative heating', which would be expected to have increased leaf temperature more. Bearing that in mind, the mean leaf temperature increase under 'no radiative heating' was 0.56°C compared to 2.0°C under 'solar' conditions (Tab. 8.1), a 360% increase. This indicates that stomatal closure under maximal 'solar' conditions accounts for ~25% of leaf warming and radiative heating ~75%. However, taking into account the greater stomatal conductance reduction in the polytunnels at Lancaster, the effect of total radiation would be marginally lower, with ~30% of leaf warming caused by stomatal closure and ~70% caused by radiative heating, when total radiation differences between treatments are close to maximum.

8.3.4 Summary of the Relative and Absolute Effects of Partial Stomatal Closure and Radiation Loading on Leaf Temperature

It has been identified that radiative heating caused by absolute total radiation ranged 200-700%, and that leaf temperature increases exponentially with enhanced total radiation (Section 8.3.1; Fig. 8.2). Analysis of the relationship between differences in total radiation and leaf temperature between UV treatments, for multiple experiments with variable differences in total radiation between UV treatments, again reveals an exponential increase in leaf temperature with enhanced radiation loading differences (Section 8.3.3; Fig. 8.3), substantiating the exponential relationship. Comparing experiments conducted with ‘no radiative heating’ and those under ‘solar’ conditions (Tab. 8.1) indicated that stomatal closure accounts for ~30% of the leaf temperature increase and ~70% is attributable to radiative heating from the differences in radiation loading between treatments under maximal solar conditions (Section 8.3.3). This demonstrates the relative effects of stomatal closure and radiative heating, and that leaf warming can be enhanced 200-700%, increasing exponentially with total radiation.

Where absolute temperature increase can be attributed to only one leaf warming mechanism, leaf warming caused by radiative heating alone ranged 0.21°C (Antalya 2018; Section 8.3.2). to 1.5°C. Leaf temperature increase caused by radiation loading in the climate cabinet (total radiation difference between control and UV treatments was 53.6 W m⁻²) was quantified as 0.16°C (Fig. 3.12, p. 53), corroborating that observed in Antalya 2018 where the radiation differences between treatments was similarly low (67.0 W m⁻²). This demonstrates the range of absolute leaf temperature increases attributable to stomatal closure and radiative heating.

Leaf warming caused by stomatal closure alone was a mean of 0.56°C across two experiments (ranging 0.23-0.65°C; Tab. 8.1; Section 8.4.2), in broad agreement with that observed in the climate cabinet experiments with respect to the global maximum (PGIAS: 0.66°C; GPAS: 0.52°C; Fig. 3.4, p. 42), substantiating that UV-induced warming in response to UV radiation is ~0.5°C (mean), up to a maximum of ~0.7°C. This demonstrates the range of absolute leaf temperature increases attributable to stomatal closure alone.

Radiative heating has the potential to have a greater effect on leaf warming than stomatal closure, when differences in radiation loading are low stomatal closure dominates leaf warming but when it is high radiation loading dominates. The balance between stomatal closure and radiative heating is dependent on UV irradiance / dose and radiation loading. Stomatal closure is dependent on external UV irradiance / dose and subsequent transmission through the different plastics. Radiation loading is dependent on ambient total radiation and subsequent transmission through the different plastics. Thus the balance between these warming mechanisms will vary depending on the relative inputs of each, as observed by the substantial difference between the experiments in polytunnels at Lancaster where radiation loading was high and the experiments in the CE room where there were no radiation loading differences between treatments during measurements.

Thus my overall conclusions from this synthesis of the experiments conducted are:

1. Exposure to UV radiation causes partial stomatal closure that increases leaf temperature by up to ~0.7°C.
2. The magnitude of leaf temperature increase is dependent on:
 - a. The degree of stomatal closure determined by the UV irradiance / dose.

- b. The radiation loading that is caused by differences in total radiation, resulting from the total radiation transmission properties of different plastic claddings, dependent on latitude and season.

This leads to a final question: How much variation exists in the transmission properties of the different plastic claddings available for use in commercial protected horticultural cultivation and scientific studies. Such variability could affect differences in leaf warming related to radiation loading in addition to UV-induced leaf warming caused by partial stomatal closure.

8.4 An Initial Assessment of the Transmission Properties of a Range of Commercial Cladding Plastics

The polytunnel experiments were focussed on the same two plastics: a UV-transparent (UV-T) and a UV-opaque (UV-O), but in reality there is no single UV-T or UV-O plastic as commercial companies market a range of products. For this reason the original reports from commercial growers may relate to plastics with different UV transmission properties to the polytunnel work in this thesis, and this thesis does not attempt to compare all UV-T and UV-O plastics in existence. Recent work (Paul *et al.*, in prep.) has investigated this range of UV manipulating plastics to determine how they vary, not only in UV radiation transmission but also PAR and total solar radiation. In the context of my research, this is clearly important since I have shown that differences in radiation loading between plastics can greatly affect leaf temperature, especially under high total radiation. Cluster analysis was used to identify ‘groups’ of plastics with similar UV radiation transmission properties (Paul *et al.*, in prep.). These groups were analysed to determine how much variation existed between the groups in their radiation (UV, PAR and total) transmission properties.

Ultimately eight distinctively different ‘groups’ of plastics were identified based on their UV-A and UV-B transmission properties in the cluster analysis (Fig. 8.4).

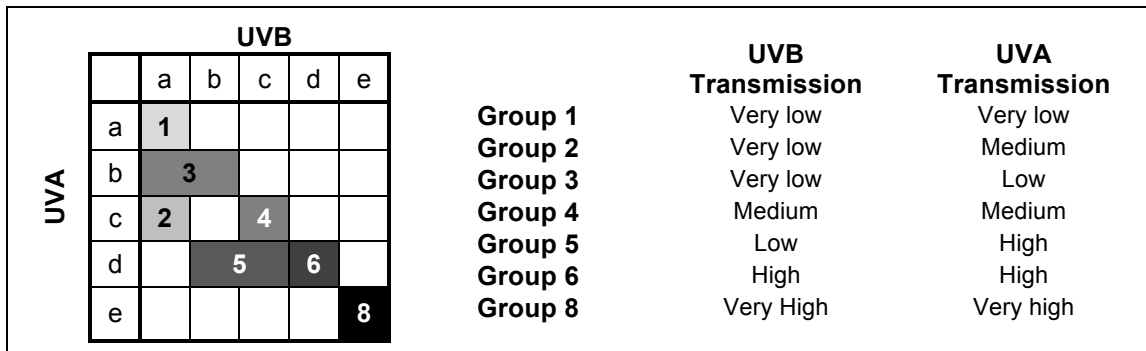


Figure 8.4: Matrix of plastic groups (numbered) for homogeneous sub-sets based on analysis of UV-A and UV-B transmission and conversion of those 8 groups into categories of transmission properties. NB Group 7 consisted of a single ‘woven’ film and has been excluded from this overview (Paul *et al.*, in prep.).

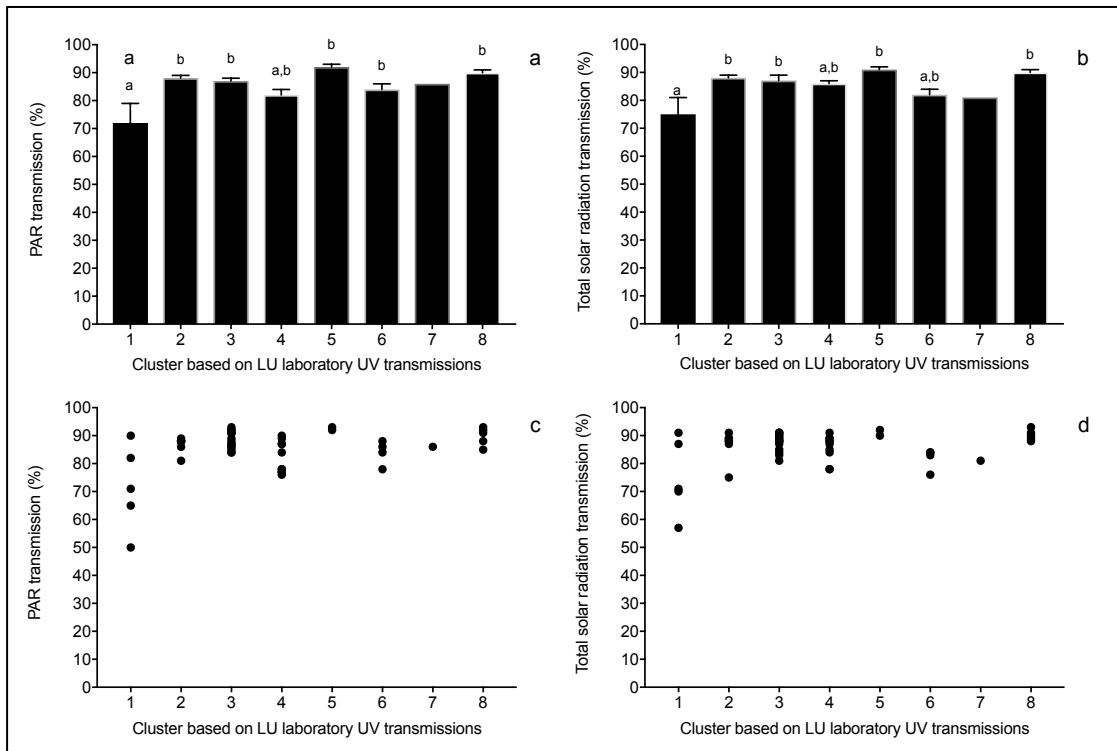


Figure 8.5: Based on groups resulting from cluster analysis of UV radiation transmission (a) analysis of PAR transmission, and (b) analysis of total radiation (290-800 nm) transmission. The results of one-way ANOVA with ‘LU lab group’ as the main factor and Tukey post-hoc sub-sets are summarised by lettering. Group 7 contained only a single plastic so was omitted from ANOVA analysis. (c) Analysis of the range of PAR transmissions within each group, and (d) the same analysis for total radiation (Paul *et al.*, in prep.).

Analysing these ‘UV groups’ of plastics for PAR and total radiation, immediately demonstrates much less variation in the transmission properties of both compared with

UV transmission (Fig. 8.5). Overall, group 1, the lowest UV radiation transmitter ('UV-opaque'), had significantly lower transmission of both PAR and total radiation than group 8 (the 'UV-transparent' group). However, it is evident that group 1 plastics contain a far greater range of PAR and total radiation transmissions than the other groups, ranging from around 50% in one exceptional 'shade film' to around 90% (Fig. 8.5: Paul *et al.*, in prep.). There were no such 'shade films' in the groups with higher UV transmission, which had consistently high transmission of both PAR and total solar radiation.

Based on this analysis, depending on the films used, a pair of 'UV-transparent' and 'UV-opaque' films might have very similar transmissions of PAR and total solar radiation, or the UV-transparent film might have substantially higher transmissions of both. This would affect leaf temperature through the separate or combined effects of UV-induced partial stomatal closure and radiative heating due to radiation imbalances. Indeed, such effects became evident as I examined my own data. In this thesis the plastics used in Lancaster (Chapter 5) transmitted 90% (UV-) and 92% (UV+) PAR, so both at the higher end of transmissions determined by Paul *et al.* (in prep.). In Antalya the plastics transmitted 83% (UV-) and 85% (UV+) when new. However, this reduced to 71% (UV-) and 83% (UV+) after 8 months on the polytunnels, due to ageing and accumulated 'dirt', which would place the UV- plastic in the lowest group (group 1).

The polytunnels at Lancaster transmitted 72% (UV-) and 89% (UV+) total radiation, a greater difference than seen in the PAR transmission, placing the plastics at the opposite ends of the scale in terms of total radiation transmission. This can explain why radiative heating caused by total radiation imbalances between the plastics was a

significant factor in leaf warming in UV+ polytunnels. In Antalya the total radiation transmission was reduced to 67% (UV-) and 80% (UV+) when new. Again there is a large difference between the plastics that contributes significantly towards leaf warming in UV+ polytunnels. UV- transmission of 67% places the plastic in group 1 only and UV+ transmission of 80% puts it in group 7, the second lowest group in terms of total radiation. After ageing and accumulation of dirt these transmissions reduced to 63% (UV-) and 78% (UV+) placing UV- at the bottom of the scale in group 1 but UV+ at the bottom of a number of different groups (groups 3, 5 and 6). This demonstrates a great variation in both plastics, varying total radiation transmission by 9% to 11% respectively, even though they are technically the same plastics (produced at different times), and were actually the same plastics (in the separate experiments in Antalya).

Thus, caution is required when selecting films for commercial cultivation or scientific studies. Any leaf temperature increases observed might be influenced by differential transmission of radiation other than UV, in addition to UV-induced partial stomatal closure that clearly increases leaf temperature in response to UV radiation alone.

8.5 Conclusions

- UV-induced partial stomata closure reduces stomatal conductance and transpiration rate, thus increasing leaf temperature.
 - Up to $\sim 0.7^{\circ}\text{C}$ leaf temperature increase attributable to stomatal closure alone.
 - When solar radiation conditions are at or near maximal stomatal closure accounts for $\sim 30\%$ of the leaf temperature increases observed.

- Differences in total radiation vary radiation loading that increases leaf temperature through direct radiative heating.
 - Up to ~1.5°C leaf temperature increase attributable to radiative heating alone.
 - When solar radiation conditions are at or near maximal radiative heating accounts for ~70% of the leaf temperature increases observed.
 - Radiative heating caused by differences in radiation loading enhances leaf temperature by 200-700%, increasing exponentially.
- Greater net (total) radiation in UV+ polytunnels enhances leaf temperature.
 - Downwelling and net solar radiation was greater in UV+ polytunnels.
 - Downwelling and net far infrared radiation was lower in UV+ polytunnels.
 - Solar radiation dominates the net radiation balance resulting in direct radiative heating of leaves.
- Ultimately the balance between UV-induced stomatal closure and radiative heating on leaf temperature is dependent on the external radiation environment (season and latitude), and the transmission properties (UV and total radiation) of the plastics.
- Recent analysis of many available plastics (Paul *et al.*, in prep.) highlights there are not only UV-transparent (UV+) and UV-opaque (UV-) plastics available, but a great range of plastics dependent on the combination of UV-A, UV-B, PAR and total radiation transmission properties, forming 8 distinct groups, highlighting that the balance of leaf warming mechanisms is dependent on the plastics used on polytunnels.

8.5.1 The Implications of Warmer Leaf Temperatures in Crops

The conclusive evidence that UV radiation increases leaf temperature in tomato through partial stomatal closure is likely to be relevant to the majority of crops, if not all, produced globally. However, a number of questions still exist that require further investigation. Does higher leaf temperature correspond with an increase in whole plant temperature? Does this lead to early maturity, as suggested by the original reports from commercial growers utilising UV-transparent plastic claddings? Do warmer crops translate into greater yields? Growth and photosynthesis increase up to an optimal temperature, beyond which further temperature increases are detrimental (Berry and Bjorkman, 1980; Gent, 1986; Long, 1991; Sage and Kubien, 2007). The model of Gent (1986) between growth rate and temperature in tomato indicates that a 2°C temperature increase at 15°C would enhance growth rate by 17% whereas at 35°C growth rate would reduce by 10%. Thus, an increase in leaf and crop temperature is not necessarily beneficial in all circumstances.

A clear benefit of greater leaf temperature, and presumably overall crop temperature, is the ability to extend the growing season at the start and end, enabling greater overall production. However, in locations with warm climates such as southern Turkey, crops such as tomato cannot be grown in mid-summer due to high temperatures meaning a further increase in temperature would perhaps detrimentally extend the non-growing mid-summer period. Thus, if using the same plastic throughout a growing season there would be a trade-off between the benefits enjoyed at the start/end of the season and the detriment in mid-season. It may be that certain plastic claddings, such as UV-transparent, could be used at specific points in the season e.g. start and end, with UV-opaque cladding used mid-season to eliminate the effect of UV radiation on leaf temperature. It may be that UV-transparent cladding is best utilised in cooler climates,

such as the UK, and plastics that lean towards UV-opaque in warmer climates such as southern Turkey. Furthermore, increased temperature may benefit certain crops more than others, so UV-transparent cladding would be best utilised with specific crops, but this would require further investigation. Ultimately, with climate change induced global warming, increased leaf and crop temperatures may not be beneficial at all in some locations with already warm climates. However, a reduction in total water use caused by UV-induced partial stomatal closure, could be a benefit in dry climates where climate change increases drought conditions. Thus, a number of different considerations and trade-offs may need to be analysed in order to optimise the use of UV-transparent plastic claddings for polytunnels.

Finally, what effect does enhanced leaf temperature have on plant interactions with other organisms? The general consensus is that UV radiation inhibits leaf chewing herbivores such as caterpillars, lessening severity, through plant synthesis of chemical defences (Paul *et al.*, 1997; Schweiger *et al.*, 2014) and stimulation of jasmonate-mediated defences (Demkura *et al.*, 2010). However, phloem feeders such as aphids have responded in a variety of ways to UV radiation, both negative (Salt *et al.*, 1998; Hu *et al.*, 2013; Kuhlmann and Muller, 2010) and positive (Paul *et al.*, 2012; Rechner *et al.*, 2016; Rechner and Poehling, 2014). Similar to plant growth rate, this may reflect differences in absolute crop temperature between experiments and/or the optimum temperatures for herbivory of specific species. Following the model of Satar *et al.* (2008), a 2°C temperature increase would enhance the rate of aphid increase by 90% at 15°C but cause a similar reduction at 30°C, thus emphasising the range of responses to enhanced leaf temperature that may occur. Ultimately, there are a number of different complex factors to consider when assessing the implications of enhanced

leaf temperatures on crop production, and the use of UV-transparent plastic claddings for polytunnels to enhance leaf temperature.

9 References

- Allen, D. J., McKee, I. F., Farage, P. K. and Baker, N. R. (1997). Analysis of limitations to CO₂ assimilation on exposure of leaves of two *Brassica napus* cultivars to UV-B. *Plant, Cell and Environment*, 20, 633-640.
- Allen, D. J., Noguès, S. and Baker, N. R. (1998). Ozone depletion and increased UV-B radiation: is there a real threat to photosynthesis? *Journal of Experimental Botany*, 328, 1775-1788.
- Allen, D. J., Noguès, S., Morison, J. I. L, Greenslade, P. D., McLeod, A. R. and Baker, N. R. (1999). A thirty percent increase in UV-B has no impact on photosynthesis in well-watered and droughted pea plants in the field. *Global Change Biology*, 5, 235-244.
- Aphalo, P. J., Albert, A., Björn, L. O., McLeod, A. Robson, T. M. Rosenqvist, E. (eds.) (2012). *Beyond the visible: A handbook of best practice in plant UV photobiology*. COST Action FA0906 UV4growth. Helsinki: University of Helsinki, Division of Plant Biology.

- Atmospheric Chemistry Observations & Modeling. (2019) *Tropospheric ultraviolet and visible radiation model*. National Center for Atmospheric Research. Available at: http://cprm.acom.ucar.edu/Models/TUV/Interactive_TUV/ [Accessed 1 August 2019].
- Ballaré C. L. (2011). Light Regulation of Plant Defense. *Annual Review of Plant Biology*, 65, 335–363.
- Benz, B. W. and Martin C. E. (2006). Foliar trichomes, boundary layers, and gas exchange in 12 species of epiphytic *Tillandsia* (Bromeliaceae). *Journal of Plant Physiology*, 163, 648–656, doi:10.1016/j.jplph.2005.05.008.
- Bertolino, L. T., Caine, R. S. and . and Gray, J. E. (2019). Impact of Stomatal Density and Morphology on Water-Use Efficiency in a Changing World. *Frontiers in Plant Science*, 10:225.
- Bickford, C. P. (2016). Ecophysiology of leaf trichomes. *Functional Plant Biology*, 43, 807-814. <http://dx.doi.org/10.1071/FP16095>.
- Caldwell, M. M. (1971). Solar UV irradiation and the growth and development of higher plants. In: *Photophysiology*. Ed. by A. C. Giese. Vol. 6. New York: Academic Press, 131–177.
- Caldwell, M. M., Robberecht, R. and S. D. Flint. (1983). Internal filters: Prospects for UV-acclimation in higher plants. *Physiologia Plantarum*, 58, 445-450.

- Caldwell M. M., Camp L. B., Warner C. W. and Flint S. D. (1986). Action spectra and their key role in assessing biological consequences of solar UV-B radiation change. In: Worrest R. C., and Caldwell M. M. (eds.) *Stratospheric Ozone Reduction, Solar Ultraviolet Radiation and Plant Life*. Springer, Berlin, pp 87–111, ISBN 3-540-13875-7.
- Caldwell, M. M. and S. D. Flint. (1994). Solar Ultraviolet Radiation and Ozone Layer Change: Implications for Crop Plants. In: *Physiology and Determination of Crop Yield*, (eds.) Boote, J. K., Bennett, J. M., Sinclair, T. R. and Paulsen, G. M.. ASA-CSSA-SSSA, Madison, WI.
- Caldwell, M. M. and S. D. Flint. (2006). Use and Evaluation of Biological Spectral UV Weighting Functions for the Ozone Reduction Issue. In: *Environmental UV Radiation: Impact on Ecosystems and Human Health and Predictive Models*. Ed. by F. Ghetti, G. Checcucci and J. F. Bornman. Vol. 57. NATO Science Series. Proceedings of the NATO Advanced Study Institute on Environmental UV Radiation: Impact on Ecosystems and Human Health and Predictive Models Pisa, Italy June 2001. Dordrecht: Springer, 71–84, doi: 10.1007/1-4020-3697-3 (cit. on p. 102).
- Caldwell, M. M., Bornman, J. F., Ballaré C. L., Flint, S. D. and Kulandaivelu, G. (2007). Terrestrial ecosystems, increased solar ultraviolet radiation, and interactions with other climate change factors. *Photochemical and Photobiological Sciences*, 6, 252-266.

- Cen, Y.-P. and Bornman, J. F. (1993). The effect of exposure to enhanced UV-B radiation on the penetration of monochromatic and polychromatic UV-B radiation in leaves of *Brassica napus*. *Physiologia Plantarum*, 87, 249–255, doi: 10.1111/j.1399-3054.1993.tb01727.
- Chater, C. C. C., Oliver, J., Casson, S. and Gray, J. E. (2014). Putting the brakes on: abscisic acid as a central environmental regulator of stomatal development. *New Phytologist*, 202, 376–391.
- Clark, J. B., Lister, G. R. (1975). Photosynthetic action spectra of trees. II. The relationship of cuticle structure to the visible and ultraviolet spectral properties of needles from four coniferous species. *Plant Physiology*, 55, 407–413.
- Ceulemans, R., Hinckley, T. M. and Impens, I. (1989). Stomatal response of hybrid poplar to incident light, sudden darkening and leaf excision. *Physiologia Plantarum*, 75, 174-182.
- Dai, Q., Peng, S., Chavez, A. Q. and Vergara, B. S. (1995). Effects of UVB Radiation on Stomatal Density and Opening in Rice (*Oryza sativa* L.). *Annals of Botany*, 76, 65-70.
- De Boeck, H. J., De Groote, De. And Nijs, I. (2012). Leaf temperature in glasshouses and open top chambers. *New Phytologist*, 194, 1155-1164.
- Dehariya, P., Kataria, S., Guruprasad, K. N. and Pandey, G. P. (2014). Photosynthesis and yield in cotton (*Gossypium hirsutum* L.) Var. Vikram after exclusion of ambient solar UV-B/A. *Acta Physiologiae Plant*, 34, 1133-1144.

- Demkura, P. V., Abdala, G., Baldwin, I. T. and Ballaré, C. L. (2010). Jasmonate-Dependent and -Independent Pathways Mediate Specific Effects of Solar Ultraviolet B Radiation on Leaf Phenolics and Antiherbivore Defense. *Plant Physiology*, 152, 1084-1095.
- Demkura, P. V. and Ballaré, C. L. (2012). UVR8 Mediates UV-B-Induced Arabidopsis Defense Responses against *Botrytis cinerea* by Controlling Sinapate Accumulation. *Molecular Plant*, 5, 642-652.
- Dobrikova, A. G., Krasteva, V. and Apostolova, E. L. (2013). Damage and protection of the photosynthetic apparatus from UV-B radiation. I. Effect of ascorbate. *Journal of Plant Physiology*, 170, 251-257.
- Eisinger, W. R., Swartz, T. E., Bogomolni, R. A. and Taiz, L. (2000). The Ultraviolet Action Spectrum for Stomatal Opening in Broad Bean. *Plant Physiology*, 122, 99-105.
- Eisinger, W. R., Bogomolni, R. A. and Taiz, L. (2003). Interactions between a blue-green reversible photoreceptor and a separate UV-B receptor in stomatal guard cells. *American Journal of Botany*, 90, 1560-1566.
- Farman, J. C., Gardiner, B. G. and Shanklin J. D. (1985). Large losses of total ozone in Antarctica reveal seasonal ClO_x/NO_x interaction, *Nature*, 315, 207-210.
- Farquhar, G. D. and Sharkey, T. D. (1982). Stomatal Conductance and Photosynthesis. *Annual Reviews*, 317-340.

- Flexas, J., Ribas-Carbo, M., Diaz-Espejo, A., Galmes, J. and Medrano, H. (2008). Mesophyll conductance to CO₂: current knowledge and future prospects. *Plant, Cell and Environment*, 31, 602-621.
- Flexas, J. and Medrano, H. (2002). Drought-inhibition of Photosynthesis in C₃ Plants: Stomatal and Non-stomatal Limitations Revisited. *Annals of Botany*, 89, 183-189.
- Flint, S. D. and M. M. Caldwell. (1996). Scaling Plant Ultraviolet Spectral Responses from Laboratory Action Spectra to Field Spectral Weighting Factors. *Journal of Plant Physiology*, 148, 107–114.
- Flint, S. D. and M. M. Caldwell. (2003). A biological spectral weighting function for ozone depletion research with higher plants. *Physiologia Plantarum*, 117, 137–144.
- Franks, P. J. and Farquhar, G. D. (2001). The Effect of Exogenous Abscisic Acid on Stomatal Development, Stomatal Mechanics, and Leaf Gas Exchange in *Tradescantia virginiana*. *Plant Physiology*, 125, 935-942.
- Gaberscik, A., Voncina, M., Trost, T., Germ, M. and Bjorn, L. O. (2002). Growth and production of buckwheat (*Fagopyrum esculentum*) treated with reduced, ambient, and enhanced UV-B radiation. *Journal of Photochemistry and Photobiology B: Biology*, 66, 30–36.
- Gates, D. M., Keegan, H. J., Schleter, J. C. and Weidner, V. R. (1965). Spectral properties of plants. *Applied Optics*, 4, 11–20.
- Gausman, H. W., Rodriguez, R. P., Escobar, D. E. (1975). Ultraviolet radiation reflectance, transmittance, and absorptance by plant leaf epidermises. *Agronomy Journal*, 67, 720–724.

- Gegas, V. C., Wargent, J. J., Pesquet, E., Granqvist, E., Paul, N. D. and Doonan, J. H. (2014). Endopolyploidy as a potential alternative adaptive strategy to *Arabidopsis* leaf size variation in response to UV-B. *Journal of Experimental Botany*, 65, 2757-2766.
- Gitz III, D. C., Liu-Gitz, L., Britz S. J. and Britz S. J. (2005). Ultraviolet-B effects on stomatal density, water-use efficiency, and stable carbon isotope discrimination in four glasshouse-grown soybean (*Glycine max*) cultivars. *Environmental and Experimental Botany*, 53, 343-355.
- Gitz III, D. C., Britz S. J. and Sullivan, J. H. (2013). Effect of Ambient UV-B on Stomatal Density, Conductance and Isotope Discrimination in Four Field Grown Soybean [*Glycine max* (L.) Merr.] Isolines. *American Journal of Plant Sciences*, 4, 100-108.
- Gonzalez, R., Paul, N. D., Percy, K., Ambrose, M., McLaughlin, C. K., Barnes, J. D., Areses, M. and Welburn, A. R. (1996). Responses to ultraviolet-B radiation (280-315 nm) of pea (*Pisum sativum*) lines differing in leaf surface wax. *Physiologia Plantarum*, 98, 852-860.
- Grant, L. (1987). Diffuse and specular characteristics of leaf reflectance. *Remote Sensing Reviews*, 22, 309-322.
- Grant, R. H., Heisler, G. M., Goa, W. and Jenks, M. (2003). Ultraviolet leaf reflectance of common urban trees and the prediction of reflectance from leaf surface characteristics. *Agricultural and Forest Meteorology*, 120, 127-139.

- Gray, J. E., Holroyd, G. H., van der Lee, F. M., Bahrami, A. R., Sijmons, P. C., Woodward, F. I., Schuch, W. and Hetherington A. M. (2000). The HIC signalling pathway links CO₂ perception to stomatal development. *Nature*, 408, 713-716.
- Grant, O. M., Chaves, M. M. and Jones, H. G. (2006). Optimizing thermal imaging as a technique for detecting stomatal closure induced by drought stress under greenhouse conditions. *Physiologia Plantarum*, 127, 507-518.
- He, J.-M., Xu, H., She, X.-P. Song, X.-G. and Zhao, W.-M. (2005). The role and Interrelationship of Hydrogen Peroxide and Nitric Oxide in the UV-B-Induced Stomatal Closure in *Arabidopsis* Leaves. *Functional Plant Biology*, 32, 237-247.
- He, J.-M., Zhang, Z., Wang, R.-B. and Chen, Y.-P. (2011a). UV-B-induced stomatal closure occurs via ethylene-dependent NO generation in *Vicia faba*. *Functional Plant Biology*, 38, 293–302.
- He, J.-M., Yue, X., Wang, R. and Zhang, Y. (2011b). Ethylene mediates UV-B-induced stomatal closure via peroxidase-dependent hydrogen peroxide synthesis in *Vicia faba* L.. *Journal of Experimental Botany*, 62, 2657–2666.
- He, J.-M., Ma, X.-G., Sun, T.-F., Xu, F.-F. Chen, Y.-P., Liu, X. and Yue, M. (2013). Role and Interrelationship of Ga Protein, Hydrogen Peroxide, and Nitric Oxide in Ultraviolet B-Induced Stomatal Closure in *Arabidopsis* Leaves. *Plant Physiology*, 161, 1570–1583.
- Hectors, K., Prinsen, E., De Coen, W., Jansen, A. K. and Guisez, Y. (2007). *Arabidopsis thaliana* plants acclimated to low dose rates of ultraviolet B radiation show specific changes in morphology and gene expression in the absence of stress symptoms. *New Phytologist*, 175, 255–270.

- Hectors, K., Jacques, E., Prinsen, E., Guisez, Y., Verbelen, J.-P., Jansen, M. A. K. and Vissenberg, K. (2010). UV radiation reduces epidermal cell expansion in leaves of *Arabidopsis thaliana*. *Journal of Experimental Botany*, 61, 4339–4349.
- Holmes, M. G. (1997). Action spectra for UV-B effects on plants: monochromatic approaches for analyzing plant responses. In: Lumsden, P.J. (Ed.), *Plants and UV-B: Responses to Environmental Change*. Society for Experimental Biology, Seminar Series 64. Cambridge University Press, Cambridge, 31–50.
- Holroyd G. H., Hetherington A. M. and Gray, J. E. (2002). A role for the cuticular waxes in the environmental control of stomatal development. *New Phytologist* 153: 433–439.
- Hu, Z. Q., Zhao, H. Y. and Thieme, T. (2013). PROBING BEHAVIORS OF SITOBION AVENAE (HEMIPTERA: APHIDIDAE) ON ENHANCED UV-B IRRADIATED PLANTS. *Archives of Biological Sciences*, 65, 247-254.
- Huché-Théliér, L., Crespel, L., Gourrierc, j. L., Morel, P., Sakr, S. and Leduc, N. (2016). Light signaling and plant responses to blue and UV radiations— Perspectives for applications in horticulture. *Environmental and Experimental Botany*, 121, 22-38.
- Huggins, T. D., Mohammed, S., Sengodan, P., Ibrahim, A. M. H., Tilley, M. and Hays, D. B. (2017). Changes in leaf epicuticular wax load and its effect on leaf temperature and physiological traits in wheat cultivars (*Triticum aestivum* L.) exposed to high temperatures during anthesis. *Journal of Agronomy and Crop Science*, 204, 49-61.

- Ibdah, M., Krins, A. Seidlitz, H. K. Heller, W. Strack, D. and Vogt, T. (2002). Spectral dependence of flavonol and betacyanin accumulation in *Mesembryanthemum crystallinum* under enhanced ultraviolet radiation. *Plant, Cell Environment*, 25, 1145–1154.
- Innes, S. N., Solhaug, K. A., Arve, L. E. and Torre, S. (2018). UV radiation as a tool to control growth, morphology and transpiration of poinsettia (*Euphorbia pulcherrima*) in variable aerial environments. *Scientia Horticulturae*, 235, 160-168.
- Jansen, M. A. K and Noort, R. E. (2000). Ultraviolet-B radiation induces complex alterations in stomatal behaviour. *Physiologia Planatarum*, 110, 189–194.
- Jenkins, G. I. (2009). Signal Transduction in Responses to UV-B Radiation. *Annual Reviews of Plant Biology*, 60. 407-431.
- John A. e-Education Institute. (2003) *SimSphere Workbook: Chapter 7*. Available at: <https://courseware.e-education.psu.edu/simsphere/workbook/ch07.html> [1 November 2015].
- Jones, H. G. (1985). Partitioning stomatal and non-stomatal limitations to photosynthesis. *Plant, Cell and Environment*, 8, 95-104.
- Jordan, B. R., He, J., Chow, W. S. and Anderson, J. M. (1992). Changes in mRNA levels and polypeptide subunits of ribulose 1,5-bisphosphate carboxylase in response to supplementary ultraviolet-B radiation. *Plant, Cell and Environment*, 15, 91-98.

- Kakani, V. G., Reddy, K. R., Zhao, D. and Mohammed, A. R. (2003a). Effects of Ultraviolet-B Radiation on Cotton (*Gossypium hirsutum* L.) Morphology and Anatomy. *Annals of Botany*, 91, 817-826, doi:10.1093/aob/mcg086.
- Kakani, V. G., Reddy, K. R., Zhao, D. and Sailaja, K. (2003b). Field crop responses to ultraviolet-B Radiation: a review. *Agricultural and Forest Meteorology*, 120, 191-218, doi:10.1016/j.agrformet.2003.08.015.
- Kaukoranta, T., Murto, J., Takala, J. and Tahvonen, R. (2005). Detection of water deficit in greenhouse cucumber by infrared thermography and reference surfaces. *Scientia Horticulturae*, 106, 447-463.
- Karabourniotis, G., Bornman, J. F and Liakoura, V. (1999). Different leaf surface characteristics of three grape cultivars affect leaf optical properties as measured with fibre optics: possible implication in stress tolerance. *Australian Journal of Plant Physiology*, 26, 47-53.
- Kakani, V. G., Reddy, K. R., Zhao, D. and Mohammed, A. R. (2003a). Effects of Ultraviolet-B Radiation on Cotton (*Gossypium hirsutum* L.) Morphology and Anatomy. *Annals of Botany*, 91, 817-826, doi:10.1093/aob/mcg086.
- Kakani, V. G., Reddy, K. R., Zhao, D. and Sailaja, K. (2003b). Field crop responses to ultraviolet-B Radiation: a review. *Agricultural and Forest Meteorology*, 120, 191-218, doi:10.1016/j.agrformet.2003.08.015.
- Kataria, S., Guruprasad, K. N., Ahuja, S. and Singh, B. (2013). Enhancement of growth, photosynthetic performance and yield by exclusion of ambient UV components in C3 and C4 plants. *Journal of Photochemistry and Photobiology B: Biology*, 127, 140-152.

- Kataria, S., Jajoo, A. and Guruprasad, K. N. (2014). Impact of increasing ultraviolet-B (UV-B) radiation on photosynthetic processes. *Journal of Photochemistry and Photobiology B: Biology*, 137, 55-66.
- Kataria, S. and Guruprasad, K. N. (2015). Exclusion of solar UV radiation improves photosynthetic performance and yield of wheat varieties. *Plant Physiology and Biochemistry*, 97, 400-411.
- Kipp & Zonen B. V. (2014). *CNR4 Net Radiometer: Instruction Manual*. Kipp & Zonen, Delft.
- Klem, K., Ac, A., Holub, P., Kovac, D., Spunda, V., Robson, T. M. and Urban, O. (2012). Interactive effects of PAR and UV radiation on the physiology, morphology and leaf optical properties of two barley varieties. *Environmental and Experimental Botany*, 75, 52-64.
- Komhyr, W. D., Oltmans, S. J. and Grass, R. D. (1988). Atmospheric Ozone at South Pole, Antarctica, in 1986. *Journal of Geophysical Research*, 93, 5167-5184.
- Kostina, E., Wulff, A. and Julkunen-Titto, R. (2001). Growth, structure, stomatal responses and secondary metabolites of birch seedlings (*Betula pendula*) under elevated UV-B radiation in the field. *Trees*, 15, 483-491.
- Kuhlmann, F. and Muller, C. (2010). UV-B impact on aphid performance mediated by plant quality and plant changes induced by aphids. *Plant Biology*, 12, 676-684.
- Lake, J. A., Quick, W. P., Beerling, D. J. and Woodward, F. I. (2001). Plant development: signals from mature to new leaves. *Nature*, 411, 154.

- Lambers, H., Chapin III, F. S. and Pons, T. L. (2008). *Plant Physiological Ecology*. New York: SpringerScience + Business Media.
- Liakoura, V., Stefanou, M., Manetas, Y., Cholevas, C. and Karabourniotis, G. (1997). Trichome density and its UV-B protective potential are affected by shading and leaf position on the canopy. *Environmental and Experimental Botany*, 38, 223-229.
- Liang, J. (2013). Radiation in the atmosphere. In: *Chemical Modeling for Air Resources: Fundamentals, Applications and Corroborative Analysis*, 43–63. Academic Press.
- Lichtenthaler, H. K., Ac, A., Marek, M. V., Kalina, J. and Urban, O. (2007). Differences in pigment composition, photosynthetic rates and chlorophyll fluorescence images of sun and shade leaves of four tree species. *Plant Physiology and Biochemistry*, 45, 577-588.
- Lidon, F. C. and Ramalho, J. C. (2011). Impact of UV-B irradiation on photosynthetic performance and chloroplast membrane components in *Oryza sativa* L. *Journal of Photochemistry and Photobiology B: Biology*, 104, 457-466.
- Lidon, F. J. C., Reboredo, F. H., Leitao, A. E., Silva, M. M. A., Duarte, M. P. and Ramalho, J. C. (2012). Impact of UV-B radiation on photosynthesis – an overview. *Emirates Journal of Food and Agriculture*, 24, 546-556.
- Meinzer, F. and Goldstein, G. (1985). Some Consequences of Leaf Pubescence in the Andean Giant Rosette Plant *Espeletia timotensis*. *Ecology*, 66, 512-520.

- N8 Research Partnership. (2019). *N8 researchers launch work to preserve 'climate smart' tomatoes*. N8 Research Partnership. Available at: <https://www.n8research.org.uk/n8-researchers-launch-work-to-preserve-climate-smart-tomatoes/> [Accessed 12 September 2019].
- Neugart, S. and Schreiner, M. (2018). UVB and UVA as eustressors in horticultural and agricultural crops. *Scientia Horticulturae*, 234, 370-381.
- Ni, Y., Xia, R. and Li, J. (2014). Changes of epicuticular wax induced by enhanced UV-B radiation impact on gas exchange in *Brassica napus*. *Acta Physiologiae Plantarum*, 36, 2481–2490, doi: 10.1007/s11738-014-1621-x.
- Noguès, S. and Baker, N. R. (1995). Evaluation of the role of damage to photosystem II in the inhibition of CO₂ assimilation in pea leaves on exposure to UV-B radiation. *Plant, Cell and Environment*, 18, 781-787.
- Noguès, S., Allen, D. J., Morison, J. I. L. and Baker, N. R. (1998). Ultraviolet-B Radiation Effects on Water Relations, Leaf Development, and Photosynthesis in Droughted Pea Plants. *Plant Physiology*, 117, 173–181.
- Noguès, S., Allen, D. J., Morison, J. I. L. and Baker, N. R. (1999). Characterization of Stomatal Closure Caused by Ultraviolet-B Radiation. *Plant Physiology*, 121, 489–496.
- Novotná, K., Klem, K., Holub, P., Rapantová, B. and Urban, O. (2016). Evaluation of drought and UV radiation impacts on above-ground biomass of mountain grassland by spectral reflectance and thermal imaging techniques. *Beskydy*, 9 (1-2), 21-30.

- Paul, N. D., Jacobson, R. J., Taylor, A., Wargent, J. J. and Moore, J. P. (2005). The Use of Wavelength Selective Plastic Cladding Materials in Horticulture: Understanding of Crop and Fungal Responses Through Assessment of Biological Spectral Weighting Functions. *Photochemistry and Photobiology*, 81, 1052-1060.
- Paul, N. D., Rasanayagam, S., Moody, S. A., Hatcher, P. E., and Ayres, P. G. (1997). The role of interactions between trophic levels in determining the effects of UV-B on terrestrial ecosystems. *Plant Ecology*, 128, 296-308.
- Paul, N. D., Moore, J. P., McPherson, M., Lambourne C., Croft, P., Heaton J. C. and Wargent J. J. (2012). Ecological responses to UV radiation: interactions between the biological effects of UV on plants and on associated organisms. *Physiologia Plantarum*, 145, 565-581.
- Peng, D.-L., Yang, N., Song, B., Chen, J.-G., Li, Z.-M., Yang, Y. and Sun, H. (2015). Woolly and overlapping leaves dampen temperature fluctuations in reproductive organ of an alpine Himalayan forb. *Journal of Plant Ecology*, 8, 159-165.
- Rechner, O. and Poehling, H. M. (2014). UV exposure induces resistance against herbivorous insects in broccoli. *Journal of Plant Diseases and Protection*, 121, 125-132.
- Rechner, O., Neugart, S., Schreiner, M., Wu, S. and Poehling, H. M. (2016). Different Narrow-Band Light Ranges Alter Plant Secondary Metabolism and Plant Defense Response to Aphids. *Journal of Chemical Ecology*, 42, 989-1003.
- Reyes, T. H., Scartazza, A., Castagna, A., Cosio, E. G., Ranieri, A. and Guglielminetti, L. (2018). Physiological effects of short acute UVB treatments in *Chenopodium quinoa* Willd. *Nature Scientific Reports*, 8, 371.

- Ripley, B. S., Pammenter, N. W. and Smith, V. R. (1999). Function of Leaf Hairs Revisited: The Hair Layer on Leaves *Arctotheca populifolia* Reduces Photoinhibition, but Leads to Higher Leaf Temperatures Caused by Lower Transpiration Rates. *Journal of Plant Physiology*, 155, 78-85.
- Robson, T. M. and Aphalo, P. J. (2012). Species-specific effect of UV-B radiation on the temporal pattern of leaf growth. *Physiologia Plantarum*, 144, 146–160.
- Runeckles, V. C. and Krupa, S. V. (1994). The Impact of UV-B Radiation and Ozone on Terrestrial Vegetation. *Environmental Pollution*, 83, 191-213.
- Salt, D. T., Moody, S. A., Whittaker, J. B. and Paul, N. D. (1998). Effects of enhanced UVB on populations of the phloem feeding insect *Strophingia ericae* (Homoptera: Psylloidea) on heather (*Calluna vulgaris*). *Global Change Biology*, 4, 91-96.
- Satar, S., U. Kersting, and N. Uygun. (2008). Effect of temperature on population parameters of *Aphis gossypii* Glover and *Myzus persicae* (Sulzer) (Homoptera: Aphididae) on pepper. *Journal of Plant Diseases and Protection*, 115, 69-74.
- Scherrer, D. and Körner, C. (2010). Infrared thermography of alpine landscapes challenges climatic warming projections. *Global Change Biology*, 16, 2602-2613.
- Schumaker, M. A., Bassman, J. H., Robberecht, R. and Rademaker, G. K. (1997). Growth, leaf anatomy, and physiology of *Populus* clones in response to solar ultraviolet-B radiation. *Tree Physiology*, 17, 617-626.
- Schweiger, R., Heise, A.-M., Persicke, M. and Müller, C. (2014). Interactions between the jasmonic and salicylic acid pathway modulate the plant metabolome and affect herbivores of different feeding types. *Plant, Cell and Environment*, 37, 1574-1585.

- Shimazaki, K.-i., Doi, M., Assmann, S. M. and Kinoshita, T. (2007). Light regulation of stomatal movement. *Annual Review of Plant Biology*, 58, 219-247.
- Suchar, V. A. and Robberecht, R. (2015). Integration and scaling of UV-B radiation effects on plants: from DNA to leaf. *Ecology and Evolution*, 5, 2544-2555.
- Taiz, L. and Zeiger, E. (2010). *Plant Physiology*. Sunderland: Sinauer Associates.
- Teramura, A. H., Sullivan, J. H. and Ziska, L. H. (1990). Interaction of Elevated Ultraviolet-B Radiation and CO₂ on Productivity and Photosynthetic Characteristics in Wheat, Rice, and Soybean. *Plant Physiology*, 94, 470-475.
- Tossi, V., Lamattina, L., Jenkins, G. I. and Casia, R. O. (2014). Ultraviolet-B-Induced Stomatal Closure in Arabidopsis Is Regulated by the UV RESISTANCE LOCUS8 Photoreceptor in a Nitric Oxide-Dependent Mechanism. *Plant Physiology*, 164, 2220–2230.
- Tyystjarvi, E. (2008). Photoinhibition of Photosystem II and photodamage of the oxygen evolving manganese cluster. *Coordination Chemistry Reviews*, 252, 361-376.
- Wargent, J. J., Gegas, V. C., Jenkins, G. I., Doonan, J. H. and Paul, N. D. (2009a). UVR8 in Arabidopsis thaliana regulates multiple aspects of cellular differentiation during leaf development in response to ultraviolet B radiation. *New Phytologist* 183, 315–326, doi: 10.1111/j.1469-8137.2009.02855.x.
- Wargent, J. J., Moore, J. P., Ennos, A. R. and Paul, N. D. (2009b). Ultraviolet Radiation as a Limiting Factor in Leaf Expansion and Development. *Photochemistry and Photobiology*, 85, 279–286.

- Wargent, J. J., Moore, J. P., Elfadly, E. M. and Paul, N. D. (2011). Increased exposure to UV-B radiation during early development leads to enhanced photoprotection and improved long-term performance in *Lactuca sativa*. *Photochemistry and Photobiology*, 85, 279–286.
- Wargent, J. J. (2016). UV LEDs in horticulture: from biology to application. *Acta Horticulturae*, 1134, 25-32.
- Weber, J., Halsall, C. J., Wargent, J. J. and Paul, N. D. (2009a). A comparative study on the aqueous photodegradation of two organophosphorus pesticides under simulated and natural sunlight. *Journal of Environmental Monitoring*, 11, 654-659.
- Weber, J., Halsall, C. J., Wargent, J. J. and Paul, N. D. (2009b). The aqueous photodegradation of fenitrothion under various agricultural plastics: Implications for pesticide longevity in agricultural ‘micro-environments’. *Chemosphere*, 76, 147-150.
- Woodward, F. I. (1987). Stomatal numbers are sensitive to increases in CO₂ from pre-industrial levels. *Nature*, 327, 617-618.
- Williams, T. B., Paul, N. D., Dodd, I. C., Moore, J. P. and Sobeih, W. (2020). Ultraviolet (UV) transparent plastic claddings warm crops and improve water use efficiency. *Acta Horticulturae*, 1271, 1-8, doi: 10.17660/ActaHortic.2020.1271.1.
- Wuenschel, J. E. (1970). The Effect of Leaf Hairs of *Verbascum thapsus* on Leaf Energy Exchange. *New Phytologist*, 69, 65-73.

- Yan, A., Pan, J., An, L., Gan, Y. and Feng, H. (2012). The responses of trichome mutants to enhanced ultraviolet-B radiation in *Arabidopsis thaliana*. *Journal of Photochemistry and Photobiology B: Biology*, 113, 29-35.
- United Nations, Department of Economic and Social Affairs, Population Division (2017). *World Population Prospects: The 2017 Revision, Key Findings and Advance Tables*. Working Paper No. ESA/P/WP/248.
- Yang, Y., Yao, Y. and He, H. (2008). Influence of ambient and enhanced ultraviolet-B radiation on the plant growth and physiological properties in two contrasting populations of *Hippophae rhamnoides*. *Journal of Plant Research*, 121, 377–385.
- Zhao, H., Zhao, Z., An, L., Chen, T., Wang, X. and Feng, H. (2009). The effects of enhanced ultraviolet-B radiation and soil drought on water use efficiency of spring wheat. *Journal of Photochemistry and Photobiology B: Biology*, 95, 54-58.
- Zu, Y.-g., Hai, H.-H., Yu, J.-H., Li, D.-W., Wei, X.-X., Gao, Y.-X. and Tong, L. (2010). Responses in the morphology, physiology and biochemistry of *Taxus chinensis* var. *mairei* grown under supplementary UV-B radiation. *Journal of Photochemistry and Photobiology B: Biology*, 98, 152–158.

10 Appendices

Appendix 1: Leaf Temperature and Gas Exchange Responses to Ultraviolet radiation in a Controlled Environment (Individual Experiments).....	205
Appendix 2: Antalya (Turkey) Part A: Leaf Temperature and Gas Exchange Responses to Ultraviolet Radiation in Polytunnels (Summary of the 2018 Experiment).....	208
Appendix 3: Published Material (<i>Acta Horticulturae</i> , 1271, 1-8, published March 2020).....	211

Appendix 1: Leaf Temperature and Gas Exchange Responses to Ultraviolet radiation in a Controlled Environment (Summary of the Individual Experiments)

Experiment 1

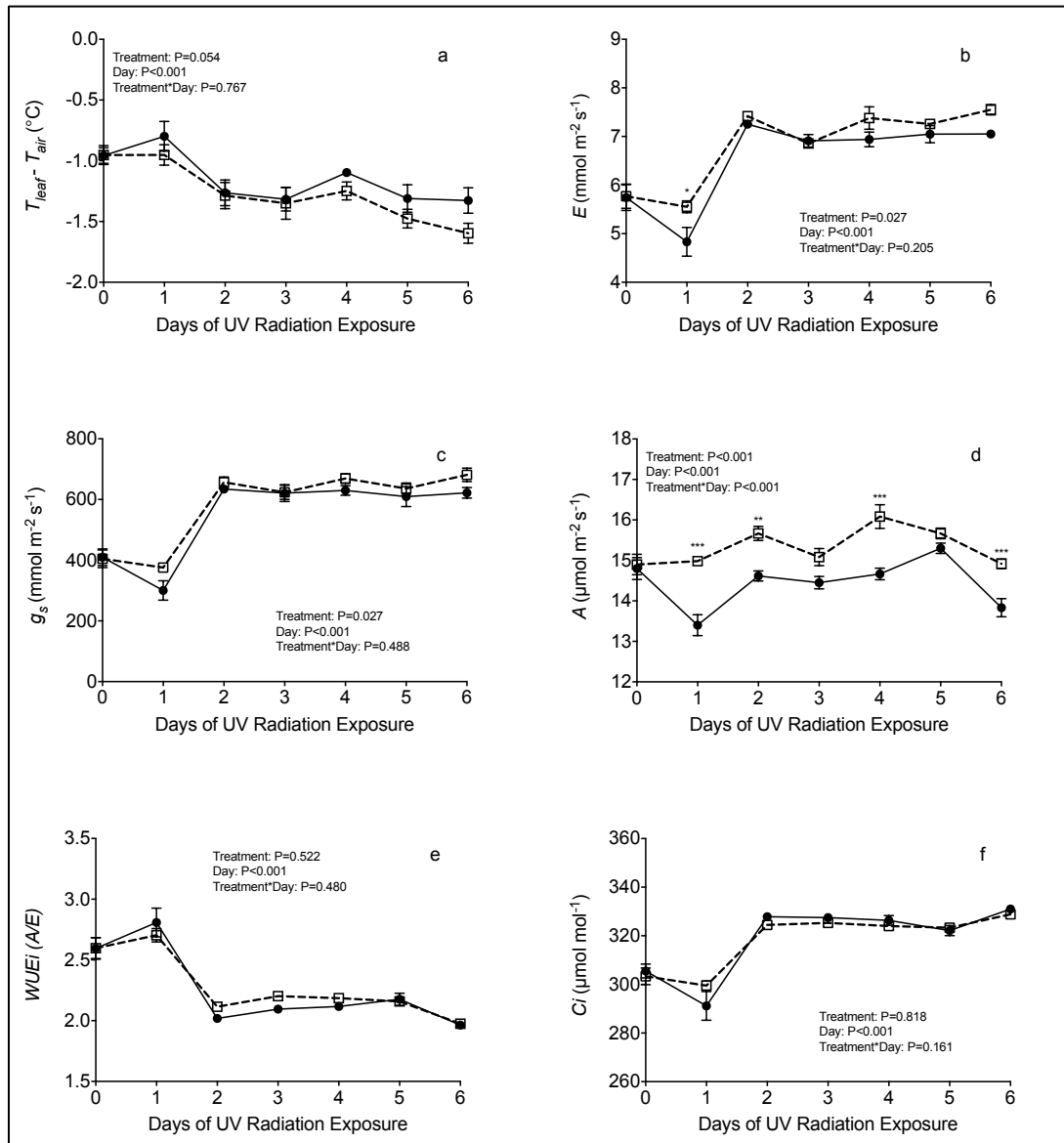


Figure 10.1: The response to UV+ (black circles and solid line) and UV- (open squares and dashed line) radiation treatments of (a) leaf temperature ($T_{leaf} - T_{air}$), (b) transpiration rate (E), (c) stomatal conductance (g_s), (d) assimilation rate (A), (e) instantaneous water use efficiency (WUE_i), and (f) intracellular CO_2 (C_i) for experiment 1. The results of repeated measures ANOVA analysis are summarised. The asterisks represent individual days where there was a significant difference between treatments (*: $P < 0.05$; **: $P < 0.01$; ***: $P < 0.001$) corrected for multiple t-tests. Error bars represent ± 1 SE but if not visible they were smaller than the symbol. Each symbol is the mean of 6 leaves ($n=6$).

Experiment 2

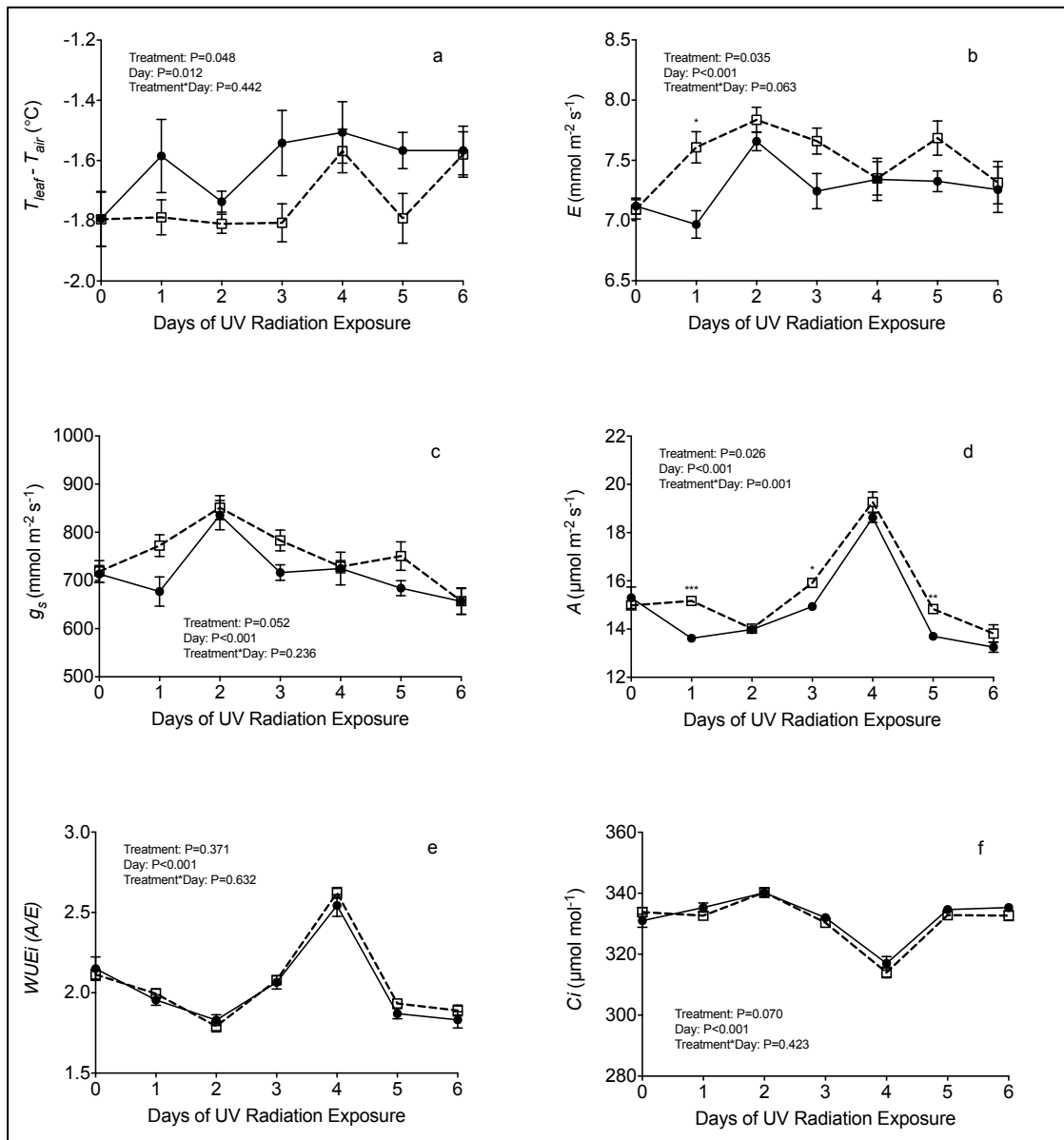


Figure 10.2: The response to UV+ (black circles and solid line) and UV- (open squares and dashed line) radiation treatments of (a) leaf temperature ($T_{leaf} - T_{air}$), (b) transpiration rate (E), (c) stomatal conductance (g_s), (d) assimilation rate (A), (e) instantaneous water use efficiency (WUE_i), and (f) intracellular CO_2 (C_i) for experiment 2. The results of repeated measures ANOVA analysis are summarised. The asterisks represent individual days where there was a significant difference between treatments (*: P<0.05; **: P<0.01; ***: P<0.001) corrected for multiple t-tests. Error bars represent ± 1 SE but if not visible they were smaller than the symbol. Each symbol is the mean of 6 leaves (n=6).

Experiment 3

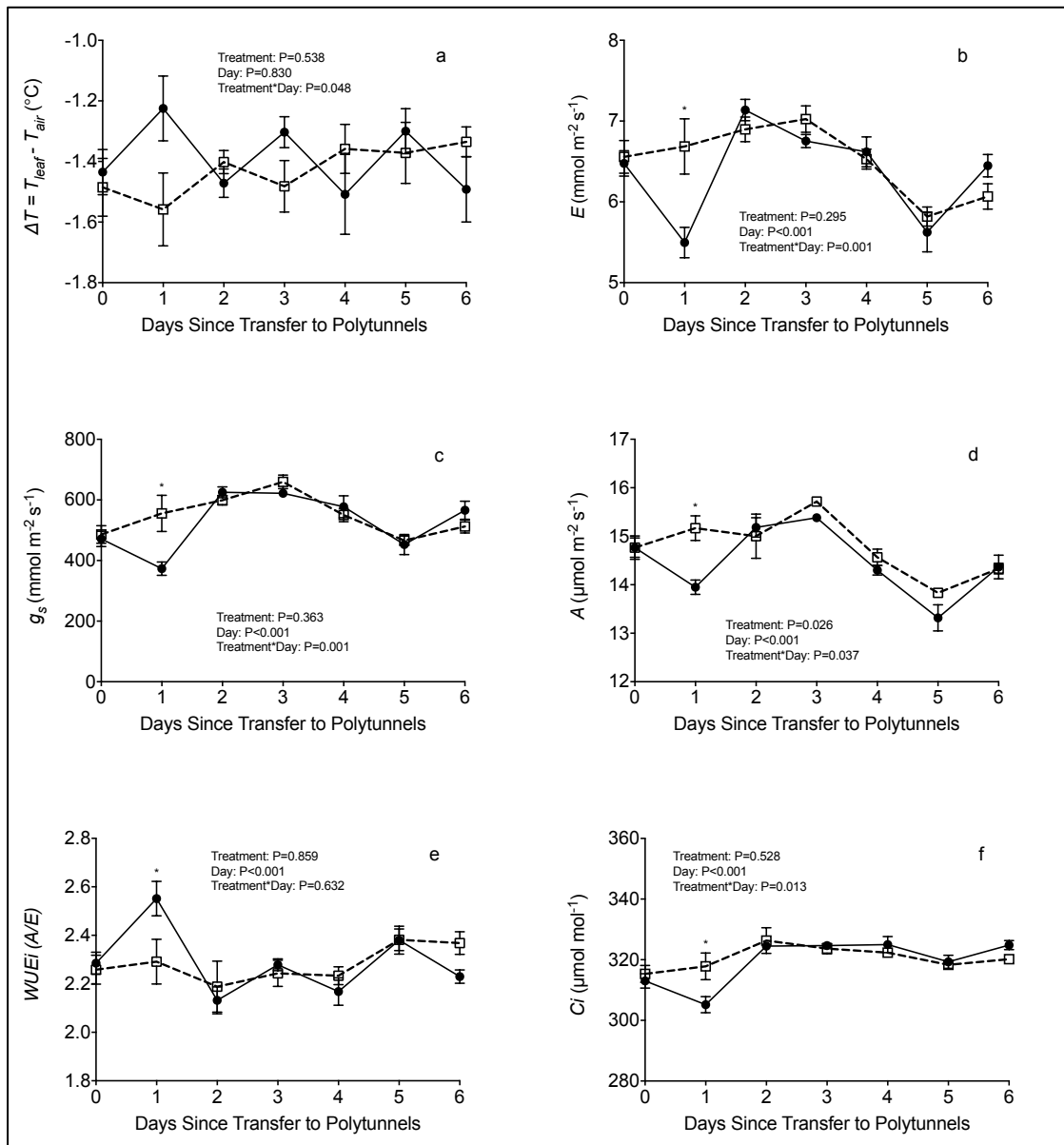


Figure 10.3: The response to UV+ (black circles and solid line) and UV- (open squares and dashed line) radiation treatments of (a) leaf temperature ($T_{leaf}-T_{air}$), (b) transpiration rate (E), (c) stomatal conductance (g_s), (d) assimilation rate (A), (e) instantaneous water use efficiency ($WUEi$), and (f) intracellular CO_2 (C_i) for experiment 3. The results of repeated measures ANOVA analysis are summarised. The asterisks represent individual days where there was a significant difference between treatments (*: P<0.05; **: P<0.01; ***: P<0.001) corrected for multiple t-tests. Error bars represent ± 1 SE but if not visible they were smaller than the symbol. Each symbol is the mean of 6 leaves (n=6).

Appendix 2: Antalya (Turkey) Part A: Leaf Temperature and Gas Exchange Responses to Ultraviolet Radiation in Poly tunnels (Summary of the 2018 Experiment)

Antalya 2018 Experiment

Prior to the experimental work in Antalya in June/July 2019, the same experiment was conducted in October 2018. The experiment location and poly tunnels were identical to those described for the 2019 experiment (Section 6.2) but lasted 6 days rather than 5 days. Statistical analyses were also replicated. Data collected with the LI-6400XT identified no significant ($P>0.05$; Fig. 6.7) treatment effects between UV+ and UV- poly tunnels for all the parameters. For each parameter there was no significant ($P>0.05$) difference between poly tunnels and no significant ($P>0.05$) interaction between poly tunnels and UV treatment. There was significant ($P<0.001$; Fig. 6.7) difference between days for each parameter, except stomatal conductance that was not significant ($P=0.872$). There was no significant ($P>0.05$; Fig. 6.7) interaction between treatment and day for all parameters.

Leaf temperature was additionally measured with an infrared temperature meter (MI-220, Apogee Instruments, Logan, USA) for comparison with the LI-6400XT measurements. The infrared temperature meter recorded a marginally greater leaf temperature especially towards the end of the week where leaf temperature was significantly ($P=0.004$; Fig. 6.8) greater in UV+ poly tunnels. Although there was a significant variation between days ($P<0.001$; Fig. 6.8) that interacted with the treatment effect ($P=0.009$; Fig. 6.8), the treatment differences diverged as the week progressed. Maximum unweighted UV irradiance was 14.5 W m^{-2} in Antalya in October 2018, which was 77% of the corresponding UV irradiance in Antalya in June/

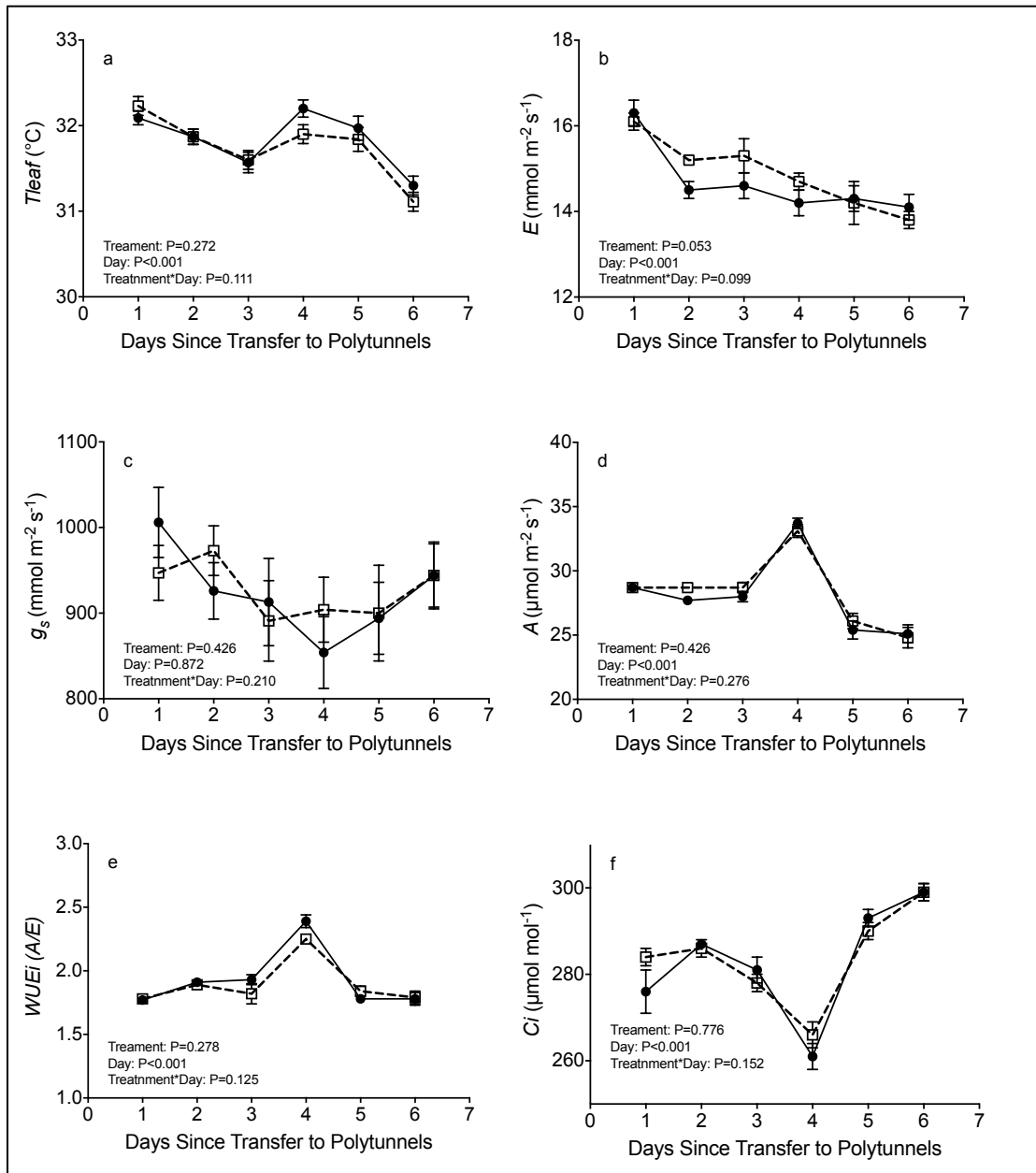


Figure 10.4: Antalya 2018: The response to UV+ (black circles and solid line) and UV- (open squares and dashed line) treatments of (a) leaf temperature (T_{leaf}), (b) transpiration rate (E), (c) stomatal conductance (g_s), (d) assimilation rate (A), (e) instantaneous water use efficiency (WUE_i), and (f) intracellular CO₂ (C_i). The asterisks represent individual days where there was a significant difference between treatments (*: $P < 0.05$; **: $P < 0.01$; ***: $P < 0.001$) corrected for multiple t-tests. Summary of repeated measures ANOVA analysis of the whole treatment period are highlighted. Error bars represent ± 1 SE ($n=27$) but if not visible they were smaller than the symbol.

July 2019 (17.9 W m^{-2}), and the UV dose was $349 \text{ kJ m}^{-2} \text{ d}^{-1}$ in 2018 compared to $551 \text{ kJ m}^{-2} \text{ d}^{-1}$ in 2019 (63% of that present in 2019), which can explain the lack of UV treatment effect in 2018 compared to the 2019 experiments. Thus, there was very little effect of UV treatment on any of the parameters, except leaf temperature measured

with the infrared temperature meter, which may indicate the effect of the differences in solar radiation transmitted into the differently clad polytunnels, which was identified in 2019.

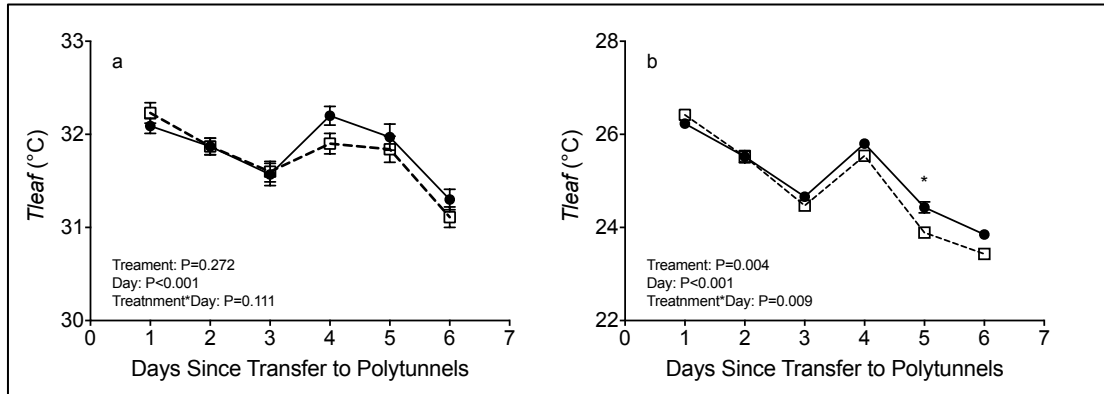


Figure 10.5: Antalya 2018: A comparison of the response to UV+ (black circles and solid line) and UV- (open squares and dashed line) treatments of (a) leaf temperature (T_{leaf}) measured with the LI-6400XT, and (b) leaf temperature (T_{leaf}) measured with an infrared temperature meter (MI-220, Apogee Instruments, Logan, USA). The asterisks represent individual days where there was a significant difference between treatments (*: $P<0.05$; **: $P<0.01$; ***: $P<0.001$) corrected for multiple t-tests. Summary of repeated measures ANOVA analysis of the whole treatment period are highlighted. Error bars represent ± 1 SE ($n=27$) but if not visible they were smaller than the symbol.

Appendix 3: Published Material (*Acta Horticulturae*, 1271, 1-8, published March 2020)

Ultraviolet (UV) transparent plastic claddings warm crops and improve water use efficiency

T.B. Williams¹, N.D. Paul¹, I. C. Dodd¹, J.P. Moore² and W, Sobeih²

¹ Lancaster Environment Centre, Lancaster University, Lancaster, LA1 4YQ; ² Arid Agritec, Enterprise & Business Partnerships, Lancaster University, Lancaster, LA1 4YQ

Abstract

Advances in the manufacturing of plastic cladding for protected crop cultivation have resulted in wavelength selective plastics capable of manipulating the transmission of solar radiation to include ultraviolet (UV: 280-400 nm). Commercial growers already utilising these plastics report early maturity associated with warmer crops. We hypothesised that UV-B radiation causes partial stomatal closure that reduces stomatal conductance and transpiration rate, thereby increasing leaf temperature (relative to air temperature). We tested this hypothesis by investigating leaf gas exchange and temperature responses of individual tomato leaves to UV-B and UV-A radiation provided by UV lamps in a controlled environment. Transient (90 minutes) exposure to UV-B radiation decreased stomatal conductance but had minimal impact on photosynthesis, thus increasing leaf temperature and instantaneous water use efficiency. Should this

enhanced water use efficiency also occur at a whole plant / canopy scale, these responses may benefit growers of protected crops in arid climates where plastic clad polytunnels are often utilised.

Keywords: protected crops, polytunnel, tomato, leaf temperature, instantaneous water use efficiency (*WUE_i*)

INTRODUCTION

Technological advances in the manufacturing of plastic cladding for protected crop cultivation have resulted in wavelength selective plastics capable of manipulating the transmission of solar radiation to include ultraviolet (UV: 280-400 nm). UV-transparent (UV-T) cladding that transmits the full range of solar UV (Paul et al., 2005; Paul et al., 2012) is already in use by commercial growers operating predominantly around the Mediterranean. Although the biology of crop responses to UV radiation has been well studied (e.g. Paul et al., 2005; Paul et al., 2012), understanding of the effects of UV-T plastics on the performance of commercial crops is still emerging. For example, we received repeated anecdotal reports from commercial growers that crops, including tomato, cultivated under UV-T cladding mature earlier than crops grown under “conventional” plastics that are opaque to all or part of solar UV radiation. Growers have associated this earlier maturity with increased leaf temperature under UV-T films. We are unaware of any published reports that exposure to solar UV radiation increases leaf temperature, but data collected on a commercial tomato farm in Antalya, Turkey confirmed that leaf temperature in a tomato crop grown under UV-T cladding was 1.9°C higher ($p < 0.05$) than under standard diffuse plastic claddings (Table 1).

Table 1. Summary of leaf temperature data provided by commercial growers from a tomato farm in Antalya, Turkey. Data compares leaf temperature under diffuse UV-transparent (UV-T) plastic cladding with diffuse standard plastic cladding which is opaque to part of solar UV radiation ($t=2.14$, $n=40$, $p<0.05$).

Cladding Type	Leaf Temperature (°C)	Standard Error (°C)
UV-T (diffuse)	33.5	0.64
Standard (diffuse)	31.6	0.63

While increased leaf temperature in response to solar UV radiation appears not to have been reported before, there is a substantial literature confirming that solar UV, especially UV-B radiation (280-315 nm) induces partial stomatal closure and so decreases stomatal conductance. This includes studies where UV radiation was provided using lamps (e.g. Nogues et al., 1998, 1999, He et al., 2005; Tossi et al., 2014) and where solar UV-B was attenuated using wavelength-selective filters (e.g. Kataria et al. 2013). These studies with differing methodological approaches demonstrate that UV-B decreases stomatal conductance independent of the experimental environment. As transpiration through stomata is one of the main leaf heat dissipation mechanisms, any closure would limit transpiration resulting in warmer leaves (Taiz and Zeiger, 2006).

In this study, we hypothesised that UV-B radiation would cause partial stomatal closure reducing transpiration rate, and thereby increasing leaf temperature (relative to air temperature). We tested this hypothesis by investigating leaf gas exchange and temperature responses of individual tomato leaves to UV-B and UV-A radiation provided by UV lamps, in a controlled environment over 90 minutes. In addition, any effect on instantaneous water use efficiency, the ratio of carbon assimilation to transpiration, was analysed.

MATERIALS AND METHODS

Plant material and cultivation

Tomato (*Solanum lycopersicum* cv. ‘Money Maker’) plants were propagated in the absence of UV-B radiation in a glasshouse at the Lancaster Environment Centre. Seeds were sown in tray inserts containing a peat-based substrate (Levington Advance M3, ICL Everris Ltd, Ipswich) and were ~2 weeks old (depending on the season) when they were transplanted individually into 2 L pots containing the same substrate. After ~4 weeks of growth from seed, the most uniform individually potted tomato plants were selected and transferred to the controlled environment to acclimate to the different conditions to those present in the glasshouse, for ~1 week prior to use in experimentation. At ~5 weeks old, the eight most uniform plants were selected for experimentation. A leaflet from the most recent fully developed leaf pair on the 5th internode was used for the experiment.

Controlled environment (CE) conditions and radiation sources

The experiments were conducted in a climate cabinet (Microclima 1750, Snijder Scientific, Tilburg, Holland). This provided relatively stable temperature and humidity control, vital for measurements of stomatal behaviour and leaf temperature, and constant PAR for each experiment repetition. A second climate cabinet was used for acclimation of plants transferred from the glasshouse. Each cabinet provided ~300 $\mu\text{mol m}^{-2} \text{s}^{-1}$ PAR without UV radiation (excluded by Lightworks sun master plastic film (Arid Agritec, Lancaster, UK) that filtered out UV radiation <400 nm) for a 16-h photoperiod. The temperature was 25°C, relative humidity was 60% and CO₂ was 400 ppm. Both Snijder climate cabinets had identical environmental settings to avoid any “transfer shock” when plants were moved between cabinets.

UV radiation was provided by a different source to PAR. Fluorescent tubes (FTs) were used to provide UV-A (Q-Lab UVA-340) or UV-B (Q-Lab UVB-313 EL, both Q-Panel Lab Products, Cleveland, USA) radiation in separate experiments. UV radiation was quantified with a spectroradiometer (model SR9910-V7, Macam Photometrics, Livingston, UK) that provided the spectral irradiance (280-800 nm) of each source (Tab. 2). UV treatments were expressed as (i) total unweighted irradiance, (ii) irradiances weighted using the plant growth inhibition action spectrum (PGIAS; Flint and Caldwell, 2003) and the (iii) irradiances weighted using the generalised plant action spectrum (GPAS; Caldwell, 1971). We used PGIAS in our experimental design because its inclusion of UV-A suggests it is the more appropriate weighting function. However, since GPAS has been used in the majority of UV studies that have utilised a biological spectral weighting function (BSWF), we have quoted this to allow direct comparison with previous studies (Tab. 2). These action spectra, or BSWFs, are vital for comparison of scientific studies because UV radiation sources, whether artificial or solar, emit radiation of variable quantities at different wavelengths. To understand the relative effect of these variations the irradiance at each wavelength is weighted based on a specific biological effect (e.g. growth inhibition in PGIAS). These action spectra allow comparisons between solar UV and UV from lamps, which have very different spectral distributions. UV-A irradiances (unweighted) were matched with the unweighted UV-B irradiances (applicable to the selected weighted irradiances) to ensure an equal total radiation loading independent of the UV wavelengths applied. UV irradiance was varied by changing the distance between the experimental leaf and the UV radiation source, ensuring that leaves remained equidistant from the PAR source, by raising or lowering the lamp on a clamp.

Table 2. Unweighted and weighted irradiances at 240-800 nm. Unweighted irradiances include the Snijder climate cabinet photosynthetically active radiation source in addition to the associated UV lamp irradiance. The weighted irradiances refer to the UV irradiance alone, weighted by the generalised plant action spectrum (GPAS: Caldwell, 1971) and the plant growth inhibition action spectrum (PGIAS: Flint and Caldwell, 2003).

Treatment	Unweighted Irradiance 280-800 nm (W m⁻²)	GPAS Weighted Irradiance 280-800 nm (W m⁻²)	PGIAS Weighted Irradiance 280-800 nm (W m⁻²)
Control	45.04	0.000	0.000
UV-B FT 0.100	44.13	0.100	0.097
UV-B FT 0.260	43.25	0.260	0.251
UV-A FT 0.260e	42.87	0.029	0.111
UV-B FT 1.08	50.75	1.080	1.120
UV-B FT 2.55	56.68	2.550	2.640

Leaf gas exchange and temperature measurements

Leaf gas exchange and temperature measurements were made using a LI-COR 6400 (LI-COR Inc., Lincoln, NE, USA). The LI-COR 6400 ‘clear window’ (‘Teflon’) cuvette attachment allowed transmission of PAR and UV radiation to the experimental leaf enclosed inside. Once a leaf was enclosed inside the cuvette, the internal environment was allowed to stabilise for 15 minutes before the application of UV for 90 minutes. The LI-COR 6400 also provided an additional level of environmental control, which dampened the cyclic fluctuations in CE temperature that are inherent to climate cabinet temperature control.

Effects of leaf excision on leaf temperature

In separate experiments, gas exchange and leaf temperature measurements were also performed on leaves that were excised from the plant after 15 minutes of stabilisation in the LI-COR 6400 cuvette. Excision causes rapid and complete stomatal closure and

so provides a measure of the maximum possible effect of stomatal closure on leaf temperature under our experimental conditions.

Data processing

Air temperature fluctuations profoundly influence leaf temperature, especially if stomata are not transpiring fully due to partial closure, reducing the plant's ability to regulate leaf temperature. To account for this, the difference between leaf and air temperature ($T_{\text{leaf}} - T_{\text{air}}$) is determined for each data point. The change in this difference was then measured over the 90 minute treatment period. The effect of UV radiation on this difference between leaf and air temperature over this time period is referred to here as $\Delta T (T_{\text{leaf}} - T_{\text{air}})$ (Fig. 1), and was calculated as follows:

$$\Delta T (T_{\text{leaf}} - T_{\text{air}}) = (T_{\text{leaf}} - T_{\text{air}})_{\text{AFTER}} - (T_{\text{leaf}} - T_{\text{air}})_{\text{BEFORE}}$$

Statistical analysis

For each treatment 8 replicates were statistically analysed using a one-way repeated measures analysis of covariance (ANCOVA) with the pre-UV treatment values as the covariate and Bonferroni post hoc comparisons using SPSS version 24 (SPSS Inc. Chicago, USA). Regression analysis determined relationships between leaf temperature, stomatal conductance and PGIAS weighted UV irradiance using GraphPad Prism version 7.0d for Mac OS X (GraphPad Software, La Jolla California USA, www.graphpad.com).

RESULTS AND DISCUSSION

The time course of stomatal responses

Example time courses of the three treatments (control, leaf excision, UV-B irradiation) demonstrate typical leaf temperature responses and how ΔT ($T_{leaf} - T_{air}$) was derived from measurements of T_{leaf} and T_{air} (Figure 1). For each experiment, a leaf was enclosed in the LI-COR 6400 cuvette then data was logged. Conditions inside the cuvette were allowed to stabilise for 15 minutes, then the treatment was maintained (Fig.1a), the leaf was excised (Fig.1b) or UV-B was applied (Fig.1c). In each case T_{air} remained relatively stable ($\pm 0.2^\circ\text{C}$) throughout. Control leaves also exhibited relatively stable T_{leaf} resulting in a stable ΔT ($T_{leaf} - T_{air}$). Excised leaves exhibited a sharp increase in T_{leaf} and ΔT ($T_{leaf} - T_{air}$) a few minutes after excision, which gradually plateaued. UV-B treated leaves exhibited an immediate but more gradual increase in T_{leaf} and ΔT ($T_{leaf} - T_{air}$).

UV radiation reduces stomatal conductance and increases leaf temperature

Increased UV-B irradiances (PGIAS weighted) significantly reduced stomatal conductance (Fig. 2a), and significantly increased ΔT ($T_{leaf} - T_{air}$) (Fig. 2b). UV-B radiation increased ΔT ($T_{leaf} - T_{air}$) by up to 0.88°C (Fig.2b), compared to a maximal temperature increase (i.e. that caused by leaf excision) of 1.14°C (Fig. 1b). Further analysis suggests that two elements contributed to leaf warming: direct radiative heating from the UV lamp and partial stomatal closure. For a given reduction in transpiration rate over the course of measurement, the concurrent increase in ΔT ($T_{leaf} - T_{air}$) was up to 0.48°C greater in response to UV treatments than in controls and in response to leaf excision. We attribute this increase to direct radiative heating from the UV source, which is clearly not present in the ‘control’ and ‘leaf excision’

treatments that provided no additional heat input. When this temperature increase caused by radiative heating from the UV lamp is deducted from the overall leaf warming results the leaf warming resulting from partial stomatal closure in response to UV radiation was up to 0.4°C . This was in response to the maximum PGIAS weighted UV irradiance used here (2.64 W m^{-2}) which is approximately double the global maximum PGIAS weighted irradiance occurring in the field.

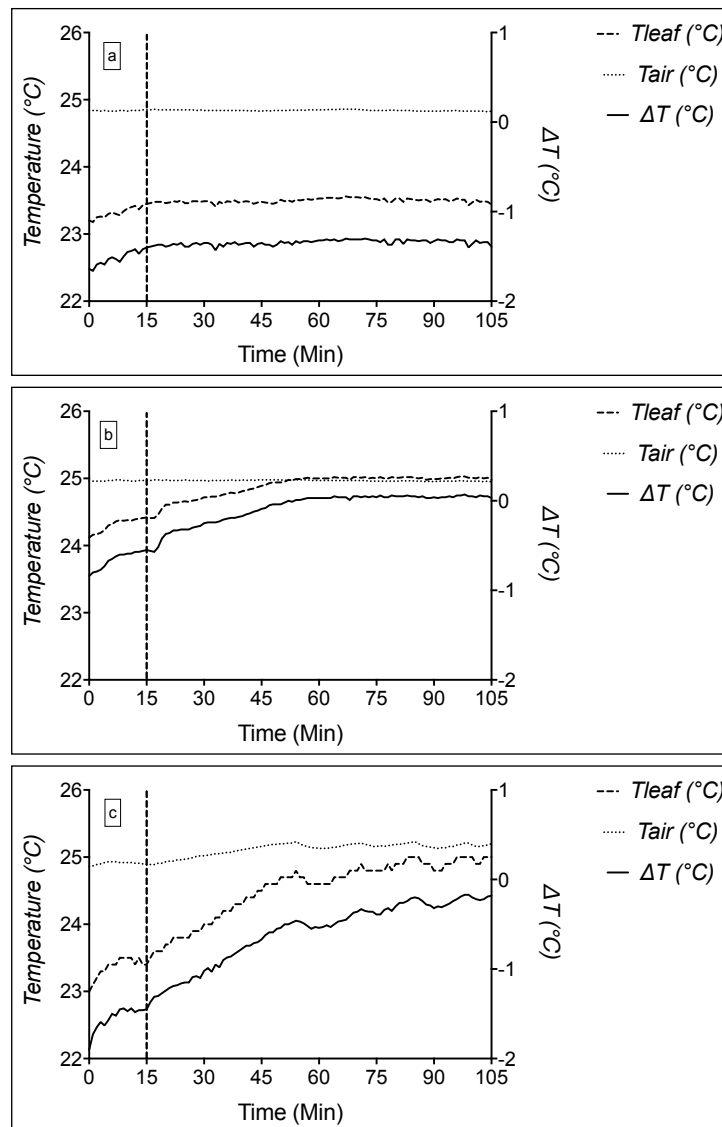


Figure 1. Example time courses of T_{leaf} , T_{air} and the resulting ΔT ($T_{leaf} - T_{air}$) for (a) Control, (b) leaf excision and (c) UV-B treatments. At zero minutes the leaf was enclosed in the LI-COR 6400 cuvette and data logging started. The conditions inside the cuvette were allowed to stabilise for 15 minutes without further treatment. After 15 minutes (vertical dashed line), the treatment was maintained (a), the leaf was excised (b) or UV-B was applied (c) for another 90 minutes. The UV treatments were weighted by the plant growth inhibition action spectrum (PGIAS: Flint and Caldwell, 2003).

In the specific radiative loading environment of the Snijder climate cabinet, leaf excision experiments demonstrated that the maximum degree of relative leaf warming ($\Delta T (T_{leaf} - T_{air})$) that could occur was 1.14°C. Thus the maximum relative leaf warming (0.4°C) attributable to UV-B radiation was 35% of the maximum possible in that environment. However, these controlled environment conditions are substantially different from the field, notably in terms of a much lower total radiative loading than is present in sunlight. As a result, partial stomatal closure caused by UV-B exposure under UV-T cladding in polytunnels would be expected to have a greater effect on leaf temperature than we recorded in our controlled environments, consistent with reports from commercial growers of leaf temperature increases of up to 2°C (Tab. 1).

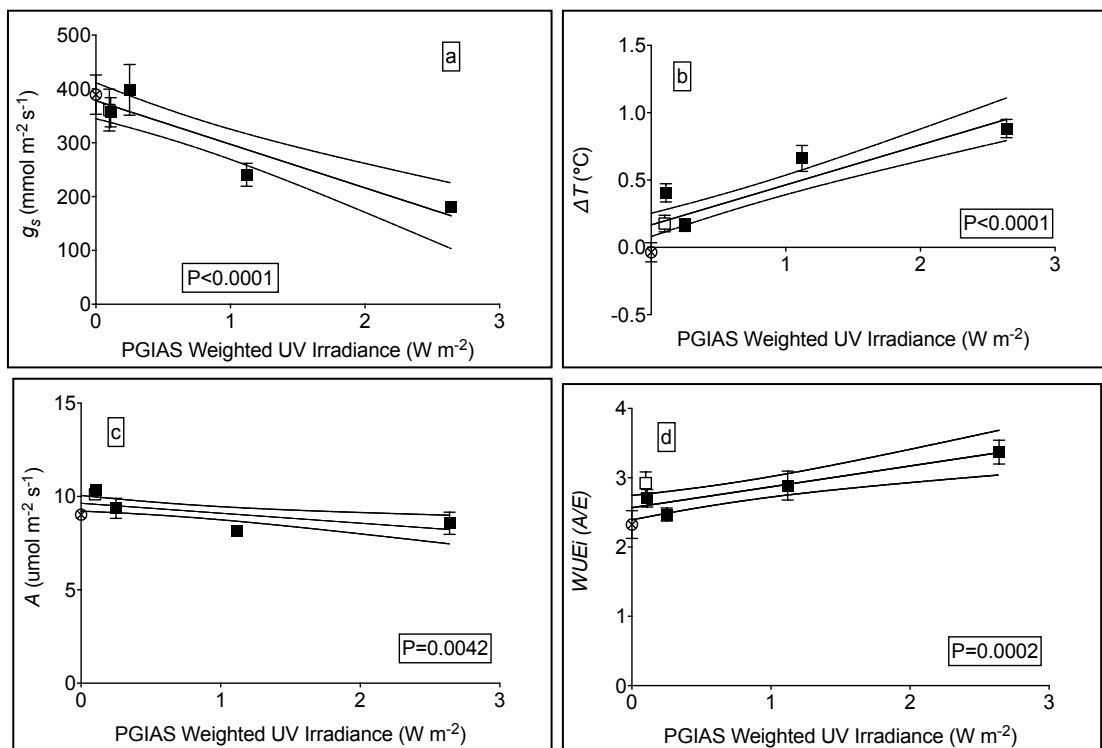


Figure 2. The dose response of (a) stomatal conductance (g_s), (b) relative leaf temperature ($\Delta T (T_{leaf} - T_{air})$), (c) CO₂ assimilation rate (A) and (d) instantaneous water use efficiency (WUE_i : the ratio of assimilation rate (A) to transpiration rate (E) to different UV treatments over 90 minutes (solid and open symbols represent UV-B and UV-A respectively, hatched circle was control). The UV treatments were weighted by the plant growth inhibition action spectrum (PGIAS: Flint & Caldwell, 2003). Regression analysis (P Values indicated) confirmed a linear model fitted best for each parameter. Dotted lines represent the 95% confidence interval of the linear regression. Error bars represent ± 1 SE (n=8).

UV radiation enhances water use efficiency

Instantaneous water use efficiency (WUE_i) was significantly increased as a result of the reduction in stomatal conductance in the absence of any significant changes in photosynthesis (Fig. 2c, d). Whether this increase in WUE_i is sustained over a longer period of UV exposure (than 90 minutes) requires additional experiments. However, the consensus in the literature is that variation in UV radiation within the ambient range rarely causes significant inhibition of photosynthesis (Aphalo et al., 2015; Kataria et al., 2014; Singh et al., 2014).

CONCLUSIONS

UV radiation significantly decreased stomatal conductance thereby increasing ΔT ($T_{leaf} - T_{air}$). Since our treatments were very short, (90 minutes) the measured responses cannot have been due to longer-term responses to UV radiation, such as changes in stomatal distribution or cuticle properties (e.g. Nogues et al., 1998, 1999; Gonzalez et al., 1996) that might affect transpiration, and hence leaf temperature, under commercial conditions. However, our data do corroborate the reports from commercial growers of higher leaf temperature and warmer crops when cultivated under UV-T plastic claddings in protected cultivation. While those reports confirm that this warming is commercially beneficial for some crops at some times of year, we recognise that under other conditions warming might lead to additional heat stress. Further investigation is required to assess the agronomic value of leaf warming under UV-T cladding, alongside the wider benefits of cultivation under such films (Paul et al., 2005; Paul et al., 2012). To our knowledge, previous reports have not included increased instantaneous water use efficiency as an agronomic benefit of exposure to

UV-B radiation. However, this response may assist growers of protected crops in arid climates to minimise their water use.

ACKNOWLEDGEMENTS

The authors want to thank the Biotechnology and Biological Sciences Research Council (BBSRC) and Arid Agritech for their funding of the research for this paper.

Literature cited

Aphalo, P. J., Jansen, M. A. K., Mcleod, A. R., and Urban, O. (2015). Ultraviolet radiation research: from the field to the laboratory and back. *Plant, Cell and Environment*, 38, 853-855 doi: 10.1111/pce.12537.

Caldwell, M. M. (1971). Solar UV irradiation and the growth and development of higher plants. In: *Photophysiology*. Ed. by A. C. Giese. Vol. 6. (New York: Academic Press), p.131–177.

Flint, S. D., and Caldwell, M.M. (2003). A biological spectral weighting function for ozone depletion research with higher plants. *Physiologia Plantarum*. 117, 137–144.

Gonzalez, R., Paul, N. D., Percy, K., Ambrose, M., McLaughlin, C. K., Barnes, J. D., Areses, M., and Wellburn, A.R. (1996). Responses to ultraviolet-B radiation (280-315 nm) of pea (*Pisum sativum*) lines differing in leaf surface wax. *Physiologia Plantarum*. 98, 852-860.

He, J.-M., Xu, H., She, X.-P. Song, X.-G. and Zhao, W.-M. (2005). The role and Interrelationship of Hydrogen Peroxide and Nitric Oxide in the UV-B-Induced Stomatal Closure in Arabidopsis Leaves. *Functional Plant Biology*, 32, 237-247.

Jansen, M. A. K and Noort, R. E. (2000). Ultraviolet-B radiation induces complex alterations in stomatal behaviour. *Physiologia Plantarum*, *110*, 189–194.

Kataria, S., Guruprasad, K. N., Ahuja, S. and Singh, B. (2013). Enhancement of growth, photosynthetic performance and yield by exclusion of ambient UV components in C3 and C4 plants. *Journal of Photochemistry and Photobiology B: Biology*, *127*, 140-152 doi: 10.1016/j.jphotobiol.2013.08.013.

Kataria, S., Anjana, J. and Guruprasad, K. N. (2014). Impact of increasing Ultraviolet-B (UV-B) radiation on photosynthetic processes. *Journal of Photochemistry and Photobiology B: Biology*, *137*, 55-66 doi: 10.1016/j.jphotobiol.2014.02.004.

Madronich, S. (1993). UV radiation in the natural and perturbed atmosphere, in *Environmental Effects of UV (Ultraviolet) Radiation*. M. Tevini, ed., (Lewis Publisher, Boca Raton), p.17-69.

Nogues, S., Allen, D. J., Morison, J. I. L. and Baker, N. R. (1998). Ultraviolet-B Radiation Effects on Water Relations, Leaf Development, and Photosynthesis in Droughted Pea Plants. *Plant Physiology*, *117*, 173–181.

Nogues, S., Allen, D. J., Morison, J. I. L. and Baker, N. R. (1999). Characterization of Stomatal Closure Caused by Ultraviolet-B Radiation. *Plant Physiology*, *121*, 489–496.

Paul, N. D., Jacobsen R. J., Taylor, A., Wargent J. J., and Moore, J. P. (2005). The use of wavelength-selective plastic cladding materials in horticulture: Understanding of crop and fungal responses through the assessment of biological spectral weighting functions. *Photochemistry and Photobiology*, *81*, 1052-1060.

Paul, N. D., Moore, J. P., McPherson, M., Lambourne C., Croft, P., Heaton J. C. and Wargent J. J. (2012). Ecological responses to UV radiation: interactions between the biological effects of UV on plants and on associated organisms. *Physiologia Plantarum*, *145*, 565-581.

Singh, S., Agrawal, S. B. and Agrawal, M. (2014). UVR8 mediated plant protective responses under low UV-B radiation leading to photosynthetic acclimation. *Journal of Photochemistry and Photobiology B: Biology*, *137*, 67-76.

Taiz, L. and Zeiger, E. (2006). *Plant Physiology*. Sunderland: Sinauer Associates.

Tossi, V., Lamattina, L., Jenkins, G. I. and Casia, R. O. (2014). Ultraviolet-B-Induced Stomatal Closure in Arabidopsis Is Regulated by the UV RESISTANCE LOCUS8 Photoreceptor in a Nitric Oxide-Dependent Mechanism. *Plant Physiology*, *164*, 2220–2230.